# MINERALOGY OF THE NO. 2 ZONE ELDORADO MINE, PORT RADIUM NORTHWEST TERRITORIES

PLATE 1

Reprinted photograph (D.D. Campbell, 1955 - courtesy H.E. Lake)

PORT RADIUM

NORTHWEST TERRITORIES

THE UNIVERSITY OF ALBERTA

# MINERALOGY OF THE NO. 2 ZONE ELDORADO MINE, PORT RADIUM NORTHWEST TERRITORIES

A THESIS
SUBMITTED TO THE FACULTY OF GRADUATE STUDIES
IN PARTIAL FULFILMENT OF THE REQUIREMENTS FOR THE DEGREE
OF MASTER OF SCIENCE

DEPARTMENT OF GEOLOGY

by

BERNARD JOHN KIELLER

EDMONTON, ALBERTA

MAY, 1962

PLATE 2

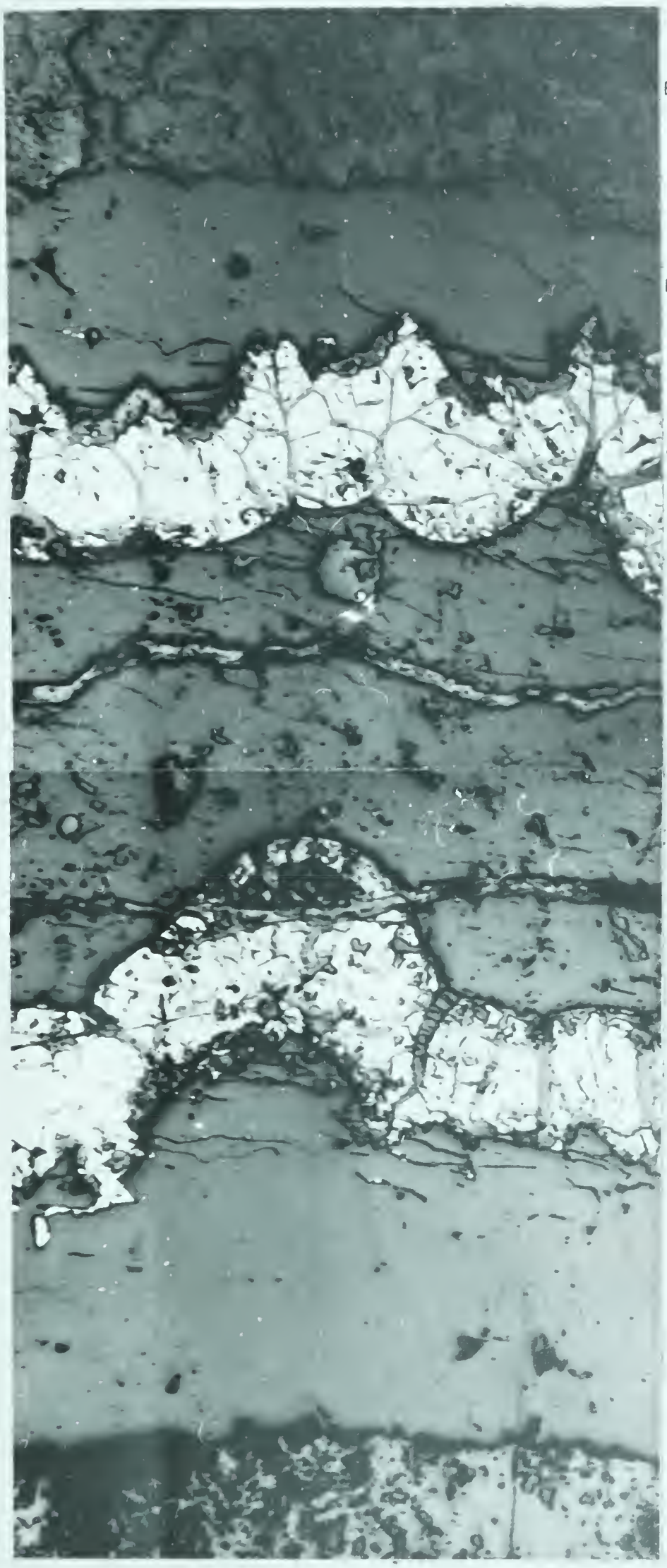


BOTRYOIDAL PITCHBLENDE VEINLET

X64

## ABSTRACT

The Eldorado ore occurs in large dilatant zones in Proterozoic sedimentary and volcanic rocks. This is partly due to the greater competency of the silicified sediments, and partly due to chemical control by the sediments on the hydrothermal solutions.

The hydrothermal solutions deposited many metallic minerals. Twenty-three hypogene metallic minerals have been identified including three rare bismuth sulfosalts, schirmerite, klaprothite and guanajuatite.

Conditions of deposition ranged from mesothermal to epithermal, with the possible exception of massive quartz and massive pitchblende which were probably deposited at higher but still mesothermal temperatures.

Two periods of hypogene pitchblende deposition have been identified. The earlier pitchblende was oxidized before the second stage of deposition. Supergene pitchblende of recent age was also observed.

ACKNOWLEDGEMENTS

The writer wishes to thank Dr. F. A. Campbell for advice and supervision in the preparation of this thesis.

Many thanks are also due to Dr. R. E. Folinsbee who obtained the samples from the Eldorado Mine; to the Eldorado geological staff for making the samples available; and to Dr. D. D. Campbell.

Finally, the writer wishes to express his gratitude to H. E. Lake who made available certain maps and Dr. D. D. Campbell's Ph. D. thesis, and to Dr. G. Hunt for supplying some samples from the Echo Bay area.

CONTENTS

# LIST OF TABLES

# LIST OF ILLUSTRATIONS

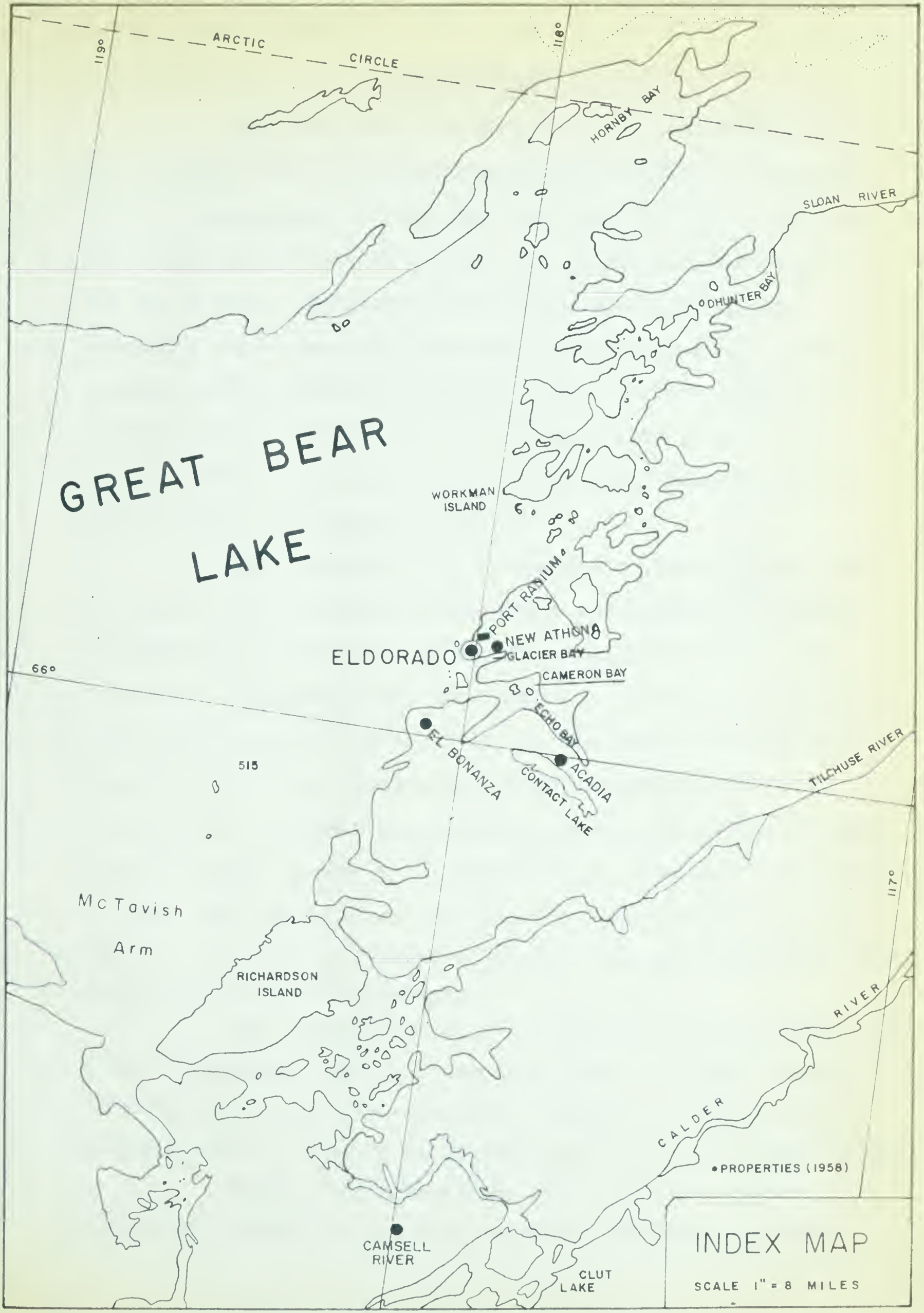
ARCTIC CIRCLE
119°
118°
HORNBY BAY
SLOAN RIVER
DHUNTER BAY
GREAT BEAR LAKE
WORKMAN ISLAND
PORT RADIUM
NEW ATHONA
ELDORADO
GLACIER BAY
CAMERON BAY
66°
ECHO BAY
EL BONANZA
ACADIA
CONTACT LAKE
TILCHUSE RIVER
515
McTavish Arm
RICHARDSON ISLAND
117°
RIVER
CALDER
• PROPERTIES (1958)
CAMSELL RIVER
CLUT LAKE
INDEX MAP
SCALE 1" = 8 MILES

FIGURE I.

# INTRODUCTION

The theme of this thesis is the mineralogy of the No. 2 Zone. The preliminary chapters, regarding the general and regional geology of the Echo Bay area and of the Eldorado Mine area, are presented to give the reader the setting of the No. 2 Zone. Information for these chapters has been liberally taken from the following sources: Campbell (1955); Campbell (1957); Edmonton Journal (Sept. 9, 1960); Feniak (1948); Feniak (1949); Kidd (1931); Kidd (1932); Kidd and Haycock (1935); Lang (1952); Lord (1946) and Parsons (1947); Murphy (1946); and Parsons (1948).

The Eldorado Mine is located on LaBine Point, on an exposed rocky peninsula that forms the northwest headland of Echo Bay on Great Bear Lake. The land rises 100 to 150 feet above the lake in the mine area but 1.25 miles northeast it is 650 feet above lake level. To the east, across LaBine Bay, is a 300 to 400 foot scarp which, except for one pronounced cleft, extends continuously north for 1.5 miles. This scarp is formed partly by a dark-coloured dike which dips gently east. The location of the Eldorado Mine area is shown in Figure 1, and the frontispiece, Plate 1, gives a pictorial representation of the topography.

The mineralization was reported by J. MacIntosh Bell of the Geological Survey of Canada in 1899. Gilbert LaBine investigated the pitchblende-silver deposits in 1930, after noticing cobalt bloom while flying over the area the year before.

Underground operations were started in 1932. Radium was extracted from the ore until 1940 when the radium

market reached a bottom, and the mine closed.

Science had learned, in the meantime, to split the atom and the need for uranium prompted the Federal government to order Gilbert LaBine to re-open the mine. In the spring of 1942, LaBine had a crew pump floodwater from the underground workings. On January, 1944, the Federal cabinet expropriated the mine and formed a Crown company, Eldorado Mining and Refining, to carry out the mining, refining, and marketing operations.

After the war, uranium continued to be produced at Port Radium (the name used for the settlement on LaBine Point). The mine was officially closed in mid September, 1960 because the underground deposits and the supply of mine tailings were exhausted.

Port Radium was to continue to be the center of exploration work by Eldorado Mining and Refining. However, pressure from private exploration companies forced the government to terminate the exploratory efforts of the Crown company.

LEGEND

DIABASE

GRANITE

GRANODIORITE

CAMERON BAY GROUP: CONGLOMERATE; TUFF; SANDSTONE.

UPPER ECHO BAY GROUP: 1 ANDESITE PORPHYRY; 2 TUFFS

+ FELDSPAR SYENITE PORPHYRY

LOWER ECHO BAY GROUP: TUFFS; SEDIMENTS

FAULT

GREAT BEAR LAKE

LINDSLEY BAY

GLACIER LAKE

GLACIER BAY

LABINE PT.

COBALT ISLAND

PORT RADIUM

CAMERON BAY

ECHO BAY

HORIZONTAL DISPLACEMENT

HOY BAY

DOWDELL POINT

CONTACT LAKE

SCALE IN MILES

0 1 2 3 4

GEOLOGY
ECHO BAY AREA
FIGURE 2

## GENERAL GEOLOGY OF THE ECHO BAY AREA

The rocks of the Echo Bay area are Precambrian. The geological sequence for the Echo Bay area is given in Table 1. Whether there is a granite older than the Echo Bay Group of sediments and volcanics in the area is unknown. Comparison with other areas in the Northwest Territories, particularily the Snare River area (Lord, 1942), indicates that there could be a granite older than the Echo Bay Group. Campbell (1955) considers the biotite granite and gneiss, southeast of the Echo Bay area, to be older than the Echo Bay Group.

### Echo Bay Group

The lower part of the Echo Bay Group consists mainly of sediments. These are dominantly siliceous argillite, but include quartzite, conglomerate, chert, and some limestone. Interbedded with the sediments are bedded tuffs. A massive crystalline tuff may be older than the sediments but the exact relationship is unknown (Murphy 1946). Campbell (1955) considers the tuffs to be younger than the sediments. He has also observed two Eldorado tuff vents, which he considers to be younger than the massive tuff.

The upper part of the Echo Bay Group consists of intrusive feldspar-syenite porhyry, and porphyritic andesite flows and pyroclastics. The feldspar-syenite porphyry is intrusive in some places and apparently extrusive in others. Crosscutting relationships, and pillows and fragmental bands have been noted. Campbell (1955) considers this rock type to

| PERIOD | ABSOLUTE AGE (M.Y.) | | |
|---|---|---|---|
| MIDDLE PROTEROZOIC | 1100 | Diabase dikes and sills | Predominately [illegible] dikes |
| | | ~~~ fracture ~~~ | Flat to low-[illegible] |
| | 1400[2] | Quartz [illegible] | Quartz-calcite; filled [illegible] veins |
| | | Diorite- [illegible] dikes and sills | Large [illegible] and [illegible] dikes |
| | | Fracture ~~~ faults | Large tension fractures, shear zones |
| | | Formby [illegible] | Sandstone, quartzite, conglomerate |
| | | Fracture ~~~ faults | Large tension fractures, shear zones |
| | 1700 | ~~~~~~~~~~~~~~~~~~~~ | Disconformity and nonconformity |
| LOWER PROTEROZOIC | 1745[1] | [illegible] granite, [illegible] granite, [illegible] | |
| | 1930[3] | [illegible] | |
| | UPDATED | Ameron Bay [illegible] | Age to [illegible] Shield [illegible] arkose, pebble conglomerate and sandstone [illegible] quartzose cement |
| | 2500 | ~~~~~~~~~~~~~~~~~~~~ | Disconformity and nonconformity |
| | ? | [illegible] | [illegible] |
| | | [illegible] | Upper part: [illegible] Lower part: [illegible] |
| | OLD COMPLEX | | |
| | 2500 ? | ~~~~~~~~~~~~~~~~~~~~ | |
| | | [illegible] | [illegible] granite; [illegible] |

AGE DATES FROM: 1. LOWDON, 1961; 2. CUMMING, WILSON, FARQUHAR, AND RUSSELL, 1955; 3. K/AR AGE DETERMINED BY DR. H. BAADSGAARD, UNIVERSITY OF ALBERTA.

be younger than even the Cameron Bay Group.

The porphyritic andesite flows consist of three units separated by massive and stratified tuff, which in part shows phenoclasts. The porphyritic andesite consists of (from oldest to youngest) porphyritic andesite, amygdaloidal andesite, porphyry, and andesite porphyry breccia.

It is postulated that there was a granitic intrusion after the deposition of the Echo Bay Group although it has never been seen. Vein quartz pebbles and a single granite pebble found in the overlying sediments suggest this intrusion according to Kidd and Haycock (1935).

Cameron Bay Group

The Cameron Bay Group overlies the Echo Bay Group probably with unconformity. It consists of red to brown massive tuffs interbedded with cobble conglomerates and sandstones with a characteristic ferruginous cement.

Intrusives

Granite batholiths, mainly of post-Cameron Bay age, lie east and south of the area. Granite also is exposed along the shore and islands north from LaBine Point and the mine workings. The Lindsley Bay granite, to the east has dimensions of 25 miles by 15 miles. The Dowdell Point granite, to the south is 35 miles wide. Another large granite body is exposed 12 miles north of LaBine Point.

The Lindsley Bay granite varies from a rather uniform massive, to a slightly gneissic biotite granite. It is medium-grained and may become somewhat porphyritic near

the borders. The Dowdell Point granite is dominantly massive although porphyritic in places. It is a fresh, coarse-grained, buff to pink, crumbly-weathering biotite granite.

A thin section, No. 4, of the Dowdell Point granite has been examined. The section comes from a sample taken in the 1612 West Line Drive of the 1675 level, near the 1612 West No. 5 drift (approximate location is marked on longitudinal section of the No. 2 Zone, Figure 7, sample No. 3936). Hydrothermal alteration appeared to be minor in the hand specimen. However, microscopic examination shows that hydrothermal alteration is significant. Composition of the granite was found to be as follows:

TABLE 2

GRANITE COMPOSITION

| Primary Minerals | | Hydrothermal Alteration Products | |
|---|---|---|---|
| Essential | % | Chlorite (prochlorite | % |
| Albite - andesine | 30.5 | | 6 |
| Orthoclase | 30 | Hematite | 1 |
| Quartz | 10 | Leucoxene | 2.5 |
| Biotite | 5 | Sericite | 8 |
| Varietal | | | |
| Ilmenite-magnetite | 6 | | |
| Apatite | <1 | | |
| Zircon | <1 | | |
| Epidote | <1 | | |
| Totals | 81.5+ | | 17.5+ |

Carlsbad-albite twins are abundant in the plagioclase. Sericitization and minor hematization of the plagioclase has occurred and hematite occurs along the grain boundaries. Alteration of orthoclase has been minor. Most of the biotite seems to be primary and is now largely

altered to chlorite. Some ilmenite has been altered to leucoxene. Euhedral zircon has been altered slightly to chlorite. Biotite from the Dowdell Point granite was separated and dated by the K/Ar method. The date was found to be 1930 million years and is shown in Table 1. This date suggests this granite may be an early segregate of the Hudsonian orogeny or it may indicate a metamorphosed updated intrusive of the Kenoran orogeny. The former interpretation in the writer's opinion is probably correct.

Granodiorite to quartz-mica diorite stocks have been distinguished from the granite in the Echo Bay area. These are older than the Dowdell Point granite. They are commonly elongated in a northwest direction. Large contact aureoles in the invaded rocks contain abundant red feldspar, chlorite, magnetite, pyrite, biotite, actinolite, and epidote. Large gossans from the weathering of the pyrite occur in places around the borders of the stocks.

These quartz-mica diorite, granodiorite, and granite intrusives seem to be of the epizonal type as defined by Buddington (1959). The intrusives are generally discordant with the relatively unmetamorphosed country rocks. The Echo Bay and Cameron Bay Groups show a low grade of metamorphism and assimilation is slight. The batholiths are composite and the successively segregated rock types show increasing felsic affinities. In the Echo Bay area a sequence from normal granite to quartz-mica diorite was intruded. The porphyries and tuffs may be consanguineous with the

grandodiorites and granites. Mineral veins associated with the intrusives are commonly zoned (temporal zoning is more apparent than spatial zoning). Aplite dikes cut the granite and pegmatitic phases are rare.

Hornby Bay Group

The Hornby Bay Group is younger than any of the granitic intrusives. This group does not outcrop in the Echo Bay area but is exposed to the north of the area in Hornby Bay and to the south on Dowdell Point and Richardson Island. The rocks present in the group are sandstone, quartzite, and conglomerate. The sediments are older than the giant quartz stockworks.

Giant Quartz Stockworks

Two very large quartz veins associated with the intrusives, one at Cameron Bay and the other on an island 4 miles north of LaBine Point, are noteworthy. There are many similar veins extending, in a zone, between Coppermine River, northeast of Great Bear Lake, to Rae on Great Slave Lake. The Rayrock Mine, approximately 44 miles north of Rae, is an example of a deposit in this type of structure. The veins are between 50 and 500 feet wide and have lengths up to 10 miles. Nearly all strike approximately N45$^{o}$ E and several occur in faults. They are giant quartz stockworks formed along large fault zones, where quartz has filled zones of displaced wallrock and rock fragments. Many contain quartz of at least two ages along with specular hematite.

Several geologists consider the veins to be

mesothermal to leptothermal. The distribution of these veins over an area at least 350 miles by 50 miles in major faults indicates a probable deep-seated source of the mineralizing solutions (Kidd and Haycock, 1935). Since the veins occur in faults which cut nearly all the known igneous rocks this suggests that they are not directly related to intrusives now exposed. The veins are probably related to an unexposed late magmatic differentiate. This suggests a complex relationship between the exposed less acid intrusives and an unexposed more acid intrusive and the giant stockworks.

Mafic Dikes

Mafic to submafic dikes are present in the area. The rocks vary in composition from diorite, diabase, and norite (Kidd and Haycock, 1935). Three samples have been examined from three localities and they are all syenodiorites. Two are highly altered hydrothermally. A description of each sample follows:

Specimen No. GB.22.1 (thin section No. 1) comes from a large flat-lying dike in the Eldorado Mine area (see figure 5). In hand specimen the rock is black, contains fine-grained phenocrysts of feldspar, set in a microcrystalline matrix. The texture appears to be diabasic to aphanitic with feldspar phenocrysts. Thus the rock in the hand specimen appears to be a diabase with minor alteration. Microscopic examination has shown that the original texture was fine granular. The mafic minerals have been highly altered to micro-crystalline chlorite and the felsic minerals have been sericitized, and

this develops the apparent grain size and texture in the hand specimen. The composition of this rock is given in Table 3.

Table 3

DIKE COMPOSITION

| Primary Minerals | % | Hydrothermal Alteration Products | % |
|---|---|---|---|
| Essential | | Chlorite | 40 |
| Feldspar | 5 | Sericite | 38 |
| (Quartz | | +Quartz | 10) |
| | | Hematite | 1 |
| Varietal | | Lawsonite | <1 |
| Hornblende | <1 | Pyrite | <1 |
| Biotite | <1 | Tourmaline | |
| Ilmenite-Magnetite | <1 | (schlorite) | 5 |
| Totals | 5+ | | 94+ |

Original primary mineral composition was as follows (estimated):

| Essential | % |
|---|---|
| Feldspar | 60 |
| Quartz | 5 |
| Hornblende | 30 |
| Biotite | 5 |
| Varietal | |
| Ilmenite-Magnetite | <1 |
| Total | 100 |

The occasional Carlsbad twin is still evident and some albite twinning can be distinguished. Most of the plagioclase has been sericitized and some chloritization and tourmalinization has taken place without destroying the original crystal outlines. The original mafic minerals have been nearly completely tourmalinized and chloritized so that just a few remnants of biotite remain. It is difficult to determine how much, if any, of the ten percent quartz is primary. Hematization has been minor. From

the above information, it appears that the rock is a chloritized (feldspar) microsyenodiorite. It is melanocratic due to chloritization and not to the original composition. Specimen No. GB.27.2 (thin section No. 2) comes from Misery Lake (Camsell River map area, to the south of LaBine Point area). The rock is dark grey, fine-grained, and granular. In the hand specimen the alteration appears to be minor. The composition is as follows:

Table 4

DIKE COMPOSITION

| Primary Minerals | % | Hydrothermal Alteration Products | % |
|---|---|---|---|
| Essential | | Sericite | 10 |
| Plagioclase (An 20) | 40 | Leucoxene | <1 |
| K-feldspar } Quartz } | 5 | | |
| Hornblende | 35 | | |
| Biotite | 9 | | |
| Varietal | | | |
| Ilmenite | 1 | | |
| Totals | 90 | | 10+ |

In the oligoclase, Carlsbad twins are more abundant than albite twins. The mineral has been sericitized in places. Hornblende is replaced by plagioclase and ilmenite. Minor chloritization of hornblende has occurred. Ilmenite cryallization was later than biotite. The rock is a (hornblende) syenodiorite porphyry.

Specimen No. GB.28.4 (thin section No. 3) comes from the Eldorado Mine, 10 level of the No. 2 Zone (see Figure 7 for approximate location). This is a steeply dipping dike

that is greyish-brown, granular, and moderately altered. Microscopic examination has shown that the rock is highly chloritized and sericitized. The composition is as follows:

Table 5

DIKE COMPOSITION

| Primary Minerals | % | Hydrothermal Alteration Products | % |
|---|---|---|---|
| Essential | | Chlorite | 23 |
| Plagioclase | 4 | Sericite | 50 |
| K-feldspar ) | | Leucoxene | 10 |
| Quartz ) | 10 | Hematite | <1 |
| Hornblende | <1 | Tourmaline (schorlite) | 2 |
| Totals | 14+ | | 85+ |

Plagioclase originally composed over 65 percent of the rock, but has been largely altered to sericite. The sericite pseudomorphs indicate plagioclase twinning was present. A very minor amount of hornblende remains unaltered. Some hematite occurs along original plagioclase boundaries. K-feldspar, probably orthoclase, is relatively unaltered and some of it may be partly secondary. Leucoxene in places shows a sub-parallel orientation. The rock is a chloritized-sericitized syenodioite.

Kidd and Haycock (1935), Murphy (1946), and others have recognized early 'diabase' dikes and late 'diabase' dikes. Kidd states on page 886,

> "A few dark-coloured dikes older than the large quartz veins occur at a few places north of the area (ie. north of Echo Bay area). They are distinguished by the presence of red feldspar."

Kidd also states that an andesite dike, south of Contact

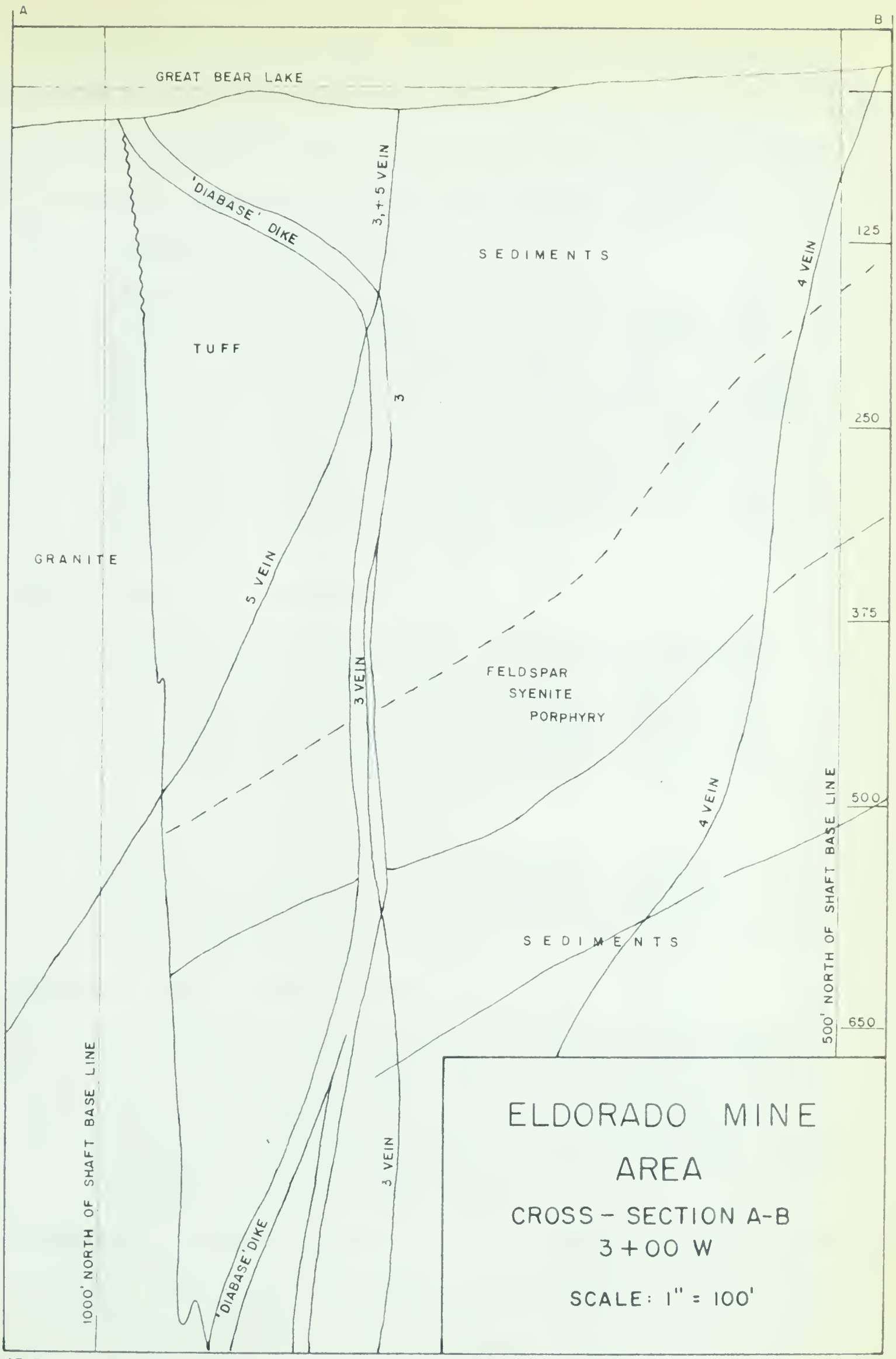


AFTER D.D.CAMPBELL, 1951

FIGURE 3

Lake, may be of this age. Dark-coloured, gently dipping, enstatite (?) mica diorite, quartz norite, and diabase dikes outcrop in the area and are younger than the vein-filled structures, according to Kidd and Haycock (1935).

Murphy (1946, p 42B) states,

> "Inrusives of two or three different ages are identified as diabase. The early diabase includes a number of fine-grained, dark dikes, some of them amygdaloidal. These are steep in attitude and known to be earlier than the pitchblende veins. The late diabase is a medium-grained, greyish rock of variable texture. It occurs as a flat lying sill or dike, showing columnar jointing. Narrow off-shoots of the dike are found in the mine working, cutting the veins."

Lang (1952, p 51) states,

> "The youngest rocks near the mine are diabases, divided into two groups. Early diabase dikes are cut by structures containing pitchblende. The late diabase forms flat-lying bodies that may have been continuous; apophyses of this rock cut some of the pitchblende-bearing veins."

Also Lang states on p 53,

> "The ore bodies are almost entirely confined to the stratified rocks or to places where the fault zones follow contacts between these rocks and early diabase."

Campbell (1957, p 181) states,

> "In the mine area the vein zones also cut diabase dikes and one diabase sill. The dikes, showing chilled margins, cross the vein zones and in some cases run along them, and are in turn cut by later fractures and veins. They are younger than the earliest quartz veins but older than the major mineralization of the veins."

Cross-section A-B (Figure 3), after Campbell (1957), shows a 'diabase' dike cut by a quartz vein (the No. 3 Zone of the Eldorado Mine area). Consult Figure 5 for the location of

Cross-section A-B.

The above observations indicate a close association between dikes and vein material. The earlier dike material apparently is more dioritic and occupies steeper structures, whereas, later dikes are diabasic and are flat-lying. Some dikes are earlier than the quartz vein material, and others are younger than quartz (probably includes pitchblende) but older than the metallic mineralization. The youngest dikes were intruded after most of the mineralization had taken place. The three dikes examined in this study were all syenodioritic in composition. Sample GB.22.1 is a large flat-lying dike or sill in the Eldorado Mine area. It has been hydrothermally altered and is therefore older than the metallic mineralization and may even be older than quartz. Sample GB.28.4 comes from the Eldorado Mine, level of the No. 2 Zone. It is a steeply dipping dike and is strongly altered. It may be an apophysis of the outcropping flat-lying dike. Sample GB.27.2 from a drill core taken in the Misery Lake area, is unaltered but similar to the previous two samples in original composition. Lack of alteration may be due to absence of hydrothermal solutions in that area and may not indicate that the rock is younger than the hydrothermal mineralization.

PLATE 3

FIGURE 1: Photomicrograph of granite (sample No. 3936) from 1612 West Line Drive. K-feld (probably orthoclase), ser (sericitized plagioclase), q (quartz), bio (biotite), il (ilmenite), chl (chlorite), and hem (hematite). x40

FIGURE 2: Photomicrograph of syenodiorite dike (sample No. GB.22.1) from the lower contact of the dike at LaBine Bay across from Port Radium. Ser (sericitized feldspar), chl (chlorite), and il (ilmenite). x40

FIGURE 3: Photomicrograph of syenodiorite dike (sample No. GB.27.2) from Misery Lake, Camsell River Map Area. Horn (hornblende), feld - q (feldspar and quartz), bio (biotite), and il (ilmenite). x40

FIGURE 4: Photomicrograph of syenodiorite dike (samle No. GB.28.4) from the 10 level of the No 2 Zone. Ser (sericitized feldspar), chl (chlorite), leu (leucoxene), and q (quartz. x40

PLATE 3

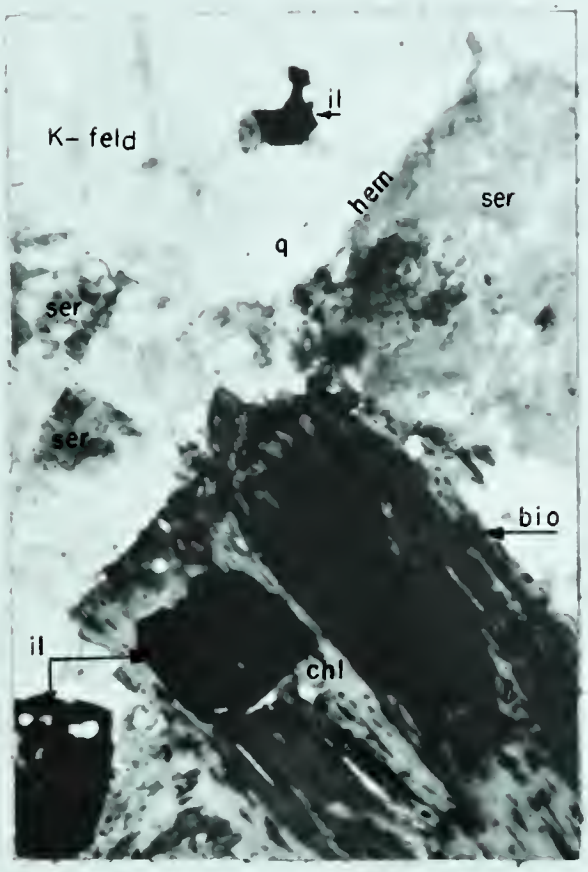


1 X40

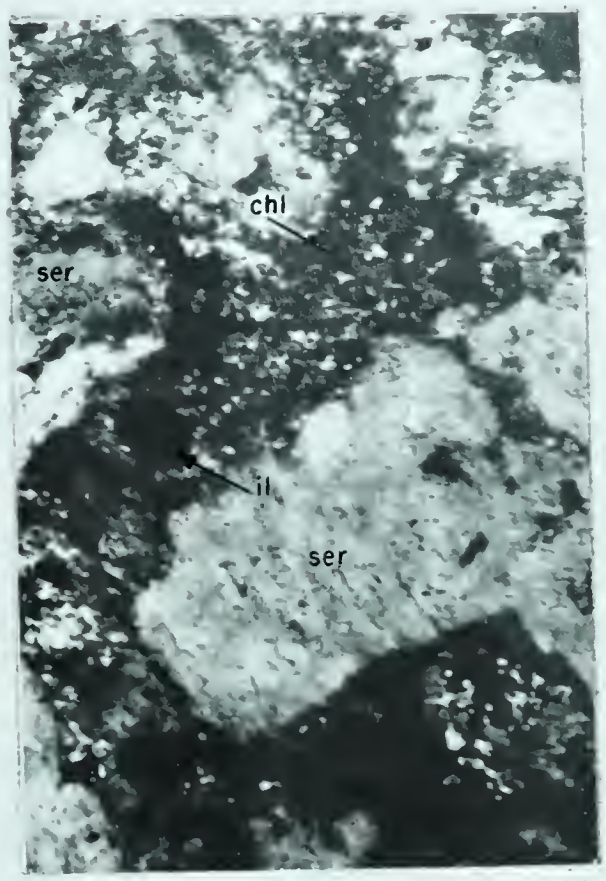


2 X40

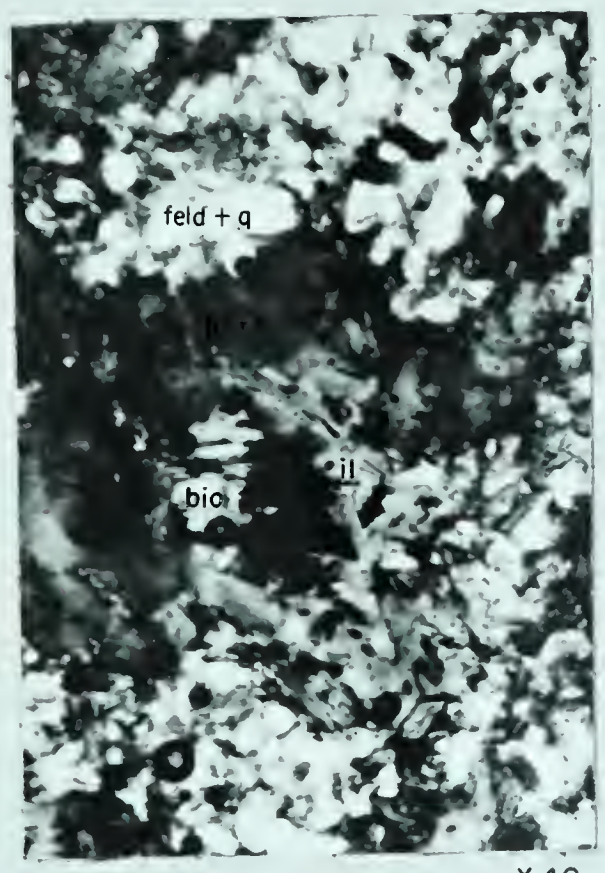


3 X40

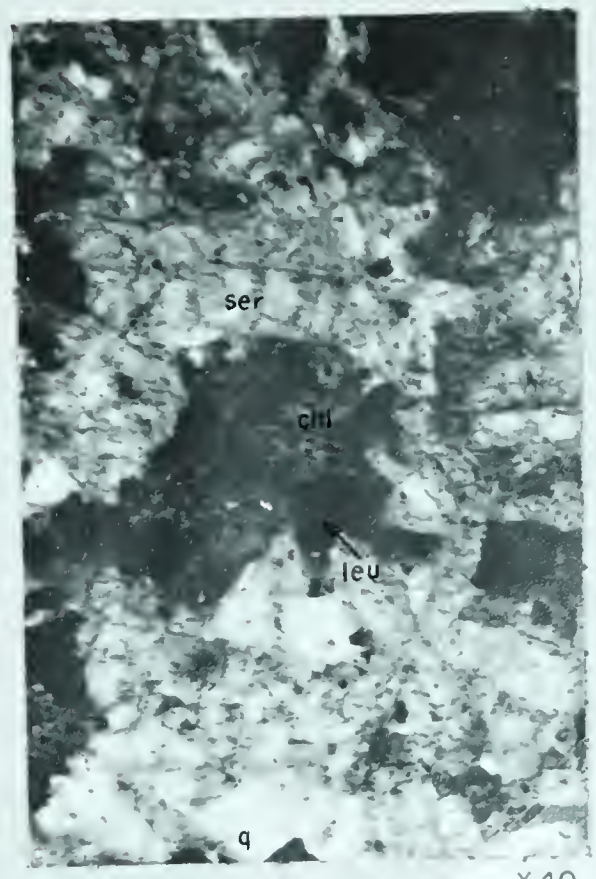


4 X40

## STRUCTURAL GEOLOGY OF THE ECHO BAY AREA

The trend of folding along the east side of Great Bear Lake is generally northwest, except in the vicinity of LaBine Point and Glacier Bay, where it is more northerly. The formations are highly contorted in the Eldorado Mine area and an accurate general attitude is difficult to determine.

Most of the fractures and faults in the Echo Bay area strike northeasterly. Some fractures strike N35°E and others are more easterly. The N35°E type of fractures are right-hand fault zones. A prominent right-hand fault at Cameron Bay appears to have a displacement horizontally about 3 miles (Figure 2). It strikes approximately N45°E and is nearly vertical. Other fractures of this type are prominent. One occupies Glacier Bay and Glacier Lake, striking approximately N35°E, and another is evident in the Eldorado Mine area (see Figure 5). Another set of fractures have an average strike of N65°E. These are composite shear fractures with right-hand or left-hand displacements. These shears are in places associated with tensional fractures, as for example in the ore zones of the Eldorado Mine. Some fractures strike S85°E and are left-hand shears. One such fault forms the No. 3 Zone in the Eldorado Mine. Dilatant zones associated with this type of shear may also be ore-bearing. Finally, a fracture in the southeastern arm of Echo Bay strikes approximately N25°W and is an extension or release tension fracture.

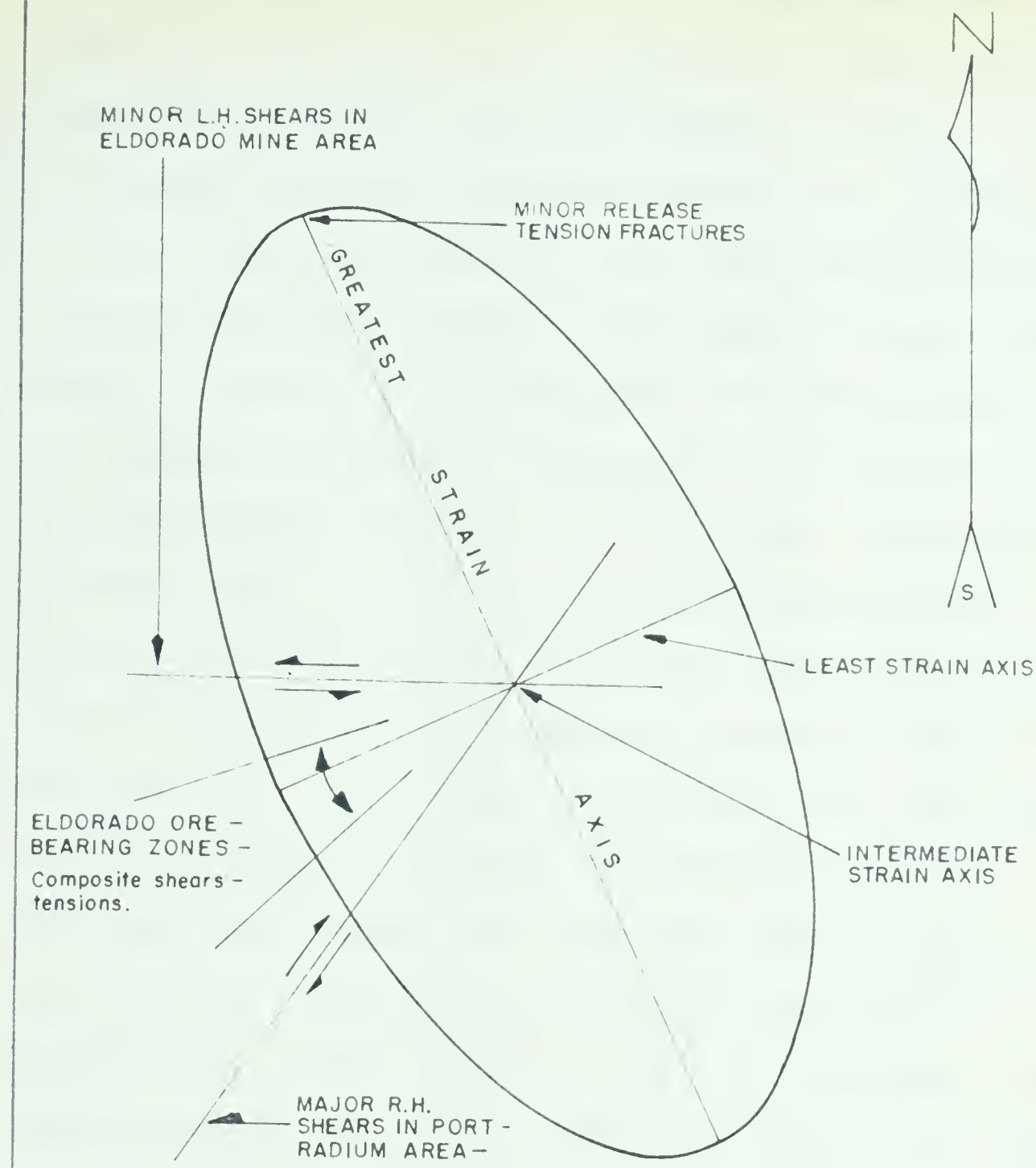


PORT RADIUM

AREA

STRAIN ELLIPSOID ORIENTATION

FIGURE 4

Kidd and Haycock (1935) suggest that the abrupt ending of the high upland along the straight shore of Great Bear Lake, together with the abundant evidence of tensional fracturing, strongly suggests control by a major north-south axis of tensional rupture. The four fracture sets mentioned indicate that the strike of the greatest strain axis was N25°W. Figure 4 is an orientation for the strain ellipsoid in the Echo Bay area. In summary, the greatest strain axis strikes N25°W, intermediate strain axis is probably near vertical, and the least strain axis strikes N65°E. Assuming that the orientation of the strain ellipsoid is correct, tension fractures and extension fractures were probably developed first. Left-hand shears were then developed and they in turn were followed by right-hand shearing, which displace the earlier fractures and faults. Upon release of the east-west and vertical stresses (possibly due to vertical intrusion), release tension fractures developed; one set is near vertical and strikes N25°E and another is nearly horizontal.

Some of the basic rocks invaded the early fractures and are cut and altered by the late vein material. These dikes have a vertical dip. However, most of the basic dike material came after the siliceous vein material had been deposited, since most of the 'diabase' dikes cut the quartz (and carbonate) veins. Some metallic mineralization and movement in the veins postdates these dikes. The late dikes which are the most abundant, occupy many late flat-lying

release tension fractures. Apophyses from the flat-lying dikes that cut the veins however are earlier than some of the metallic mineralization.

The close association of the veins and dikes is now more apparent. Some dike material was first deposited and vein-forming solutions came shortly after. The later dikes occupy the late flat-lying fractures and are apparently more mafic, although the writer has not seen any dikes more mafic than syenodiorite. There is also field evidence of an intermingling between the dike and vein materials. Sample GB.28.4, a syenodiorite, from the 10 level of the Eldorado Mine, No. 2 Zone, contains 110 $\pm$ 10 p.p.m. of uranium (average content of syenodiorite dikes is less than 1 p.p.m.). This dike is younger than the quartz and massive pitchblende mineralization, however it is hydrothermally altered and $UO_2^{+2}$ may have been introduced from solutions containing dissolved uranium. On the other hand this high uranium content may indicate the genesis of uranium and basic dikes is the same. No uranium minerals are evident but the uranium probably exists as $UO_2$. Reduction of the $UO_2^{+2}$ may have occurred in the dikes by the oxidation of $Fe^{+2}$. $Na^{+2}$ in the diabase dike could have made the invading solutions more basic and caused $Fe^{+2}$ to be more reducing than $UO_2^{+2}$ thus, facilitating precipitation of hematite and $UO_2$.

## MINERALIZATION OF THE ECHO BAY AREA

Silver and uranium are the chief mineral deposits of economic importance in the area. Copper mineralization is widespread but to date deposits of economic significance have not been found. For the purpose of this discussion the term pitchblende is used both for the crystalline unoxidized variety of uranium oxide ($UO_2$) normally called uraninite, and for the oxidized often amorphous variety as well. Many geologists have used the term pitchblende for the colloform or botryoidal variety but work on these ores indicates that crystalline unoxidized uranium oxide can also be botryoidal. The terms pitchblende and uraninite are therefore used interchangeably.

Several deposits of silver and pitchblende have been discovered in the Echo Bay area. The Eldorado property has been the most important. Other properties are shown in Figure 1.

The mineralization occurs in large quartz stockworks formed in dilatant areas in large shear zones. The country rock near most of the deposits has been much altered and contains many metasomatic minerals such as argillic minerals, chlorite, hematite, and carbonate. Minor mineral varieties include quartz, pyrite and chalcopyrite, and apatite. The metallic minerals are in part disseminated in the wall rocks of the zones, and in part in veins and veinlets with a manganiferous carbonate gangue. Quartz, earlier than the carbonate, is the dominant gangue

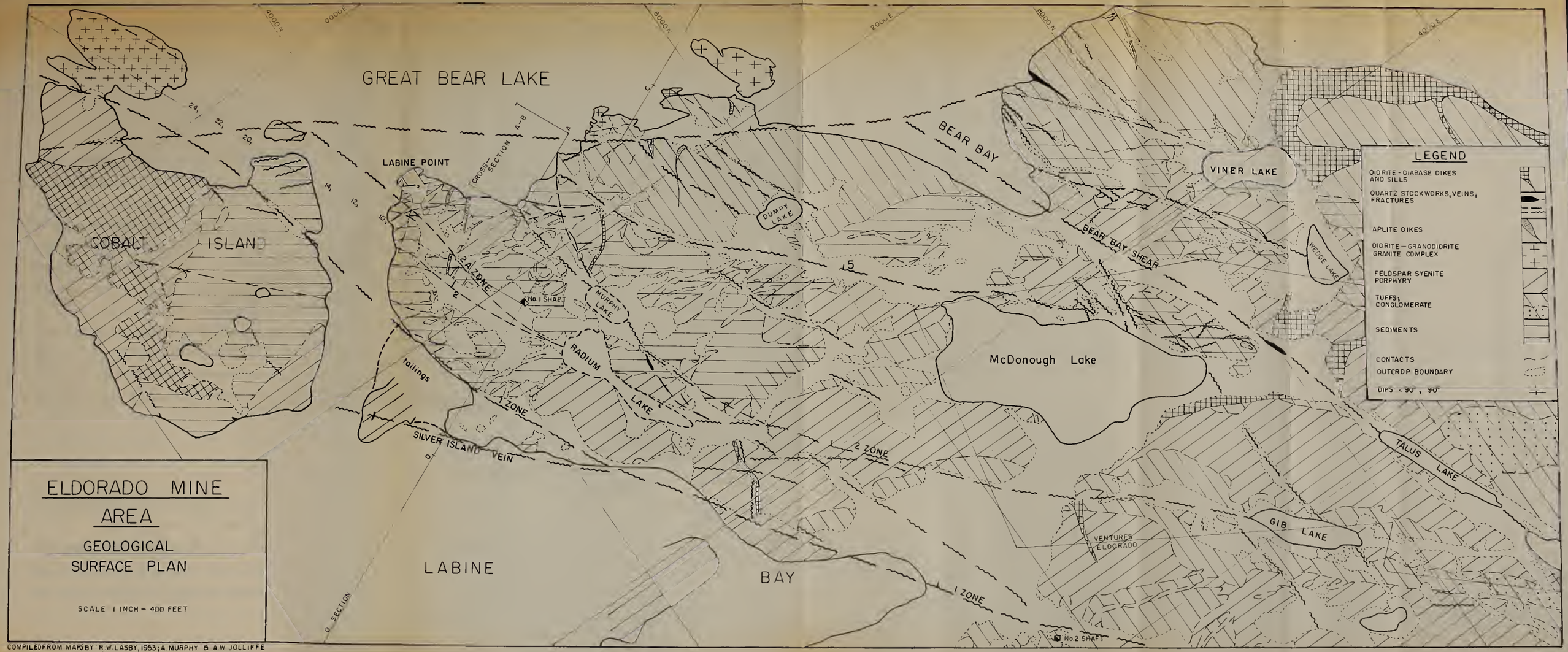
GREAT BEAR LAKE
BEAR BAY
LABINE POINT
CROSS-SECTION A-B
COBALT ISLAN
DUMPY LAKE
VINER LAKE
BEAR BAY SHEAR
WEDGE LAKE
2A ZONE
No. 1 SHAFT
MURPHY LAKE
RADIUM LAKE
tailings
1 ZONE
SILVER ISLAND VEIN
McDonough Lake
2 ZONE
TALUS LAKE
GIB LAKE
VENTURES ELDORADO
LABINE BAY
1 ZONE
No.2 SHAFT
0 SECTION
LEGEND
DIORITE - DIABASE DIKES AND SILLS
QUARTZ STOCKWORKS, VEINS, FRACTURES
APLITE DIKES
DIORITE — GRANODIORITE GRANITE COMPLEX
FELDSPAR SYENITE PORPHYRY
TUFFS, CONGLOMERATE
SEDIMENTS
CONTACTS
OUTCROP BOUNDARY
DIPS < 90°, 90°
ELDORADO MINE AREA
GEOLOGICAL SURFACE PLAN
SCALE 1 INCH = 400 FEET
COMPILED FROM MAPS BY R.W. LASBY, 1953; A MURPHY & A.W. JOLLIFFE

FIGURE 5

in the veins and veinlets.

## GENERAL GEOLOGY OF THE ELDORADO MINE AREA

The rocks are chiefly those of the lower Echo Bay Group and feldspar-syenite porphyry. Figure 5 is a geological surface plan of the Eldorado Mine area. Mafic dikes outcrop near the Eldorado Mine. They are generally gently dipping to nearly horizontal. Underground along the No. 2 Zone, there are dikes dipping 50° west and another dipping 45° east (Figure 7). Granite outcrops on the southwest tip of LaBine Island and on small points and islands along the west shore of LaBine Point. Granite is also exposed in the west end of the mine.

The Echo Bay Formations are so altered by the introduction of igneous rocks and hydrothermal solutions that at many places their original character is indeterminate. The rock is hard, fine-grained, massive, mottled reddish-brown, pink, and greenish-grey. Faint banding over areas of a few square feet indicates that it is probably an argillitic sediment. Well banded argillite and volcanic flow breccias occur in the mine area. At the northwest corner of LaBine Island (Cobalt Island) are a few feet of contorted much altered limestone.

Much of the alteration is due to the intrusion of at least five tabular bodies of feldspar-syenite porphyry. The rocks in the mine area (Lower Echo Bay Group, excluding the tuffs) contain at least 20 percent metasomatic minerals.

Campbell (1957, p 180), states,

> "These metasomatic (and metamorphic) minerals are predominantly hornblende, diopside, plagioclase, magnetite, garnet, and scapolite. Adjacent to the porphyry bodies, the sediments, mostly cherts, have been completely recrystallized and the above mentioned minerals are in coarsely crystalline banded and massive aggregates."

Kidd and Haycock (1935, p 890) state that feldspathization of these rocks occurred either by crystallization or by introduction of new material, or by both, together with formation of chlorite, carbonates, magnetite, garnet, biotite, sericite, pyrite, and actinolite. Kidd and Haycock (1935) also noted some uralite, antigorite, and epidote in thin sections. They state that chlorite, carbonate, magnetite, and sericite or paragonite occur in nearly all the rocks examined. Biotite and magnetite are often closely associated, and pyrite and actinolite frequently occur together. Pyrite is sparsely disseminated at many places and abundant in some areas.

Kidd and Haycock (1935) state that the alteration described in these rocks is not confined to the mine area. On the east side of LaBine Bay, feldspathization of the argillite is in places widespread. Also, to the northwest these minerals have developed extensively. They indicate it is doubtful that the alteration of the pyrometasomatic type was caused by the adjacent granite, as elsewhere similar granite has caused no such widespread or thorough alteration. For example, at Dowdell Point the effect of the granite intrusion on the invaded rock is

simply baking and silicification. On the other hand, granodiorite stocks have caused pyrometasomatic alteration of this nature and extent elsewhere. Thus the LaBine Point rocks, may have been altered by grandodiorites. An area of granodiorite, nearly 100 feet in diameter occurs on the east-side of LaBine Bay and the extensive alteration may indicate that it is the tip of a cupola.

However, Campbell (1957, p 178), states that the granodiorite bodies are only locally fringed with haloes of recrystallization and granitization, whereas hypabyssal intrusives (feldspar-syenite porphyry) generally show very extensive haloes of recrystallization and metasomatism. The alteration material described by Kidd and Haycock may be attributed predominantly to these hypabyssal bodies rather than the granodioite plutons as postulated by Kidd and Haycock. Campbell concurs with the remarks of Kidd and Haycock by saying that the granite bodies have sharp contacts, accompanied by little or no metamorphic effects.

Campbell (1957) has observed that the principal hydrothermal alterations in order of decreasing abundance are: argillic, chloritization, hematization, and carbonatization. Minor varieties include silicification, sulfidization (pyrite and chalcopyrite), and concentrations of apatite. In addition to these Murphy (1946) notes magnetite and sericite mineralization.

The ore zones are often enveloped by a red-alteration which is due to hematization. Murphy (1946) calls

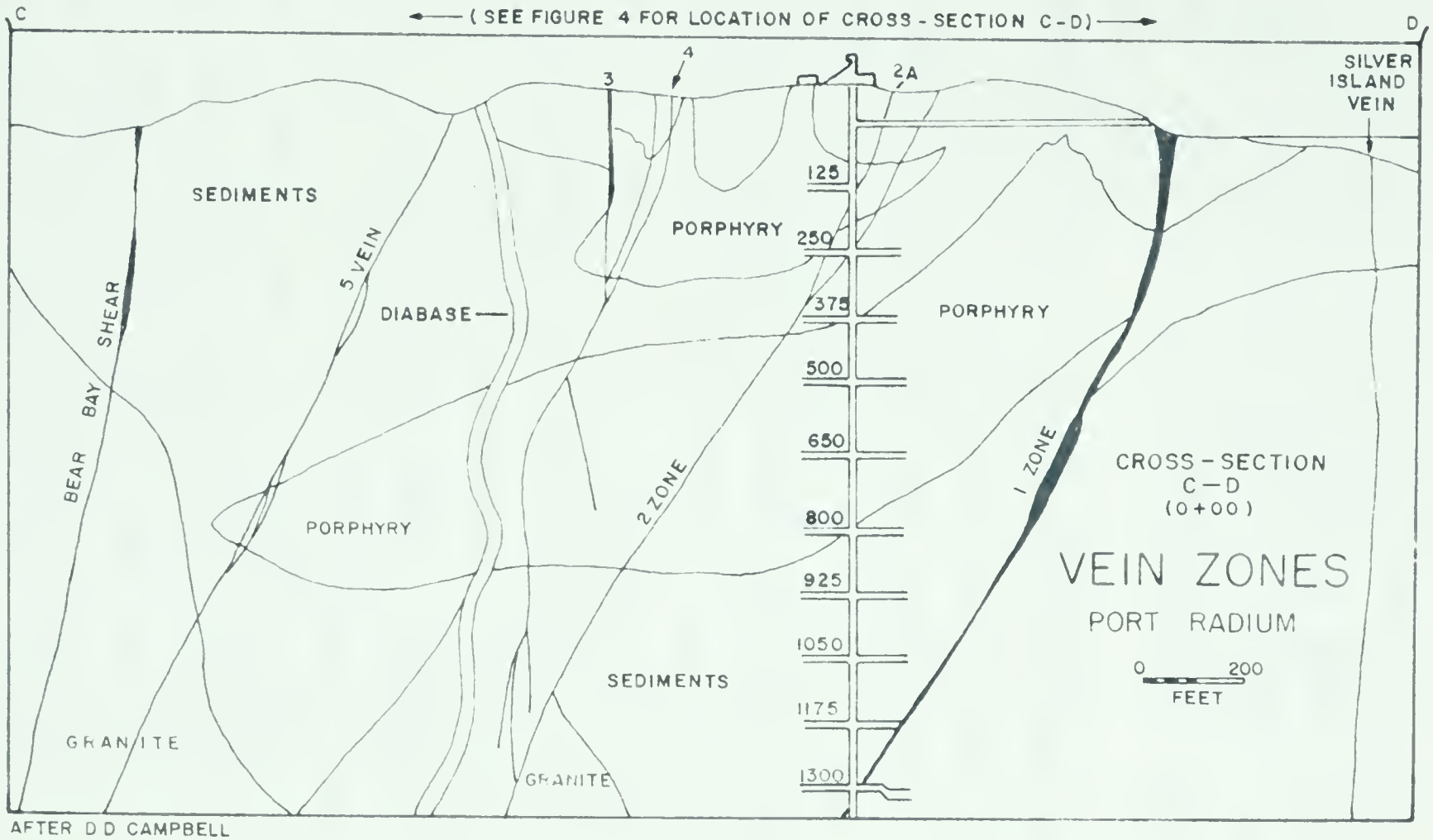


AFTER D D CAMPBELL

FIGURE 6

this envelope reddish 'jasperoid' envelopes as zones of hematized chert. These red alteration envelopes can be useful in exploration.

The granite on the westside of LaBine Point is lithologically similar to the Dowdell Point granite. A fine-grained border phase occurs at the tip of LaBine Point. Sharp-walled dikes of pink orthoclase-quartz aplite cut the main granite mass.

## STRUCTURAL GEOLOGY OF THE ELDORADO MINE AREA

Figure 6 (Cross-section C-D) shows the relationship of the vein zones, dikes and country rocks. The general trend of the rocks is northerly in the mine area. The Echo Bay Group is extensively contorted which may be due primarly to the batholithic intrusions in the area. The folding may or may not be related to the fracturing. If folding was caused by the post-Echo Bay exposed intrusions, fracturing and folding would be unrelated since the fractures cut most of the rocks, except the late dikes. Although the general trend of folding for the Echo Bay area is northwest the intrusions in the vicinity of the Eldorado Mine may have caused the local trend to be north to northeast.

Murphy (1946) states that some dikes cut vein-faults but are themselves displaced by mudseams. Other dikes are definitely cut by the veins. The mud seams indicate movement along the quartz vein after implacement of the late dikes. He suggests that the movements took place at shallow depths due to,

"the complexity of the faulting and the brec-
ciated 'open' appearance of the fault zones."

This is in accordance with the epizonal depth of erosion (Buddington, 1959).

Most of the uranium ore occurs over a strike length of 4,500 feet between LaBine Point and Crossfault Lake. There are three main ore-zones on the Eldorado property. They are regularly disposed at about 600-foot intervals, and trend approximately N65E, converging in that direction. The three ore-zones have been numbered from south to north, respectively, 1, 2, and 3 (see Figure 7 for junction between zones 2 and 3). Zones 1 and 2 dip steeply northwest, but No. 3 Zone is vertical or dips south. Other fractures in the Eldorado Mine area are the Silver Island Vein, Nos. 4, 5 (Dumpy), 7, 8, and Bear Bay Shear.

All the zones are a composite of shear and tension fractures. Some zones have gouge-covered slip planes predominantly, and others are brecciated dilatant zones. The ore is confined to the dilatant zones. Tensional fracturing is dominant in the more competent sediments, whereas, other less competent rock-types have fewer tension fractures. Ore is concentrated in the competent rocks near their contact with incompetent units, and bulges developed at such contacts are favorable loci of ore zones. Mineralization is also strongly concentrated at the junction of zones such as the No. 2 and the No. 3. Steep portions of the zones have more tension fractures than the less steep parts and have been

the favorable site for ore deposition. No. 1 Zone is a strong shear zone up to 40-feet in width and extends for over 5,000 feet. The apparent horizontal displacement is 300-feet and the movement is left-handed. Nos. 2 and 3 Zones are structurally minor fractures. They consist of narrow, subparallel shear and related tension fractures. The ore occurs in discontinuous tension fractures. Murphy (1946) states,

> "Displacements do not exceed 20-feet and movements in opposing directions have been observed in different parts of the zones."

The Nos. 4 and 5 Zones and Bear Bay Shear (Figure 5) are strong shear zones with minor tensional fracturing. Zones 7 and 8 are strong brecciated tensional zones similar to the No. 3 Zone.

## MINERALIZATION OF THE ELDORADO MINE AREA

The veins are composed primarily of quartz, carbonate, and hematite in varying proportions, with a minor amount of chlorite. Deposition has taken place in four distinct stages according to Kidd and Haycock (1935). Complex mineral relationships were produced, depending on the timing of the fracturing and the heterogeneous spatial zoning of the solutions. In large shear zones, stockworks of narrow, persistent veins have formed. All veins carry numerous inclusions of the wall rocks and, as an extreme instance, No. 3 vein is a breccia (consisting of several discontinuous fractures according to Lang, 1952) cemented by a little vein material.

No. 1. Zone

This zone shows the most complex mineral relationship of any zone in the area. The earliest filling has been white or pale brown quartz with occasional rosettes of specular hematite. Minor pyrite is associated with the quartz. There are seams and inclusions of chlorite and a little carbonate. The quartz shows no banding, and may in fact be hypothermal. The next stage is a banded, hematite-stained quartz which fills fractures of the earlier quartz or replaces it. Numerous vugs, occasionally a few feet in diameter, are lined with crystals of carbonate, hematite, quartz and chalcopyrite. Carbonate was the last gangue mineral to be deposited. Parts of the hematitic-quartz vein are a dense rose-red chert.

Late shearing has opened portions of the hanging-wall, along the northwest side of the zone and botryoidal pitchblende was deposited in the openings. It is brecciated in places and cemented by the pale brown so called early quartz. This means that some pitchblende at least has been earlier than the pale-brown quartz. Also in the hanging-wall are lenses of pale chalcopyrite several feet long, which are earlier than the shear. The pale colour is due to sworms of relict pyrite grains.

Narrow bands of sulphides, arsenides, bismuth, silver and pitchblende are found in the cherty phases of the quartz-hematite veins. Some Co-Ni minerals are crystallized on comb quartz, which in turn, contain chalcopyrite crystals. The remaining space is filled with white

to buff carbonate and chalcopyrite, and in some places euhedral native bismuth. Kidd and Haycock (1935) suggests that the latter shoots of ore may represent a third stage of mineralization. Various metallic minerals are segregated separately in lenses in the vein, although intergrowths are not unusual in these lenses. The metallic minerals are not co-extensive indicating a heterogeneous distribution of the solution, or conditions necessary for precipitation were locally unfavourable. The limits of the ore are apparently well defined. Native silver content is high in the upper portion of the ore zone whereas pitchblende, particularily the massive variety, occurs in greater abundance in the lower portion.

According to Murphy (1946) the last stage of mineralization consisting of minor fillings of veins and vugs by quartz, carbonate, and chalcopyrite, is later than the late diabase dikes. Where one dike cuts the No. 1 Zone, it is itself cut by a few veinlets of quartz and carbonate. Carbonate veins in the diabase on Cobalt Island contain metallic bismuth and Ni-Co minerals. At Gunbarrel Inlet, forty miles south, a calcite vein cutting the late diabase contains silver.

Movement along the No. 1 Zone was of long duration. Three feet of gouge is found in the footwall, and branch faults lace their way through the zone giving rise to weak ground. A few veinlets of quartz and carbonate, possibly belonging to the youngest stage of mineralization,

are found in the gouge. In a few places, lenses of massive chalcopyrite, several feet wide, with a dense 'muddy' appearance, appear to have replaced the gouge.

No. 2 and No. 3 Zones

Each zone has its own characteristics. There is no evidence in No. 2 and No. 3 Zones of the extended period of mineralization recognized in the large shear zones. Various sections of these veins show distinct and different parts of the general sequence of mineralization and it appears the openings must have been accessible for relatively brief and critical periods.

No. 2 Zone

Banded carbonates, including some rhodochrosite, compose parts of the vein. Pitchblende occurs as seams and botryoidal crusts, and a few sections are rich in silver. Hematite, chalcopyrite, and Ni-Co minerals are common, and fluorite may be present. This zone shows no displacement and consists predominantly of tension fractures with minor chloritic shears. Strong quartz-hematite veins contain some of the pitchblende. Other shoots are sparsely mineralized zones in which pitchblende is spotted through the schist, accompanied by a few stringers of quartz and carbonate.

The metamorphism of the rocks has been especially intense along this zone so that locally the rock has abundant chlorite, magnetite, pyrite, and the other minerals of this association scattered through it. Chalcopyrite and galena are found disseminated in streaks and patches in the

country rock replacing pyrite of the pyrometasomatic

TABLE 6: Mineralogy and Paragenesis

(After Kidd and Haycock 1935)

PYROMETASOMATIC
- Magnetite
- Pyrite
- Arsenopyrite

HYDROTHERMAL STAGES

Type 1
- Pitchblende
- Quartz
- Safflorite - Rammelsbergite
- Polydymite
- Gersdorffite
- Glaucodot
- Hematite
- Molybdenite

Type 2
- Smaltite - Chloanthite - Quartz - Hematite
- Ni-skutterudite and Skutterudite
- Cobaltite
- Native bismuth
- Witherite
- Unknown 1

Type 3
- Pyrite, Arsenopyrite, Hematite, Native
- Bismuth, Unknown 1
- Lollingite
- Unknown 5
- Dolomite
- Barite
- Sphalerite
- Galena
- Tetrahedrite
- Freibergite
- Bornite
- Chalcopyrite
- Unknown 2
- Chalcocite
- Manganese carbonate

Type 4
- Stromeyerite
- Jalpaite
- Argentite
- Hessite
- Native silver

SUPERGENE STAGE
- Argentite ?
- Native silver ?
- Covellite
- Alteration products

suite. Chalcopyrite and galena also occur in cracks in pitchblende. Native silver is present at several places, especially in the northeast section of the zone, where it occurs in rhodochrosite and is associated with chalcopyrite and galena. Native bismuth occurs with the Ni-Co minerals. Niccolite is associated with rhodochrosite in the northeast end of the zone. Supergene alteration is extensive near the surface.

No. 3 Zone

Although this zone resembles No. 2 in that vein material is scarce, it has some similarities to the No. 1 Zone. It is a single vein (actually several brecciated discontinuous fractures as previously mentioned) rather than a stockwork. Pitchblende lenses with brown quartz occurs in the shear zone. Some pitchblende is disseminated with chalcopyrite; and occasional isolated masses of pitchblende also occur. The shearing apparently post-dates the pitchblende lenses that occur in tension fractures. White quartz, with occasional vugs and specks of copper minerals, cements the breccia. Comb quartz and Co-Ni veins are present and one of these cuts a pitchblende lens. In as much as quartz has been deposited on the Co-Ni minerals it is apparent that some quartz is later than these.

The walls of the country rock and horses are altered from greenish-grey to brick-red suggesting strongly oxidizing solutions.

Kidd and Haycock (1935) have identified forty metallic minerals and several nonmetallic minerals from the Eldorado Mine. Some are of supergene origin but most are hypogene (including the pyrometasomatic suite). Table 6 gives the minerals they identified in paragenetic sequence.

MINERALOGY OF THE NO 2 ZONE

The mineralogy of the No. 2 Zone is complex, in that a large number of minerals are present and several of these are rare bismuth sulfosalts. For this study twelve samples were obtained for an examination. From these 17

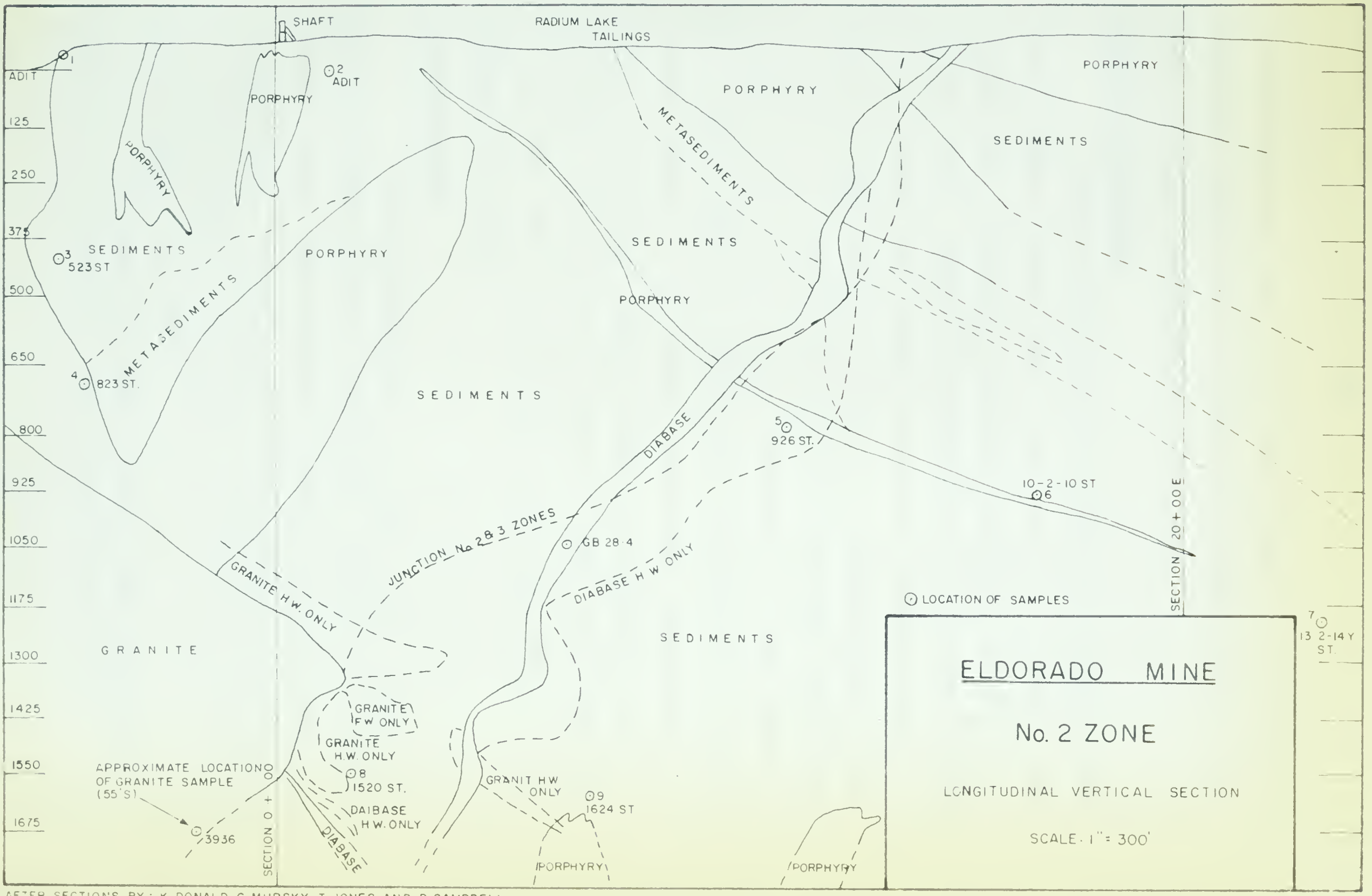


AFTER SECTIONS BY: K.DONALD, G.MURSKY, T. JONES AND D.CAMPBELL.

FIGURE 7

polished sections were prepared and studied to determine the assemblage present and to attempt an interpretation of the genesis of the mineralization.

Location of Samples

Twelve samples were available for study by the writer. Nine samples were obtained from the Eldorado geological staff through the Geology Department, University of Alberta. These samples are numbered 1 to 9 and are located on the vertical longitudinal section of the No. 2 Zone, Figure 7. One sample (No. GB.28.3), obtained from G. Hunt, is typical of hydrothermally altered wall rock. The exact location is not known, but is believed to be from the No. 2 ore - zone. Sample No. 1812, from 310 sub-drift, is one of several donated to the Geology Department, University of Alberta, by Preboy. Another sample was donated to the Department of Geology by E. Walli in 1936. The sample is No. 4557 and comes from the No. 2 Zone, 1212 stope of the Eldorado Gold Mines.

Identification

Seventeen polished sections of the samples were made for mineralographic examination. Minerals were identified by colour, polarization properties, hardness, and textural habit. Confirmation of identification was made by the X-ray diffraction technique. Both 57.3 mm. and 114.5 mm. powder cameras were used.

Vaseline was used to hold a small amount of sample on a glass fibre. The glass fibres were not

amorphous as expected but showed a certain amount of ordering. For this reason cristobalite lines were obtained on X-ray photographs when small quantities of sample were used. When the fibre was covered with sample, no cristobalite lines were obtained. The 4.12 Å and 3.72 Å d-spacings were the cristobalite lines identified.

Measurements of the X-ray patterns of the minerals were made with a viewer. The Index to the X-ray powder data file (1957 and 1960) were used to determine the minerals.

Minerals Present

The study indicates that the following types of compounds are present: oxides of iron and uranium; arsenides and sulfarsenides of nickel, cobalt, and iron; a sulfosenide of bismuth; sulfides of iron, zinc, lead, copper, and other elements; bismuth sulfosalts of silver, lead, and copper; and native bismuth. Quartz and dolomite were the only nonmetallic minerals found in the samples examined.

Oxides

Magnetite, hematite, and pitchblende are the metallic oxides present.

Magnetite ($Fe_3O_4$): The colour in hand specimen is iron-black and the colour when seen in polished section is dark-grey. The mineral is isotropic, hard, and strongly magnetic. Crossed-nicols shows the mineral is istropic. Magnetite occurs only in sample GB.28.3.

Hematite ($Fe_2O_3$); Hematite occurs as a finely disseminated mineral with pitchblende in massive and comb quartz. Most

of the hematite mineralization gives a red internal reflection but some occurrence of a medium-grey to grey-white specularite were observed. The mineral is hard and strongly anisotropic. One sample was X-rayed, and identified as hematite.

Pitchblende ($UO_2$ to $U_3O_8$): Study under the microscope indicates the presence of four types of pitchblende, designated types 0,1,2,3. The differences appear to be due to different states of oxidation.

Pitchblende 0 and 2 ($UO_2$): Pitchblende 0 and Pitchblende 2 are similar, and are differentiated because pitchblende 2 is younger than pitchblende 0. It is therefore not possible to determine which is present when only one occurs. The megascopic colour is a dark-grey with a 'pitchy' lustre. A polished surface under the microscope is grey. The hardness is intermediate (barely scratched with steel). Most of the material is isotropic, however, in one location it was observed to anisotropic with faint internal reflections noted. This mineral was X-rayed and it gave a pitchblende pattern corresponding closely to that shown on card number 9-174 of the X-ray powder data file (1957 and 1960). The data indicates that the mineral is tetragonal gamma uranium di-oxide ($UO_{2.32 - 0.01}$). One sample of isotropic pitchblende, probably pitchblende 2, was also X-rayed. The lines obtained were weak but discernable, and are shown on Table 7.

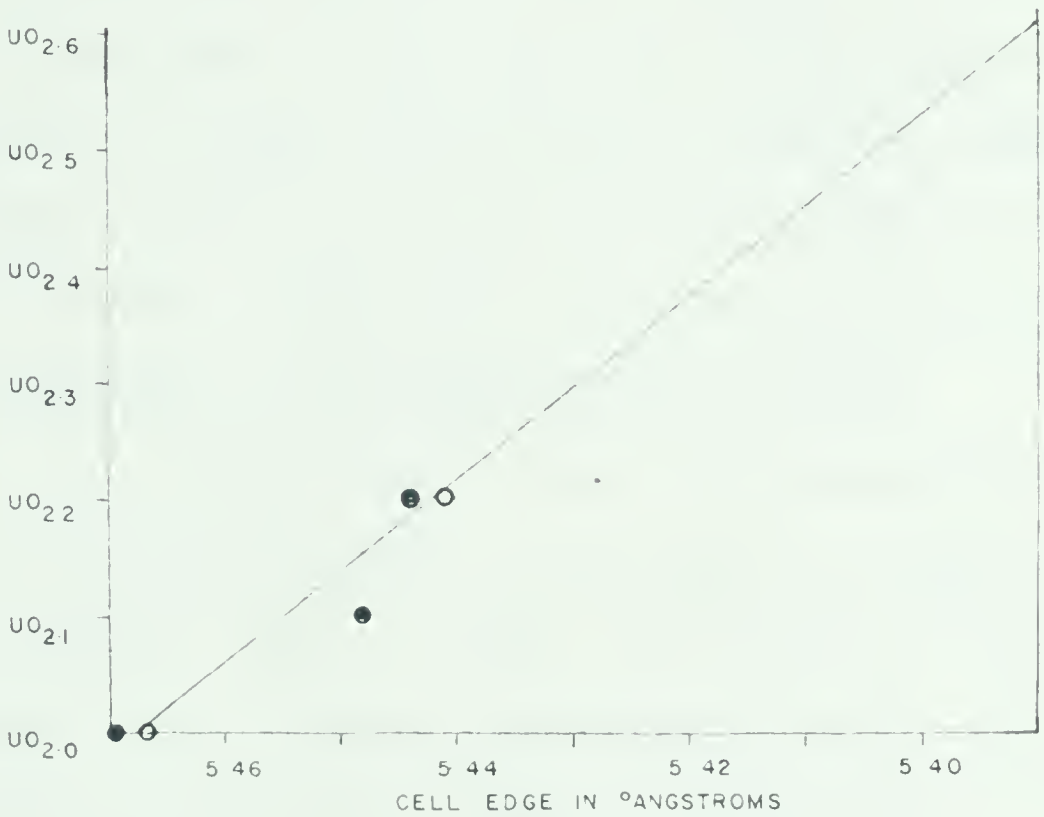
UO2·6
UO2 5
UO2 4
UO2·3
UO2 2
UO2·1
UO2·0
5 46
5 44
5 42
5 40
CELL EDGE IN °ANGSTROMS

FIGURE 8

TABLE 7

PITCHBLENDE 2 X-RAY DATA

| dÅ | I+ | hkl |
|---|---|---|
| 3.15 | 100 | (111) |
| 2.72 | 50 | (200) |
| 1.92 | 50 | (220) |

+ Intensities in this pattern and following patterns are visual estimations.

The average cell dimension determined from the three lines is 5.455 Å. Brooker and Nuffield (1952) related the state of oxidation to the cell size. The unit cell edge of 5.45 Å, as in this case, gives the state of oxidation as $UO_{2.1}$ (Figure 8). Wasserstein (1951), however, suggests that the decrease in cell edge from 5.47 Å for $UO_2$ is due to radioactive decay. Later the pitchblende age of deposition will be determined using Wasserstein's method.

Pitchblende 1 and 3 (approximately $U_3O_8$): The colour in hand specimen is dark-grey to black and the colour of a polished section under a microscope is medium-grey. The mineral can be readily scratched by steel. It is isotropic as were pitchblendes 0 and 2, respectively. Pitchblende 1 and 3 are therefore the same and are differentiated only in their association. The exact composition is not known but believed to be close to $U_3O_8$.

Pitchblende 4 ($UO_2$): The colour is light-grey and the lustre metallic, and it is light-grey when viewed in polished section. The mineral is hard and isotropic. Pitchblende 4 was X-rayed and the following data shown in Table 8 were obtained.

TABLE 8

PITCHBLENDE 4 X-RAY DATA

| dÅ | I | hkl | dÅ | I | hkl |
|---|---|---|---|---|---|
| 3.16 | 100 | (111) | 1.05 | 40 | (511) |
| 2.72 | 80 | (200) | - o.982 | 5 | |
| 1.93 | 90 | (220) | 0.967 | 20 | (440) |
| 1.64 | 85 | (311) | 0.927 | 30 | (531) |
| 1.57 | 30 | (222) | 0.911 | 10 | (600) |
| 1.36 | 10 | (400) | 0.865 | 20 | (620) |
| 1.25 | 60 | (331) | 0.834 | 5 | (533) |
| 1.22 | 50 | (420) | 0.822 | 5 | (622) |
| 1.11 | 40 | (422) | 0.800 | 1 | (444) |
| | | | - Unknown | | |

The average cell dimensions determined from all the lines is 5.47 Å. This cell size indicates no oxidation or radioactive decay thus the material has a composition of $UO_2$ (Figure 8).

Arsenides and Sulfarsenides

Five minerals of this group have been identified. they are niccolite, rammelsbergite, gersdorffite, glaucodot, and skutterudite.

Niccolite (NiAs): The colour in hand specimen is coppery-pink, and the colour in polished section is coppery-pink to yellow. The mineral is hard and strongly anisotropic. Table 9 shows a typical niccolite pattern.

TABLE 9

NICCOLITE X-RAY DATA

| dÅ | I | | hkl | dÅ | I | | hkl |
|---|---|---|---|---|---|---|---|
| 3.12 | 30 | | (100) | - 1.21 | 5 | | |
| - 2.83 | 10 | | | 1.18 | 5 | | |
| 2.65 | 100 | | (101) | 1.15 | 40 | th | (211) |
| 2.50 | 45 | th | | 1.07 | 65 | | (212) |
| 2.35 | 10 | | | 1.06 | 10 | | |
| 2.17 | 10 | | | 1.04 | 25 | | (300) |
| - 2.01 | 5 | | | 1.03 | 60 | | (114) |
| 1.96 | 95 | | (102) | - 1.01 | 5 | | |
| - 1.86 | 30 | | | - 1.00 | 5 | | |
| 1.80 | 85 | | (110) | - 0.980 | 1 | | |
| - 1.73 | 5 | | | 0.969 | 40 | | (213) |
| 1.63 | 5 | | | 0.949 | 10 | | (105) |
| - 1.58 | 5 | | | - 0.924 | 10 | | |
| 1.49 | 55 | | (201) | 0.905 | 20 | th | (220) |
| 1.48 | 55 | | (103) | - 0.887 | 5 | | |
| - 1.43 | 5 | | | 0.858 | 20 | | (311) |
| - 1.37 | 1 | | | 0.847 | 10 | | (222, 205) |
| 1.33 | 70 | | (202) | 0.821 | 30 | | (312) |
| - 1.30 | 5 | | | 0.810 | 20 | | (106) |
| - 1.28 | 5 | | | 0.804 | 30 | | (304) |
| 1.25 | 25 | | (004) | - Unknown | | | |

th = thick

Niccolite is hexagonal, with cell dimensions $a_o$ = 3.62 Å and $c_o$ = 5.0$^3$ Å.

Rammelsbergite ($NaAs_2$): This mineral is a very bright white in the hand specimen and a brighter white when viewed under the microscope. The mineral is hard and strongly anisotropic. Several samples were X-rayed, and all gave similar patterns. The best pattern is shown in Table 10.

TABLE 10

RAMMELSBERGITE X-RAY DATA

| dA° | I | hkl | dA° | I | hkl |
|---|---|---|---|---|---|
| 3.63 | 10 | (011) | 1.40 | 1 | (131) |
| 2.98 | 10 | (101) | 1.36 | 1 | (221) |
| 2.80 | 80 | (110) | 1.30 | 1 | (132) |
| 2.55 | 100 | (111) | 1.27 | 1 | (222) |
| 2.47 | 100 | (012) | 1.25 | 1 | (213) |
| 2.39 | 7 | (020) | 1.23 | 4 | (024) |
| 2.20 | 5 | (021) | 1.20 | 1 | (040) |
| 2.01 | 7 | (112) | 1.15 | 1 | (133, 231, 301) |
| 1.86 | 75 | (121) | 1.13 | 1 | (223, 301) |
| 1.82 | 7 | (013) | 1.11 | 1 | (311, 204) |
| 1.71 | 7 | (200) | 1.08 | 1 | (232, 214) |
| 1.69 | 7 | (103) | 1.06 | 2 | (115, 034) |
| 1.63 | 8 | (122) | 1.05 | 1 | (142) |
| 1.59 | 8 | (113, 211) | 1.03 | 1 | (025, 321) |
| 1.54 | 3 | (031) | 1.02 | 2 | (134) |
| 1.48 | 3 | (202) | 1.01 | 2 | (043, 224) |
| 1.44 | 4 | (212) | 0.975 | 1 | (143, 241) |

Rammelsbergite is orthorhombic with cell dimensions of $a_o = 3.43$ Å, $b_o = 4.82$ Å, and $c_o = 5.94$ Å.

Gersdorffite (NiAsS); The colour of gersdorffite is similar to rammelsbergite. However, the colour in polished is a less intense white, tending toward a greyish white. The mineral is hard and isotropic. The X-ray pattern is as follows in Table 11. From these data the calculated cell edge is 5.61 Å.

TABLE 11

GERSDORFFITE X-RAY DATA

| dÅ | I | hkl | dÅ | I | hkl |
|---|---|---|---|---|---|
| 2.81 | 85 | (200) | 1.49 | 60 | (321) |
| 2.50 | 100 | (210) | 1.22 | 10 | (421) |
| 2.28 | 90 | (211) | 1.19 | 10 | (332) |
| 1.98 | 45 | (220) | 1.07 | 20 | (511) |
| 1.86 | 5 | (221) | 1.04 | 15 | (521) |
| - 1.75 | 7 | | 0.992 | 20 | (440) |
| 1.69 | 95 | (311) | 0.964 | 10 | (600, 442) |
| 1.62 | 2 | (222) | 0.909 | 10 | (611, 532) |
| 1.55 | 60 | (320) | - Unknown | | |

Glaucodot ( (Co,Fe)AsS ): The mineral is light-grey to white in the hand specimen, and a light-pinkish-grey colour in polished section. The hardness is intermediate (barely scratched with steel), and the mineral is weakly anisotropic. Several X-rays were taken of different samples. The best pattern gave the information shown in Table 12.

TABLE 12

GLAUCODOT X-RAY DATA

| dÅ | I | hkl | dÅ | I | hkl |
|---|---|---|---|---|---|
| - 3.89 | 100 | | -1.90 | 20 | |
| 3.56 | 5 | (061) | 1.81 | 70 | (2.12.1) |
| - 3.46 | 5 | | 1.77 | 10 | (063) |
| - 3.35 | 40 | | 1.73 | 10 | (400,083) |
| - 3.22 | 30 | | 1.49 | 20 | |
| - 3.07 | 30 | | 1.48 | 10 | |
| 2.97 | 10 | | 1.41 | 20 | |
| 2.86 | 10 | (0.10.0) | 1.39 | 10 | |
| 2.78 | 70 | (260) | 1.32 | 5 | |
| 2.48 | 80 | (261) | 1.30 | 5 | |
| 2.39 | 60 | (280, 062) | 1.27 | 5 | |
| - 2.29 | 20 | | 1.25 | 10 | |
| 2.13 | 60 | (222) | 1.22 | 10 | |
| 2.02 | 70 | (2.10.1) | 1.19 | 10 | |
| 1.97 | 30 | (262) | 1.15 | 10 | |

- Unknown

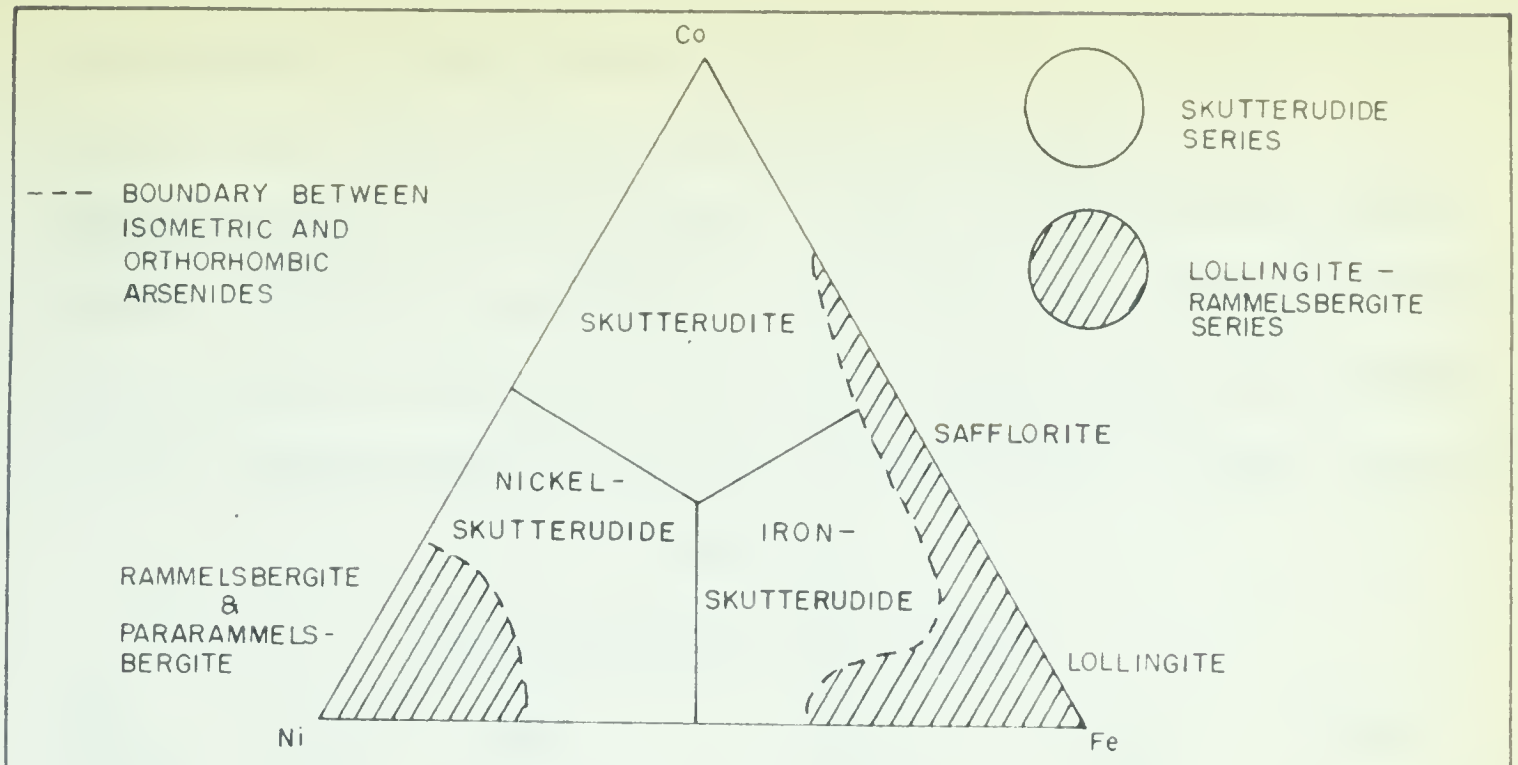


FIGURE 9 RELATIONSHIP AND NOMENCLATURE OF THE HIGHER ARSENIDES OF Co, Ni, AND Fe.

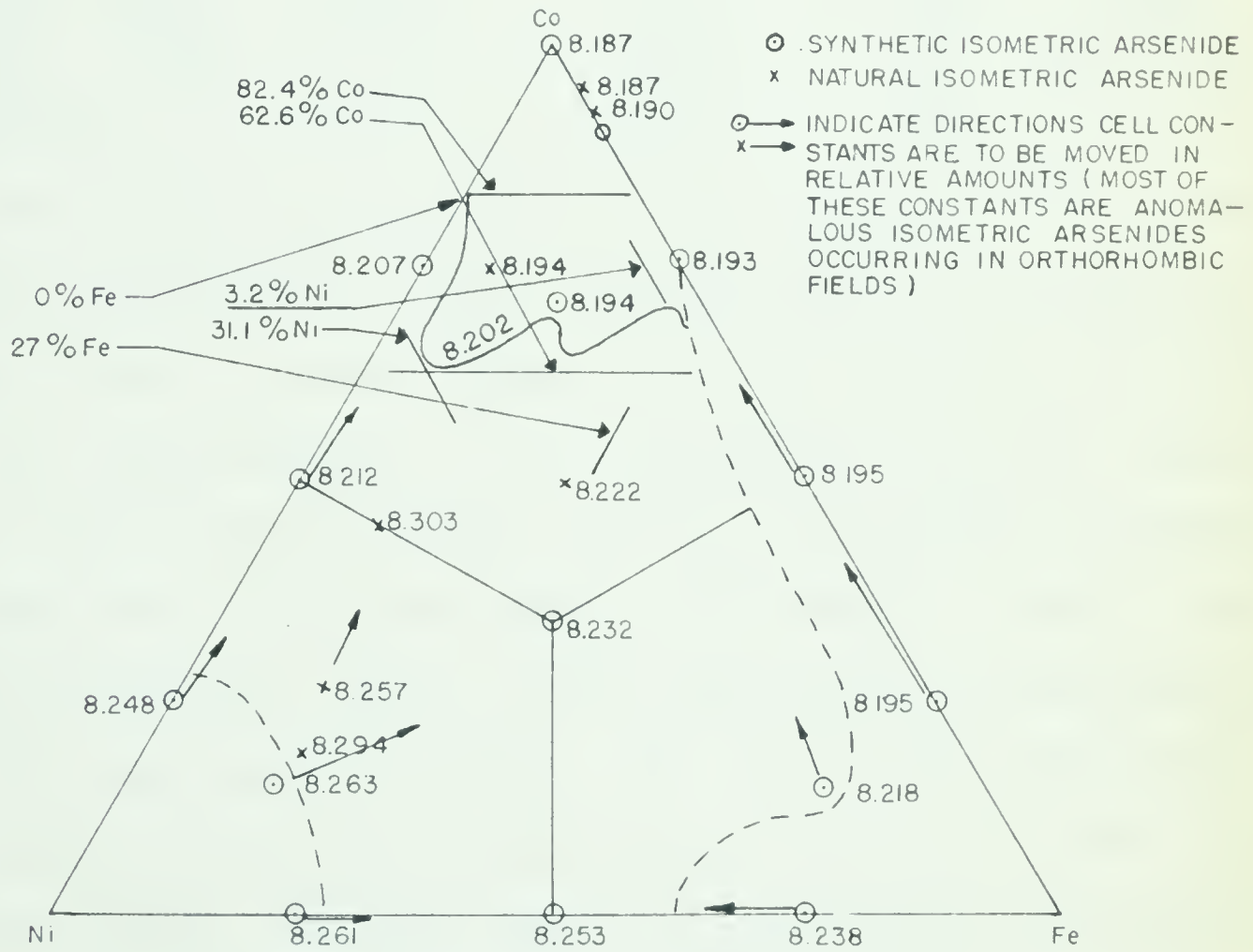


RELATIONSHIP BETWEEN LATTICE CONSTANT AND COBALT – NICKEL – IRON RATIO IN THE ISOMETRIC ARSENIDES.

FIGURE 10

The mineral is orthorhombic and the cell dimensions are as follows: $a_o$= 6.84 Å, $b_o$= 28.65 Å, and $c_o$= 5.82 Å.

Skutterudite ( $(Co,Ni,Fe)As_3$ ): The microscopic and megascopic colours are similar to rammelsbergite and gersdorffite. The mineral is hard and isotropic. One sample was X-rayed and the skutterudite pattern shown in Table 13 was obtained:

TABLE 13

SKUTTERUDITE X-RAY DATA

| dÅ | I | hkl | dÅ | I | hkl |
|---|---|---|---|---|---|
| - 12.89? | <1 | | - 2.02 | 10 | |
| 4.12 | 80 | (200) | - 2.01 | 10 | |
| 3.34 | 20 | (211) | 1.92 | 10 | (411, 330) |
| 2.88 | 60 | (220) | - 1.88 | 10 | |
| - 2.80 | 10 | | 1.82 | 20 | (420) |
| 2.65 | 10 | | 1.75 | 10 | (332) |
| 2.59 | 100 | (310) | 1.67 | 20 | (422) |
| 2.49 | <1 | | 1.61 | 20 | (431, 510) |
| 2.19 | 30 | (321) | - 1.53 | 5 | |
| - Unknown | | | -1.48 | <1 | |

In this study a modified form of the classification of the higher arsenides of cobalt, nickel, and iron proposed by Holmes (1947) is used. Figure 9 is a triangular presentation of the classification of the isomorphous isometric triarsenides and the discontinuous series of isomorphous orthorhombic diarsenides. The dashed line is literally a 'fence' between the two distinct series. The orthorhombic diarsenides occur in the cross-hatched fields. The solid lines within the triangle are arbitrary divisions in the isometric and orthorhombic fields. Mineral names for these areas are indicated. Smaltite and chloanthite are discredited heterogeneous isometric diarsenides. Skutterudite and nickel-skutterudite are, respectively, the proper names for smaltite and

chloanthite. Isometric diarsenides do not exist. The composition of the isometric triarsenides examined in this study is determined by using Holmes' relationship between lattice constant and cobalt-nickel-iron ratio triangular diagram shown in Figure 10. The calculated edge is 8.202 Å and the 8.202 contour line is shown on the diagram. The mineral is skutterudite with an approximate composition of 72.50 percent Co, 17.15 percent Ni, and 13.50 percent Fe. These percentages are averages of the maximum and minimum possible for each element for a skutterudite with $a_o$= 8.202 Å.

Sulfoselenide

Guanajuatite ($Bi_2(Se,S)_3$): This is a silver-grey mineral. The mineral was not examined microscopically and occurred as needles in a vug in sample No. 1812. X-ray data shown in Table 14 were obtained:

TABLE 14

GUANAJUATITE X-RAY DATA

| dÅ | I | hkl | dÅ | I | hkl |
|---|---|---|---|---|---|
| 3.56 | 100 | (130) | - 1.04 | 10 | |
| 3.15 | 100 | (230, 121, 211) | - 1.02 | 20 | |
| 2.86 | 90 | (040, 221) | -1.01 | 5 | |
| - 2.82 | 45 | | - 0.988 | 15 | |
| 2.57 | 60 | (240) | - 0.973 | 10 | |
| 2.47 | 45 | (231, 321) | - 0.961 | 10 | |
| 2.34 | 20 | (041) | - 0.933 | 5 | |
| 2.25 | 50 | (141, 340) | - 0.922? | 5 | |
| 2.14 | 50 | (241, 421) | -0.917 | 10 | |
| 2.04 | 30 | (002) | - 0.906 | 10 | |
| 1.98 | 65 | (341, 431) | - 0.897 | 10 | |
| 1.94 | 30 | (060)? | - 0.893 | 10 | |
| 1.87 | 30 | (610) | - 0.880 | 10 | |
| - 1.79 | 10 | | - 0.871 | 20 | |
| 1.75 | 70 | (351, 132) | - 0.863 | 10 | |
| 1.63 | 10 | | - 0.856 | 30 | |
| 1.58 | 60 | | - 0.842 | 10 | |
| 1.51 | 45 | | - 0.832 | 15 | |
| 1.47 | 10 | | - 0.822 | 10 | |
| 1.41 | 55 | | - 0.816 | 25 | |
| 1.37 | 10 | | - 0.814 | 25 | |
| 1.36 | 10 | | - 0.810 | 25 | |
| 1.33 | 15 | | - 0.806 | 10 | |
| 1.30 | 10 | | - 0.804 | 10 | |
| 1.27 | 20 | | - 0.799 | 10 | |
| - 1.26 | 5 | | - 0.797 | 10 | |
| - 1.23 | 10 | | - 0.794 | 10 | |
| 1.21 | 10 | | - 0.791 | 10 | |
| - 1.17 | 20 | | - 0.787 | 10 | |
| - 1.16 | 20 | | - 0.785 | 10 | |
| -1.13 | 10 | | - 0.782 | 10 | |
| - 1.12 | 20 | th | - 0.780 | 10 | |
| - 1.08 | 10 | | - 0.778? | 1 | |
| - 1.06 | 10 | | - 0.777? | 1 | |
| - Unknown | | | | | |

The mineral is orthorhombic and the calculated cell dimensions are $a_o$ = 11.17 Å, $b_o$ = 11.47 Å, and $c_o$ = 4.08 Å.

Iron sulfides

Pyrite, marcasite, and pyrrhotite are the three iron sulfides found in this study.

Pyrite ($FeS_2$): A light brass-yellow mineral was identified as pyrite. The colour when the mineral is viewed under the

microscope is lighter than the colour in hand specimen. The X-ray pattern shown in Table 15 was obtained and identified as that of pyrite.

TABLE 15

PYRITE X-RAY DATA

| dÅ | I | hkl | dÅ | I | hkl |
|---|---|---|---|---|---|
| 4.56 | 5 | | 1.21 | 20 | (420) |
| - 4.36 | 5 | | 1.18 | 5 | (421) |
| - 3.89 | 10 | | - 1.17 | 5 | |
| - 3.31 | 5 | | 1.15 | 10 | (332) |
| 3.13 | 30 | (111) | - 1.14 | 5 | |
| - 3.00 | 5 | | - 1.12 | 5 | |
| - 2.86 | 10 | | 1.10 | 10 | (422) |
| 2.70 | 80 | (200) | - 1.08 | 5 | |
| 2.42 | 70 | (210) | - 1.06 | 5 | |
| - 2.15 | 70 | | - 1.05 | 10 | |
| - 2.14 | 5 | | 1.04 | 30 | (511) |
| 1.91 | 70 | (220) | - 1.03 | 10 | |
| - 1.87 | 10 | | - 1.02 | 10 | |
| 1.63 | 20 | (311) | - 1.01 | 10 | |
| - 1.59 | 5 | | 1.00 | 20 | (432) |
| 1.56 | 25 | (222) | - 0.997 | 10 | |
| 1.50 | 25 | (230) | 0.990 | 10 | (521) |
| 1.45 | 30 | (321) | - 0.974 | 10 | |
| - 1.42 | 5 | | 0.958 | 30 | (440) |
| - 1.39 | 5 | | - 0.929 | 5 | |
| - 1.37 | 10 | | - 0.920 | 5 | |
| - 1.33 | 5 | | - 0.909 | 5 | |
| - 1.31 | 5 | | 0.902 | 10 | (600) |
| - 1.27 | 10 | | 0.879 | 10 | (611) |
| 1.24 | 15 | (331) | 0.827 | 10 | (533) |
| - Unknown | | | 0.807 | 1 | (622) |

The average unit cell size of all the lines is $a_o = 5.42$ Å.

Marcasite ($FeS_2$): The megascopic colour is a very light bronze-yellow and the microscopic colour is a lighter shade. The mineral is hard and in as much as it is orthorhombic it exhibits strong anisotropism. A very good marcasite X-ray pattern was obtained. The d-spacings and visual intensities are as shown in Table 16.

TABLE 16

MARCASITE X-RAY DATA

| dÅ | I | dÅ | I | dÅ | I |
|---|---|---|---|---|---|
| - 4.65 | 50 | - 2.17 | 5 | 1.51 | 10 |
| - 3.70 | 40 | 2.06 | 5 | 1.46 | 5 |
| 3.45 | 100 | - 1.98 | 5 | 1.43 | 30 |
| - 3.00 | 20 | 1.92 | 60 | 1.22 | 1 |
| 2.70 | 80 | - 1.87 | 5 | 1.19 | 5 |
| - 2.63 | 30 | - 1.79 | 5 | 1.03 | 10 |
| - 2.52 | 10 | 1.76 | 70 | 0.991 | 20 |
| 2.41 | 70 | 1.73 | 20 | 0.965 | 5 |
| 2.32 | 70 | 1.69 | 40 | - 0.935 | 5 |
| 2.23 | 5 | 1.60 | 40 | - 0.877 | 5 |

- Unknown

Pyrrhotite ($Fe_{48.6}S_{51.4}$ to $Fe_{49.2}S_{50.8}$): The natural colour is bronze-yellow and the microscopic colour is a light bronze-yellow. The mineral is hard and strongly anisotropic. Two samples were X-rayed and both gave similar patterns. One of the patterns is shown in Table 17.

TABLE 17

PYRRHOTITE X-RAY DATA

| dÅ | I | hkl | dÅ | I | hkl |
|---|---|---|---|---|---|
| - 4.39 | 10 | | 2.21 | 40 | |
| - 3.85 | 70 | | 2.08 | 60 th | (102) |
| - 3.57 | 60 | | 1.92 | 65 th | |
| - 3.53 | 30 | | - 1.86 | 20 | |
| - 3.42 | 50 | | - 1.81 | 15 | |
| - 3.21 | 40 | | 1.76 | 65 | |
| 3.00 | 100 | | 1.73 | 20 | |
| 2.87 | 30 | | - 1.68 | 30 | |
| 2.70 | 80 | | - 1.66 | 5 | |
| - 2.57 | 5 | | 1.64 | 50 | |
| 2.49 | 20 | | 1.60 | 30 | |
| - 2.42 | 70 | | - 1.57 | 20 | |
| - 2.32 | 20 | | 1.50 | 40 th | |
| - 2.26 | 30 | | 1.43 | 20 th | |

- Unknown

The atomic percent Fe determined from curves published by Arnold (1962, p. 75) and Arnold and Reichen (1962, p. 106), is 49.2 percent for the above sample and 48.6 percent Fe for the other sample X-rayed. It is therefore apparent that the pyrrhotite is very near troilite (50 percent Fe).

Sulfides

In addition to the iron sulfides, sphalerite, galena, bornite, chalcopyrite, covellite, and stromeyerite are present.

Sphalerite (ZnS): The sphalerite is too fine-grained to see in hand specimen. The microscopic color is grey and is lighter than unoxidized pitchblende. The mineral is soft and isotropic and shows ruby-red internal reflection. An excellent sphalerite X-ray pattern was obtained, and the data are shown in Table 18.

TABLE 18

SPHALERITE X-RAY DATA

| | dÅ | I | hkl | dÅ | I | hkl |
|---|---|---|---|---|---|---|
| | 3.0909 | 100 | (111) | 1.2063 | 10 | (420) |
| | 2.6914 | 30 | (200) | 1.1817 | 10 | |
| - | 2.4622 | 10 | | 1.1032 | 70 | (422) |
| - | 2.0759 | 5 | th | 1.0411 | 50 | (511) |
| | 1.9064 | 100 | (220) | 0.95720 | 30 | (440) |
| | 1.6258 | 90 | (311) | 0.91500 | 55 | (531) |
| | 1.3503 | 45 | (400) | 0.85639 | 40 | (620) |
| | 1.2406 | 60 | (331) | 0.82655 | 20 | (533) |

- Unknown

The $a_o$ values for each line were plotted against the function described by Nelson and Riley (1944). The $a_o$ obtained by extrapolation to $\theta = 90^\circ$ is 5.4138 Å. The data used in making this extrapolation must be accurately determined as small

variations in reading the lines cause a significant variation in the extrapolated cell size. Since many of the sphalerite lines are thick, it is difficult to be certain what the exact reading is for each line and it was found that 0.2 mm. shrinkage of the photograph is a significant factor. Using the curve published by Skinner, Barton, and Kullerud (1959, p. 1041) the FeS content for 5.4138 Å is approximately 9 percent FeS.

Galena (PbS): In polished section the mineral is white, and it is soft and sectile. The polishing may develop scratches and triangular pits in the surface of the galena. Galena is generally isotropic but some shows anomalous weak anisotropism. The galena X-ray pattern is given in Table 19.

TABLE 19

GALENA X-RAY DATA

| dÅ | I | dÅ | I | dÅ | I |
|---|---|---|---|---|---|
| 3.43 | 100 | 1.79 | 50 | 1.36 | 5 |
| 2.97 | 95 | 1.71 | 25 | 1.33 | 7 |
| 2.10 | 90 | 1.48 | 5 | 1.21 | 6 |

Bornite ($Cu_5FeS_4$): The megascopic colour is brownish-bronze, and it tarnishes to a light-purple. In polished section it is pinkish-brown to orange, and tarnishes to a light purple. Under polarized light, bornite is generally isotropic, but in places shows an anomalous weak anisotropism. Some twinning is present which may have developed under stress and this may have strained the lattice enough to cause the anisotropism. Table 20 shows the X-ray data obtained.

TABLE 20

BORNITE X-RAY DATA

| dÅ | I | | dÅ | I | | dÅ | I |
|---|---|---|---|---|---|---|---|
| 3.22 | 40 | | 2.02 | 20 | | 1.43 | 10 |
| 3.13 | 40 | | 1.93 | 100 | | 1.34 | 10 |
| 2.84 | 30 | - | 1.88 | 5 | | 1.22 | 15 |
| 2.74 | 40 | - | 1.81 | 25 | | 1.12 | 20 |
| 2.43 | 55 | - | 1.74 | 30 | | 1.02 | 20 |
| - 2.31 | 20 | | 1.65 | 30 | | 1.00 | 5 |
| 2.15 | 25 | | 1.53 | 20 | | 0.929 | 5 |

- Unknown

Chalcopyrite ($CuFeS_2$): The megascopic and microscopic colour of chalcopyrite is brass-yellow. The mineral is soft and anisotropic. One sample was X-rayed and the pattern shown in Table 21 was obtained.

TABLE 21

CHALCOPYRITE X-RAY DATA

| dÅ | I | hkl |
|---|---|---|
| 3.03 | 100 | (112) |
| 2.60 | 1 | (020, 004) |
| - 2.08 | 5 | |
| 1.87 | 80 | (024) |
| 1.59 | 60 | (132) |
| 1.20 | 25 | (136, 143) |
| 1.07 | 30 | (244) |
| 1.01 | 25 | (152) |
| 0.958 | 5 | |

- Unknown

Chalcopyrite is tetragonal with cell dimensions of $a_o = 5.21$ Å and $c_o = 10.43$ Å.

Covellite (CuS): This mineral has not been seen in the hand specimen. The microscopic colour varies from an indigo-blue to an iridescent-orange or red. It is soft and anisotropic.

Stromeyerite ( $(Cu,Ag)_2S$ ): This mineral is too fine-grained in the hand specimen to be easily seen. The colour in polished section is a light-grey to almost white. The

mineral is soft, moderately sectile, and strongly anisotropic. An X-ray pattern is similar to A.S.T.M. (1957 and 1960) cards 2-0578 and 2-0694 but is distinct from either. The pattern, however, was identified as stromeyerite and the differences can be accounted for by the variations in Ag and Cu in the mineral. Table 22 shows the X-ray data.

TABLE 22

STROMEYERITE X-RAY DATA

| dÅ | I | dÅ | I | dÅ | I |
|---|---|---|---|---|---|
| - 4.17 | 100 | 1.99 | 10 | 1.44 | 45 |
| - 3.49 | 20 | 1.87 | 65 | - 1.36 | 10 |
| 3.06 | 70 | 1.83 | 10 | - 1.32 | 10 |
| 2.89 | 90 | 1.76 | 10 | 1.23 | 15 |
| - 2.66 | 30 | - 1.70 | 55 | - 1.09 | 10 |
| 2.55 | 75 | 1.64 | 5 | - 0.940 | 5 |
| 2.48 | 80 | - 1.60 | 10 | - 0.877 | 5 |
| 2.33 | 20 | 1.53 | 10 | - 0.831 | 5 |
| 2.20 | 5 | 1.49 | 35 | - 0.791 | |
| 2.09 | 10 | | | | |

- Unknown

Antimony sulfosalts

Tetrahedrite ( $(Cu,Fe,Ag,Pb,Zn)_{12}Sb_4S_{13}$ ): The mineral cannot be seen in the hand specimen as it is too fine-grained. In polished section it is a light grey colour and with crossed-nicols it appears isotropic. The hardness of the mineral is soft to intermediate. The X-ray data obtained are shown in Table 23.

TABLE 23

TETRAHEDRITE X-RAY DATA

| dÅ | I | dÅ | I | dÅ | I |
|---|---|---|---|---|---|
| 2.96 | 100 | 1.55 | 60 | 1.05 | 30 |
| 2.56 | 20 | 1.48 | 55 | 1.00 | 25 |
| 2.09 | 90 | 1.44 | 5 | 0.989 | 30 |
| 2.00 | 10 | 1.36 | 30 | 0.939 | 35 |
| 1.88 | 10 | 1.32 | 50 | 0.895 | 35 |
| 1.83 | 70 | 1.28 | 10 | 0.831 | 20 |
| 1.78 | 70 | 1.20 | 45 | 0.823 | 10 |
| 1.70 | 35 | 1.17 | 5 | 0.793 | 20 |
| 1.66 | 20 | - 1.14 | 40 | | |
| | | - Unknown | | | |

Bismuth sulfosalts

Two minerals that are commonly thought to be rare have been found to be rather common in the No. 2 Zone. They are schirmerite and Klaprothite.

Schirmerite ( $(Ag,Pb)_6Bi_4S_9$ ): The mineral is too fine-grained to observe in the hand specimen. Mineralographic examination indicates the following properties of this mineral: a very light purple-grey with weak pleochroism, soft, and very weakly anisotropic. Short (1940) does not report this mineral. Both Palache, Berman, and Frondel (1946) and the A.S.T.M. file (1957, 1960) report the mineral but fail to give the crystal system to which it belongs. Several samples were X-rayed and one of the patterns is given in Table 24.

TABLE 24

SCHIRMERITE X-RAY DATA

| dÅ | I | dÅ | I | dÅ | I |
|---|---|---|---|---|---|
| 3.00 | 100 | - 1.74 | 10 | 1.19 | 15 |
| 2.85 | 10 | - 1.73 | 5 | 1.12 | 10 |
| 2.75 | 15 | 1.69 | 30 | 1.09 | 10 |
| 2.59 | 40 | 1.56 | 50 | - 1.08 | 5 |
| - 2.49 | 5 | 1.50 | 20 | 1.05 | 20 |
| 2.44 | 20 | 1.46 | 20 | - 1.03 | 5 |
| 2.28 | 20 | - 1.42 | 5 | - 1.02 | 1 |
| 2.12 | 10 | - 1.39 | 5 | - 1.01 | 5 |
| 2.03 | 30 | 1.31 | 10 | - 0.998 | 10 |
| - 1.96 | 10 | 1.29 | 5 | - 0.958 | 10 |
| 1.90 | 20 | 1.27 | 5 | -0.940 | 5 |
| 1.83 | 75 | 1.24 | 15 | - 0.899 | 10 |
| 1.78 | 20 | 1.20 | 15 | | |
| - Unknown | | | | | |

Klaprothite ($Cu_6Bi_4S_9$): The natural colour of this mineral is grey. The mineralographic examination indicates the following properties: very light grey to white, soft, sectile, strongly anisotropic. These properties are similar to stromeyerite; and in fact cannot be distinguished from stromeyerite microscopically very readily. However, klaprothite develops a bright orange tarnish whereas stromeyerite does not seem to tarnish as quickly. Several samples were X-rayed. Table 25 shows an excellent pattern that was observed for one of the samples.

TABLE 25

KLAPROTHITE X-RAY DATA

| dÅ | I | dÅ | I | dÅ | I |
|---|---|---|---|---|---|
| - 3.47 | 40 | 1.59 | 30 | - 1.08 | 40 |
| 3.24 | 20 | 1.54 | 20 | - 1.04 | 10 |
| 3.07 | 100 | 1.50 | 20 | - 1.01 | 35 |
| 2.82 | 40 | 1.44 | 20 | - 0.990 | 20 |
| 2.66 | 95 | 1.41 | 20 | - 0.963 | 10 |
| - 2.47 | 40 | 1.39 | 20 | - 0.946 | 10 |
| 2.40 | 10 | - 1.35 | 25 | - 0.935 | 10 |
| 2.18 | 90 | - 1.32 | 20 | - 0.924 | 20 |
| 2.04 | 10 | - 1.30 | 10 | - 0.909 | 5 |
| 1.98 | 80 | - 1.27 | 30 | - 0.898 | 5 |
| - 1.92 | 30 | - 1.23 | 20 | - 0.890 | 20 |
| 1.90 | 30 | - 1.20 | 30 | - 0.871 | 10 |
| 1.81 | 60 | - 1.17 | 10 | - 0.862 | 10 |
| - 1.78 | 40 | - 1.15 | 10 | - 0.853 | 25 |
| 1.75 | 20 | - 1.13 | 10 | - 0.837 | 10 |
| 1.73 | 20 | - 1.10 | 10 | - 0.831 | 5 |
| 1.68 | 65 | - 1.09 | 10 | - 0.789 | 5 |
| - 1.64 | 40 | | | | |
| - Unknown | | | | | |

Bismuth (Bi)

The only native element identified is bismuth. The megascopic colour is coppery-silver, and the microscopic colour is creamy-white. The mineral is soft and very sectile. Perfect basal cleavage is perceptible. Distinct pleochrism and strong anisotropism are microscopic properties of this hexagonal mineral.

Nonmetallics

Quartz and dolomite are the dominant gangue minerals. Chlorite and biotite occur in some samples. Five or six perfect crystals of one mineral, occurring with copper minerals, were unidentified. The mineral is epidote, sphene, or zircon.

Supergene Uranium Minerals

Secondary uranium minerals were observed. They

were not identified, except pitchblende 4, because this study is involved primarily with the pypogene metallic minerals.

## MODE OF OCCURRENCE AND PARAGENESIS

The textural relationships of the minerals will be described in paragenetic sequence. Some departure from this sequence will of necessity take place when a mineral has been deposited at more than one time. The determinants employed in developing the sequence of deposition are the generally accepted criteria of superposition, replacement, and veining plus, in some cases, a knowledge of phase relationships.

### Magnetite

Magnetite was one of the earliest minerals to be deposited. Kidd and Haycock (1935, p. 905) have reported rare occurrences in the southwest end of No. 2 Zone. The minerals occurs in the country rocks, dominantly bordering granodiorite and the ore zones. In this study, magnetite was seen only in sample No. GB.28.3. Here, it is massive and is associated with very coarse (one-half inch) biotite. Plate 4, Figure 1, shows early magnetite completely enclosed by later sulfide mineralization.

### Quartz

The dominant early gangue is a massive quartz. This is followed by comb quartz which has filled openings in the early massive variety. Plate 5, figure 8, shows a typical example of the comb quartz occurrences. Both forms of quartz occurs in all the samples. Quartz veinlets,

PLATE 4

FIGURE 1: Photomicrograph of sample GB.28.3. Magnetite medium-grey - mag) replaced by gangue (black) and enclosed by pyrrhotite (white - po). Sphalerite (grey - sp) exsolution veinlets in pyrrhotite. x625

FIGURE 2: Photomicrograph of sample 7. Specular hematite (white - spec) in gangue (quartz). x255

FIGURE 3: Photomicrograph of sample 3. Oriented specularite (white - spec) in quartz-carbonate gangue. x625

FIGURE 4: Photomicrograph of sample 2. Hematite spherules (hem), originally goethite, in carbonate gangue. x255

FIGURE 5: Photomicrograph of sample 9, showing massive quartz (q) being replaced by pitchblende 0 and 1 (p). Most of pitchblende 0 (white) has been oxidized to pitchblende 1 (medium grey). x100

FIGURE 6: Photomicrograph of sample 3. Similar to figure 5. Pitchblende 0 (white - p) has been oxidized to pitchblende 1 (medium grey - p). Dolomite (dol) has replaced pitchblende 1. x255

FIGURE 7: Photomicrograph of sample 8 which shows similar quartz (q)-pitchblende 1 (p) relationship as figure 5. x40

FIGURE 8: Photomicrograph of sample 7. Pitchblende veinlet (p), that has been largely oxidized, in quartz (q). x40

PLATE 4

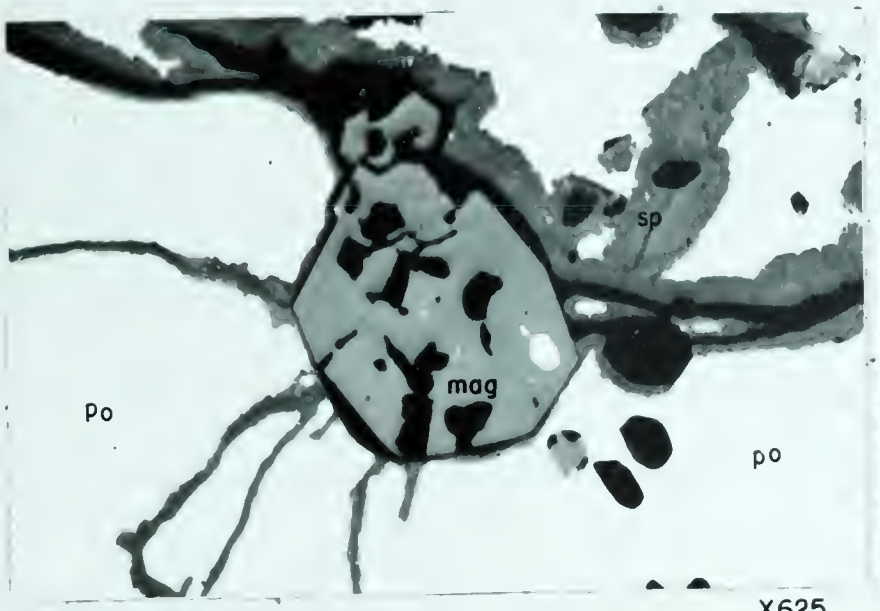


1 X625


2 X255


3 X625

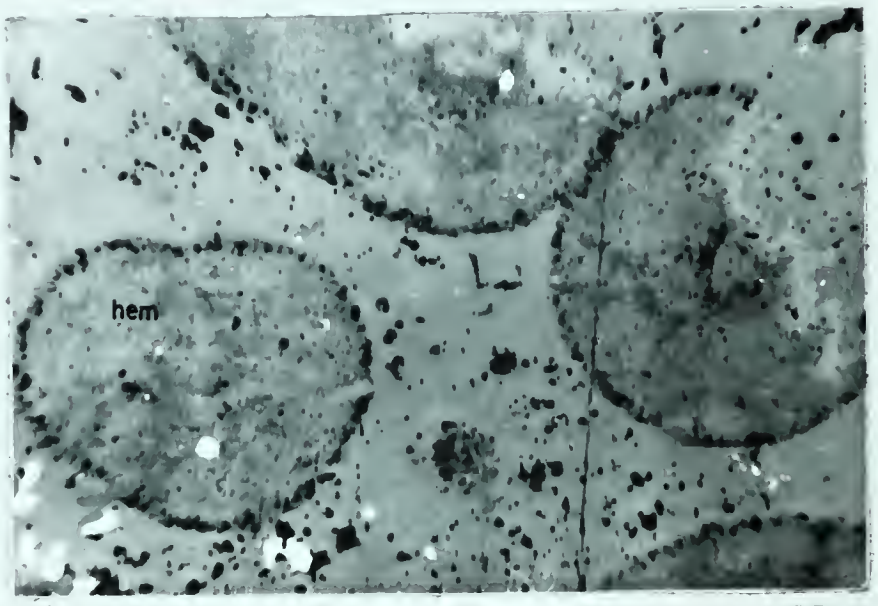


4 X255

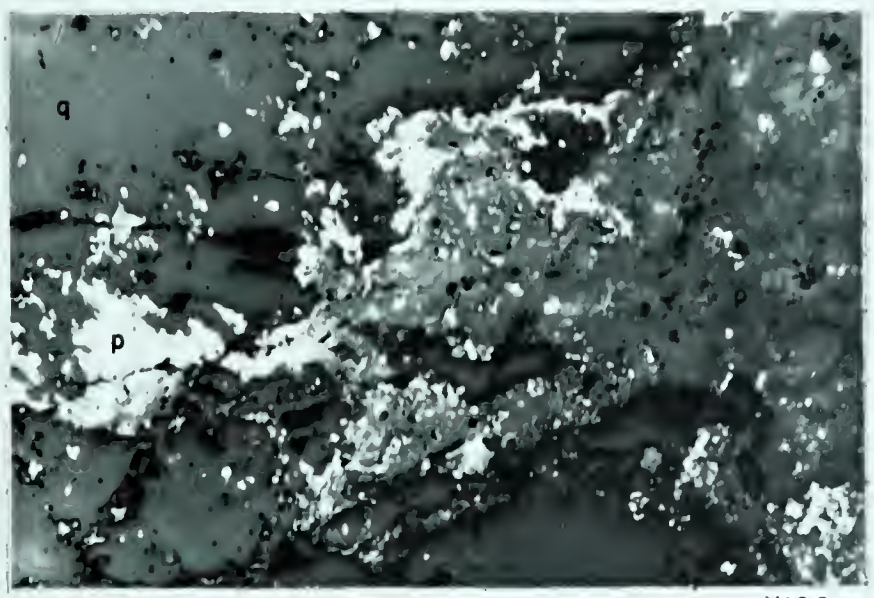


5 X100

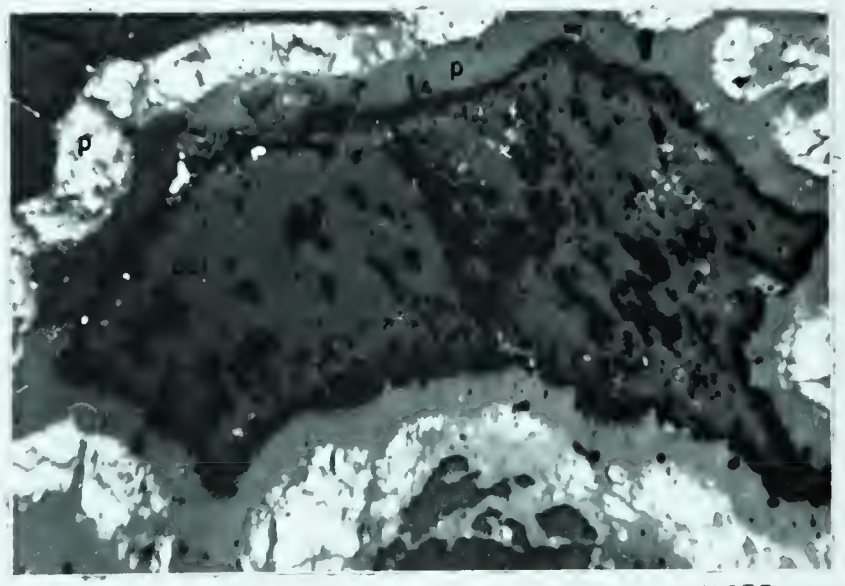


6 X 255

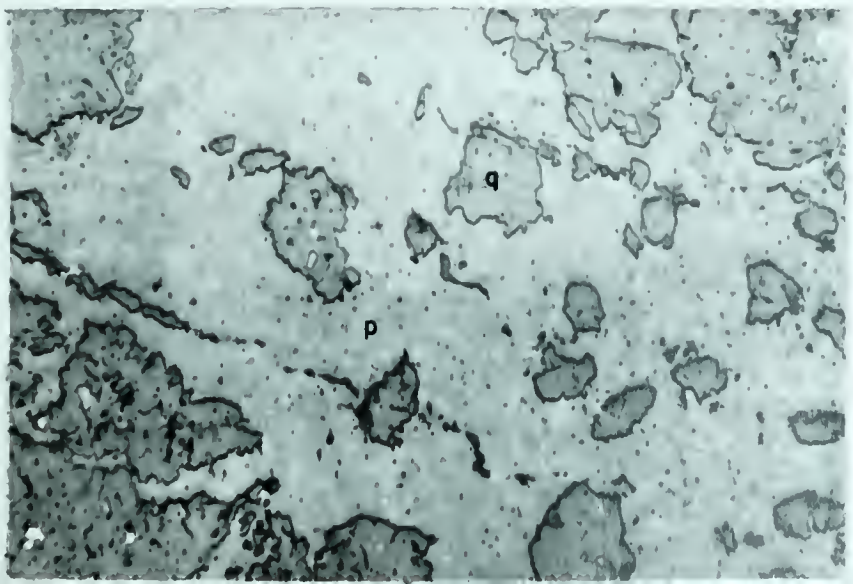


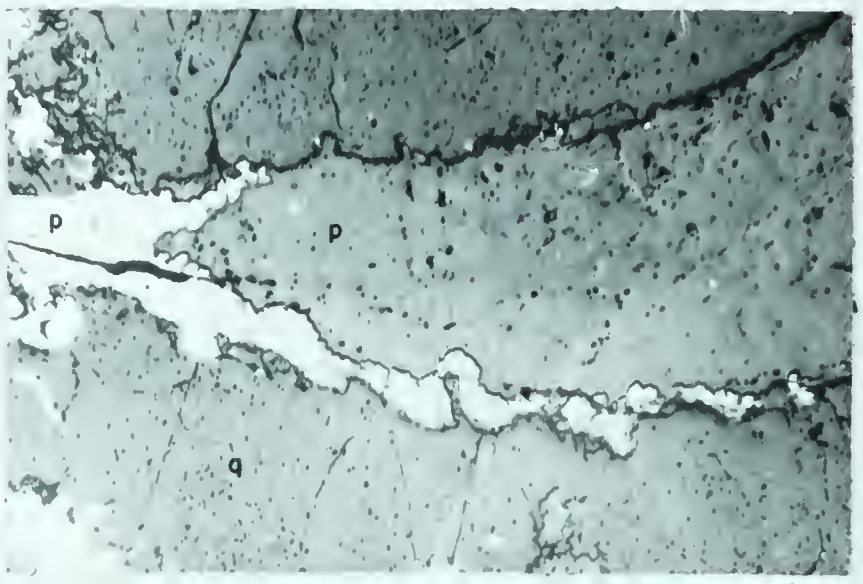

which cut the early massive quartz, are also common. The veinlets can be quartz-filled or contain comb quartz fillings in microscopic fractures. Plate 2 (frontispiece 2) is an example of a quartz-filled veinlet, cutting early massive quartz.

Hematite

Precipitation of disseminated $Fe_2O_3$ in massive quartz began early. It is common in all samples. Less common forms are specularite and botryoidal hematite. Specularite occurs in samples 3, 7, and 8. Exact relationship to the arsenides and younger mineralization is not known, but specularite may be in places later than the arsenides and may even be later than dolomite. Specular hematite is definitely younger than comb quartz (see Plate 4, Figure 2). Some blades of specularite show a parallel orientation and were possibly aligned by a stress field. Plate 4, Figure 3, shows the long axis of specular hematite at right angles to the possible maximum stress direction. Botryoidal hematite occurs only in sample 2 (Plate 4, Figure 4). It is suggested that botryoidal $Fe(OH)_3$ was originally precipitated, and then goethite, FeO(OH), was formed upon expulsion of HOH. Further expulsion of HOH formed hematite which retained the typical botryoidal form of goethite. The equations involved are as follows:

$$Fe(OH) \longrightarrow FeO(OH) + HOH\uparrow$$

$$2FeO(OH) \longrightarrow Fe_2O_3 + HOH\uparrow$$

Precipitation of goethite must have occurred at a low

temperature (around 150°C) at the time of, or earlier than, the carbonate deposition.

Pitchblende 0 and 1

Pitchblende 0 was deposited with hematite. The time of deposition was later than massive quartz but earlier than comb quartz. Most of pitchblende 0 has been oxidized to pitchblende 1. Pitchblende 0 and 1 are dominantly massive but some botryoidal gelatinous precipitates did occur and gave rise to the botryoidal variety shown in Plate 4, Figure 6. Plate 4, Figure 5 shows highly oxidized pitchblende 0 replacing massive quartz. Some pitchblende 0, partly oxidized, veins massive quartz (Plate 4, Figure 8). Loose pieces of brecciated massive pitchblende 0 and 1 are also common. Pitchblende 0 and 1 occur in all ore samples examined.

Pitchblende 2 and 3

Pitchblende 2 and occurs throughout the No 2 Zone and has similar physical properties to pitchblende 0. It can be differentiated only in that it cuts pitchblende 0 and is only slightly oxidized. Furthermore, pitchblende 2 is botryoidal and may occur in various forms. Pitchblende 2 veinlets (Plate 2, frontispiece 2 and Plate 5, Figure 1) cut massive pitchblende 0(and 1). Sample 2 shows brecciated wall rock, and massive quartz with hematite that has been encrusted with pitchblende 2. Loose spherules (Plate 5, Figures 4 and 5) have been observed in several samples, particularly in sample 2 where the spherules occur between

breccia fragments. Layers (Plate 5, Figure 7), and remnants of layered pitchblende 2 (Plate 5, Figure 2), are present in several samples. In sample 6, a 1.5 inch vein of layered pitchblende occurs. In general, both the early and the late pitchblende have been brecciated. Photomicrographs which exhibit brecciation are Plate 5, Figure 5; Plate 7, Figure 5; and Plate 8, Figure 5. One occurrence of pitchblende pseudomorphous after pyrite is seen in Plate 5, Figure 6. Pitchblende 3 occurs in the syneresis cracks of pitchblende 2.

Pitchblende 4

This mineral (Plate 7, Figure 8) was seen only in sample 7 where it is a filling in a quartz vug. It is massive with no syneresis cracks. The composition is $UO_2$ (Figure 8) and this thought to be a recently precipitated mineral of supergene origin.

Bismuth

Native bismuth is present in samples 4, 1812, and 4557. In sample 4, it is irregular and fine-grained (Plate 8, Figure 3). Sample 1812 contains bismuth crystals that have been replaced and enclosed by carbonate. Bismuth dendrites (Plate 6, Figures 1, 2, and 7) occur in sample 4557. The dendrites are composed of oriented rhombohedral crystals rimmed and replaced by niccolite, schirmerite, and klaprothite (Plate 6, Figures 1, 2, and 3). Plate 6, Figure 4, shows gersdorffite rimming the dendrites and replaced by carbonate. In this case, the carbonate has

PLATE 5

FIGURE 1: Photomicrograph of sample 1 where pitchblende 1 (p-1) is replaced by botryoidal pitchblende 2 (p-2) veinlet that has been oxidized, probably recently, to pitchblende 3 (p-3). White mineral along syneresis cracks of pitchblende 1 is galena. x255

FIGURE 2: Photomicrograph of sample 4. Remnants of botryoidal pitchblende layers (p) - replaced by quartz (medium grey). x40

FIGURE 3: Photomicrograph of sample 2. Brecciated wall rock (dark grey) or early quartz and hematite fragments crusted with botryoidal pitchblende (p) and separated by gangue (quartz - medium grey). x40

FIGURE 4: Photomicrograph of sample 2. Similar to Figure 3 but more crustification has occurred. Pitchblende (p) crusting breccia fragments (dark grey). Some 'loose' spherules between fragments occur. Bornite is bor and cp is chalcopyrite. x40

FIGURE 5: Photomicrograph of sample 2. Large botryoidal pitchblende (p) spherule with galena (white) in syneresis cracks. Bornite (bor). x40

FIGURE 6: Photomicrograph of sample 9. Pitchblende (p) pseudomorphic spherule with galena (gn) x255

FIGURE 7: Photomicrograph of sample 6 showing displaced and cracked botryoidal pitchblende (p). White mineral along syneresis cracks is chalcopyrite. x40

FIGURE 8: Photomicrograph of sample 7 where supergene pitchblende 4 (p-4) has filled a quartz vug. x100

PLATE 5

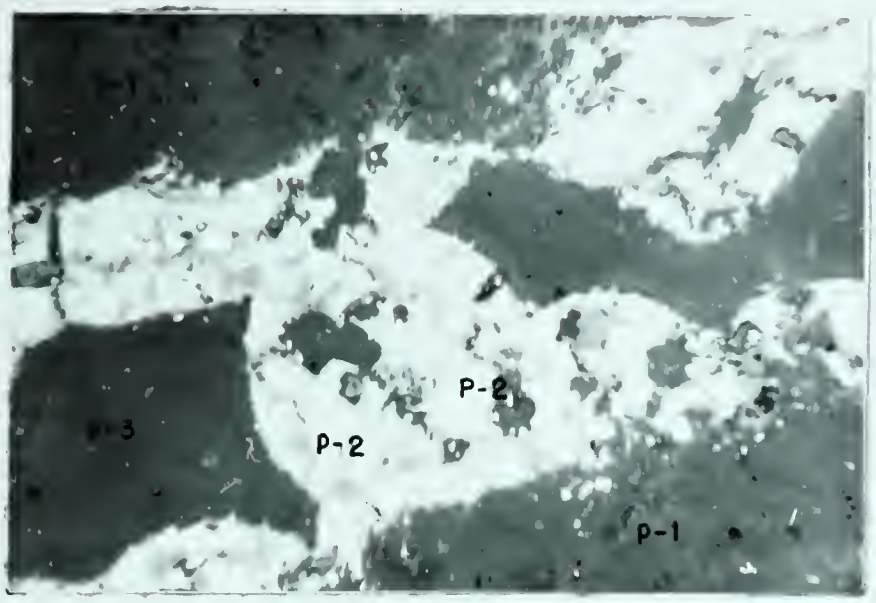


1 X255

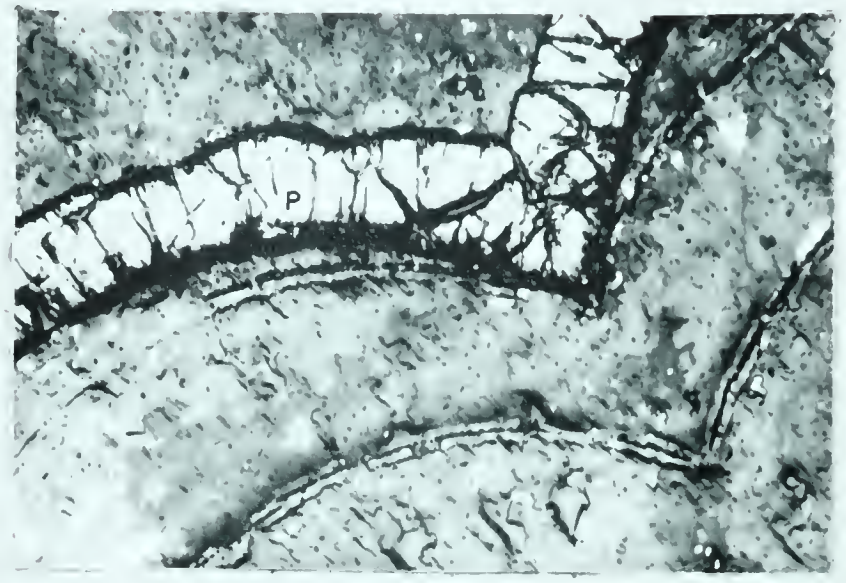


2 X40

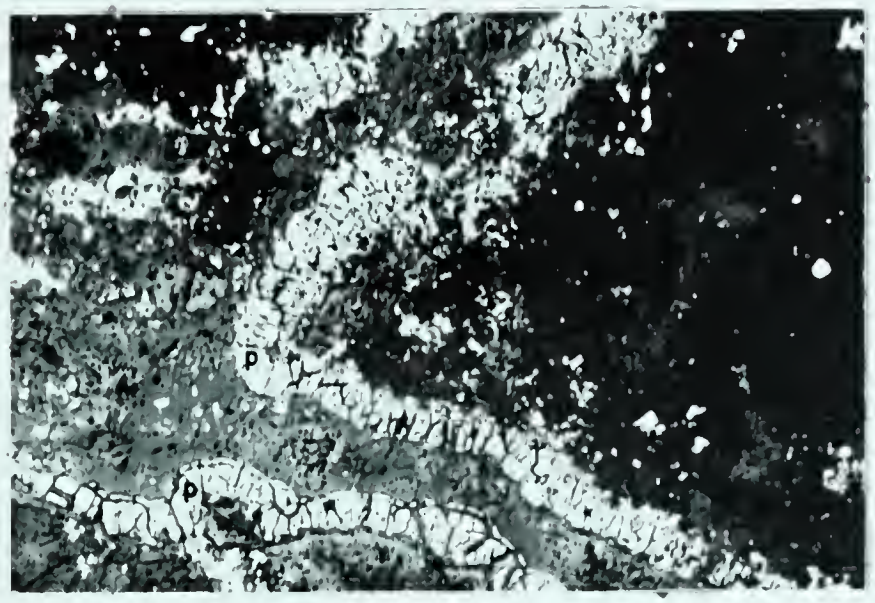


3 X40

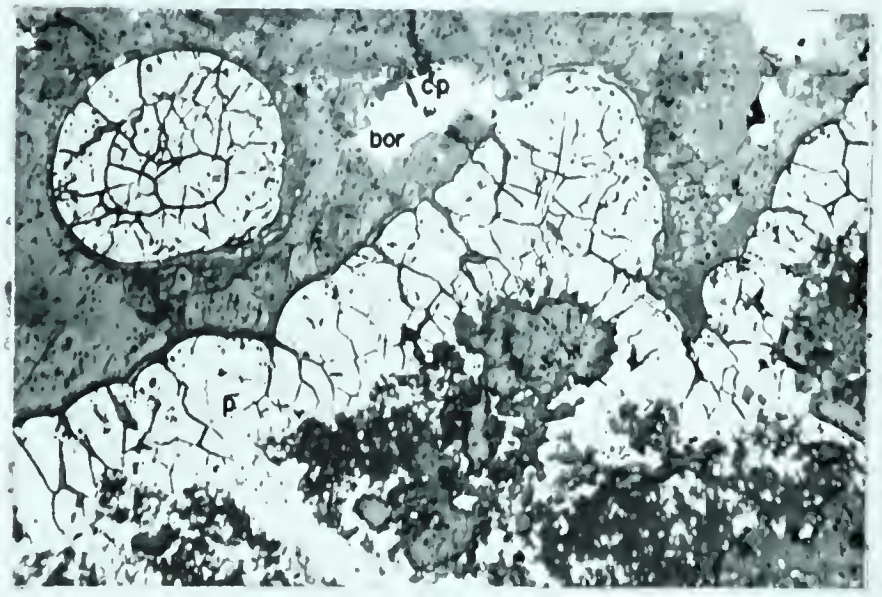


4 X40

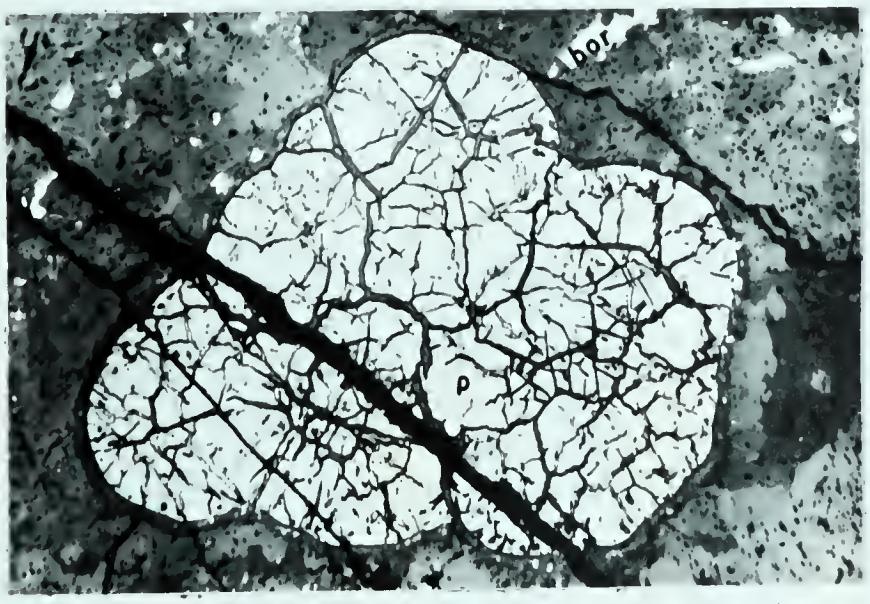


5 X40

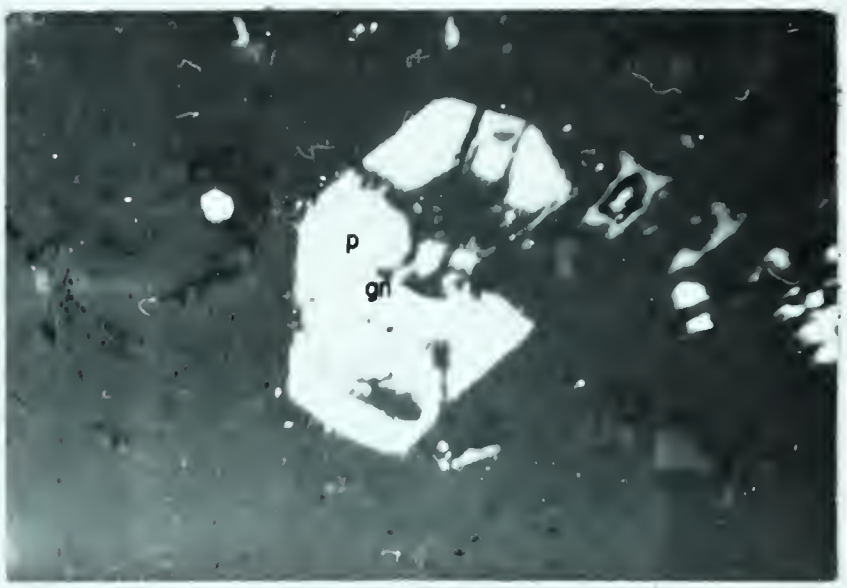


6 X255

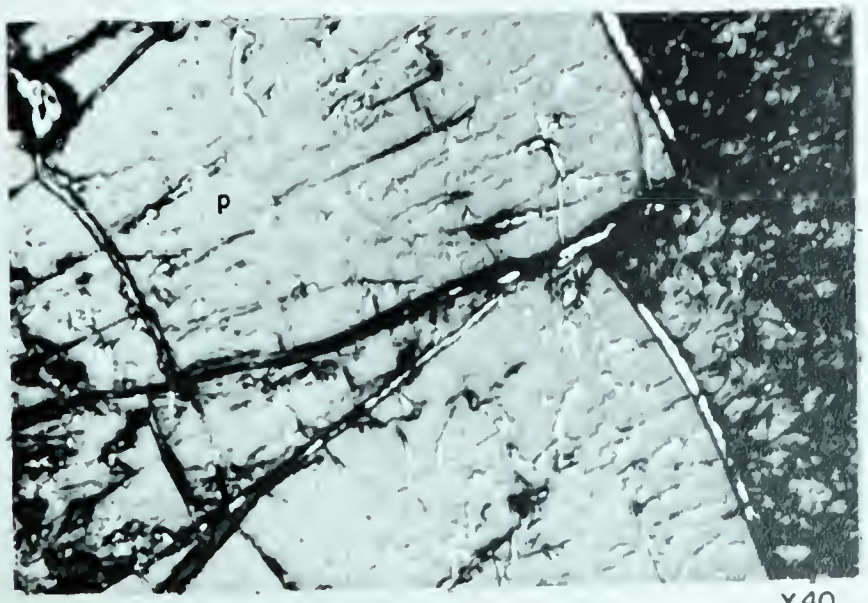


7 X40

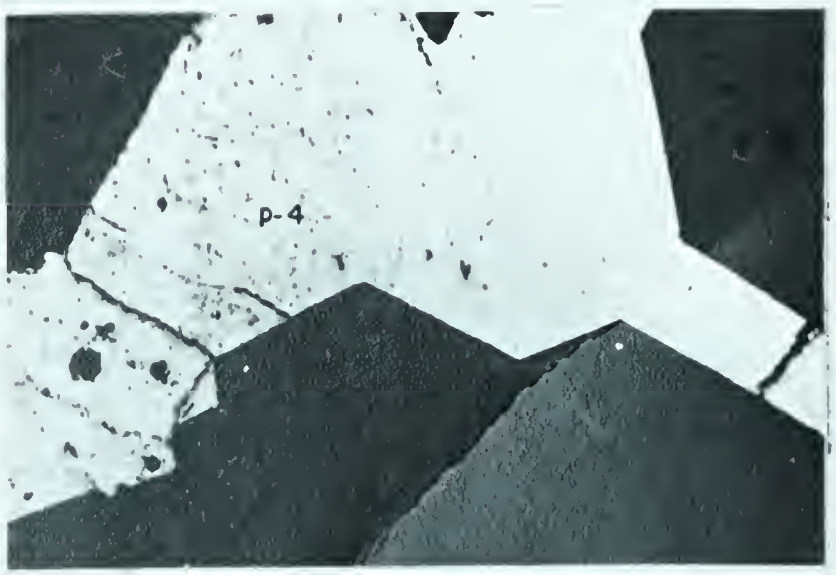


8 X100

replaced the original bismuth core in the gersdorffite. The arsenide dendrites in sample 5 also rim carbonate (and bismuth sulfosalts) which have replaced skeletal native bismuth (Plate 6, Figures 3,5,6, and 8).

Much discussion has taken place regarding arsenide dendrites rimming native silver and in some cases native bismuth. Some geologists believe that the silver or bismuth has replaced the cores of arsenide dendrites. Bastin (1950, pp. 44 - 46) suggests that the interpretation that silver or bismuth as a replacement of the core of arsenide dendrites is incorrect. Todd (1926) supports this idea in his discussion of the Gowganda dendritic types. He states:

> "The constant presence of a layer of skutterudite surrounding the silver offers strong evidence that the arsenide was precipited upon the silver. It is hard to conceive how this definite arrangement could have been arrived at in any other way."

Bastin points out that Van der Veen noted that in some occurences in the Erzgebirge and at Cobalt, the cores within the arsenide envelopes were calcite rather than silver. Van der Veen believed that the original dendrites were calcite which were rimmed by arsenides and replaced by native silver. Bastin indicates that Kiel has shown that at Marienberg, Germany, and at Cobalt, silver dendrites are partially replaced by calcite. Bastin noted that silver cores are the rule and carbonate cores the local exception. This, however, is not the case in the No 2 Zone, where the cores are carbonate (Plate 6). The author believes, however, that

PLATE 6

FIGURE 1: Photomicrograph of sample 4557. Bismuth dendrite (bi) rimmed by Klaprothite (kla) x40

FIGURE 2: Photomicrograph of sample 4557. Bismuth dendrite (bi) rimmed by niccolite (nic), schirmerite (sch), klaprothite (kla) and largely replaced by carbonate (medium grey). x40

FIGURE 3: Photomicrograph of sample 5. Rammelsbergite (white - ram) dendrites replaced partly by glaucodot (grey-white - glau). Core is carbonate (dark grey) and in places skeletal glaucodot (light grey). x40

FIGURE 4: Photomicrograph of sample 4557 where gersdorffite (gers) has rimmed bismuth which has since been totally replaced by carbonate (medium grey) x40

FIGURE 5: Photomicrograph of sample 5. Rammelsbergite (ram) dendrites. Skeletal glaucodot (glau) has replaced skeletal bismuth. Core filled by carbonate (black). Sch is schirmerite. x100

FIGURE 6: Photomicrograph of sample 5. Similar to Figure 6. Rammelsbergite (ram) and glaucodot (glau) dendrites. x100

FIGURE 7: Photomicrograph of sample 4557. Same as Figure 2 - larger scale. Bismuth (bi) rimmed by niccolite (nic), schirmerite (sch), and klaprothite (kla). x100

FIGURE 8: Photomicrograph of samples. Arsenide dendrite. Rammelsbergite (white - ram) partly replaced by glaucodot (grey-white - glau). Skeletal mineral is glaucodot (glau) and grey (sch) is schirmerite x100

PLATE 6


1 X40

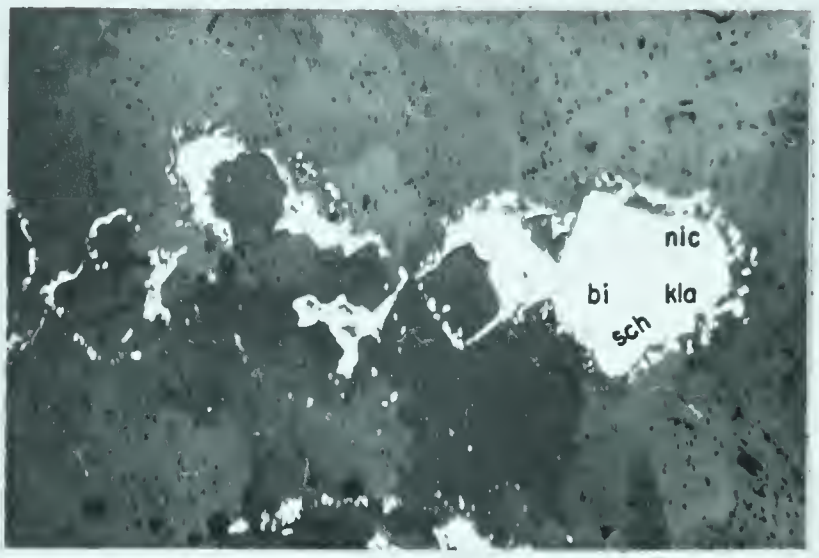


2 X40

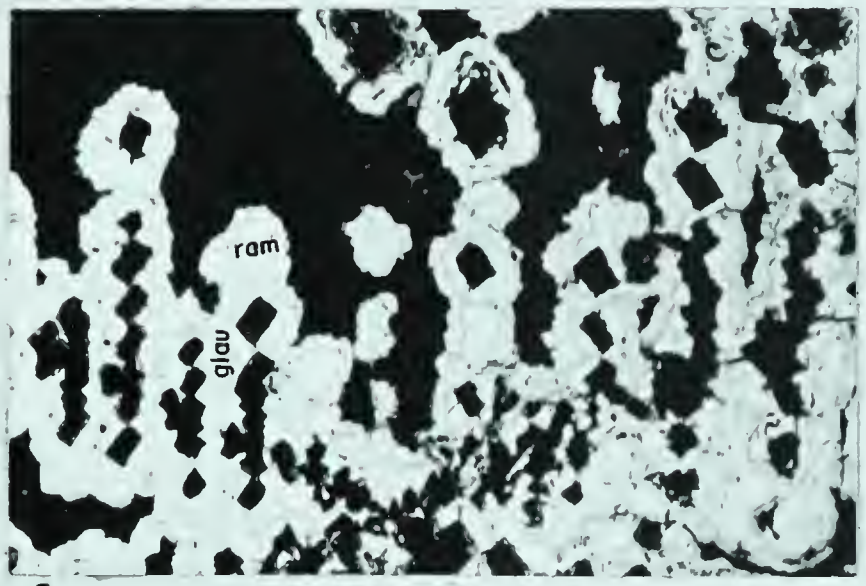


3 X40


4 X40

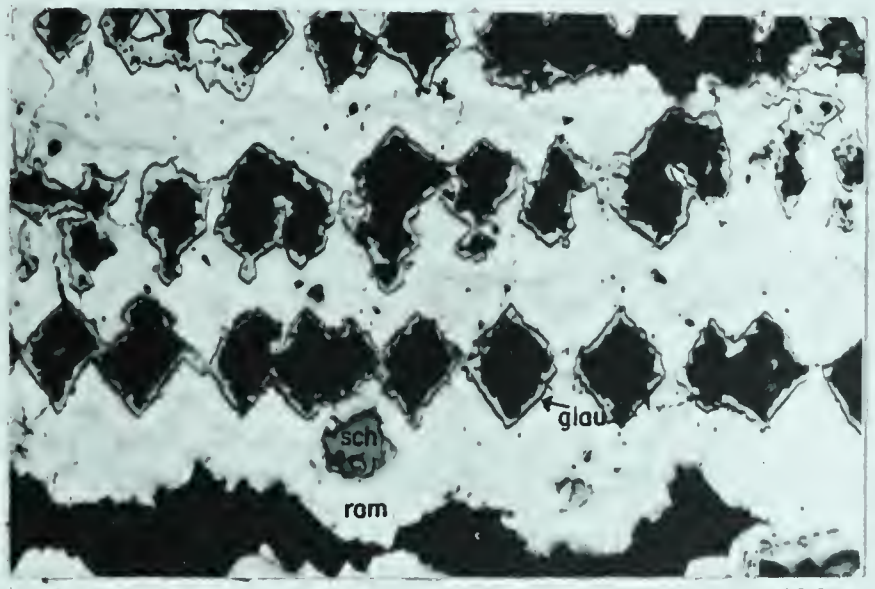


5 X100

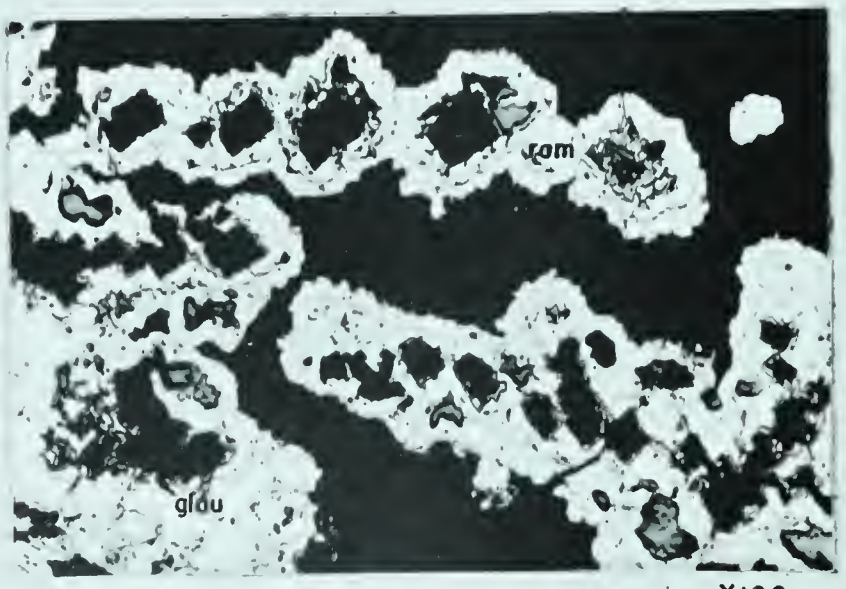


6 X100


7 X100


8 X100

the bismuth (skeletal in places) has been replaced by the carbonate and not carbonate by bismuth. Some cores consist of bismuth sulfosalts which could develop when native bismuth was dissolved and redeposited as schirmerite or klaprothite (Plate 8, Figure 1). Plate 6, Figure 5 seems to show that the dendrites were skeletal bismuth that were rimmed by rammelsbergite, and then replaced by glaucodot. Finally dolomite filled the core of the pseudoskeletal glaucodot (glaucodot has replaced skeletal bismuth). Bastin, on examination of the ores of the Miller Lake O'Brien Mine at Gowganda notes partial or entire replacement of spider-like silver outlines by calcite. Plate 8, Figure 6, shows a similar outline of calcite rimmed by klaprothite. The writer believes that the spider-like outline of dolomite was bismuth which has been replaced by carbonate. Another explanation is that the skeletal spider-like native bismuth has been replaced by klaprothite and the core filled by carbonate. It is postulated, therefore, that bismuth was deposited after comb quartz and before all the metallic mineralization except magnetite, hematite, pitchblende, and perhaps some iron sulfides. This theory has an important thermal implication which will be discussed under geothermometry.

Niccolite

Niccolite occurs in samples 4557 and 5. In 4557 (Plate 6, Figure 7), it was observed in one location where it rims bismuth and has been largely replaced by

klaprothite. In sample 5, an appreciable amount of niccolite is present in the core of rammelsbergite (Plate 7, Figure 1). The interpretation of the mineral relationships is that niccolite has replaced pitchblende and has been in turn replaced by rammelsbergite along the pitchblende-niccolite contact. The concentration of arsenic in the solutions may have been low at first and this feature would favour the formation of niccolite as the first arsenide precipitated. Thus, on this basis, it is rather arbitrarily placed before rammelsbergite in the paragenetic sequence.

Rammelsbergite

This mineral is definitely earlier than all arsenides with the exception of niccolite. It is present in sample 5, where it exhibits several modes of occurrence. It may be botryoidal and have formed after pitchblende as is shown in Plate 7, Figure 1. Irregular masses are shown in Plate 7, Figures 2 and 3. Dendritic rammelsbergite rimming replaced bismuth dendrites is shown in Plate 6, Figures 3, 5, 6, and 8. Rammelsbergite was deposited earlier than glaucodot as is shown by the replacement along crystal growth layers (Plate 6, Figure 8), and the veining of rammelsbergite by glaucodot (Plate 7, Figure 3).

Gersdorffite

Gersdorffite occurs in sample 4557 where it has rimmed bismuth dendrites or replaced skeletal bismuth dendrites (Plate 6, Figure 4). It is similar in composition to glaucodot except that it is a nickel sulfarsenide instead

of cobalt-iron sulfarsenide. It is placed before glaucodot in the sequence since the solutions appear to have been nickel-rich at first, and after rammelsbergite since it is similar to glaucodot.

Glaucodot

This mineral is common in samples 3, 5, 8, and 9. It is present as skeletal dendrites (Plate 6, Figures 5 and 8), and as rims, replacements, and veins in rammelsbergite (Plate 6, Figures 3, 5, 6, and 8; Plate 7, Figures 2 and 3). Plate 7, Figure 4 and 5 shows disseminated glaucodot.

Skutterudite

Skutterudite occurs in sample 5 in cellular forms. It has replaced pitchblende and rammelsbergite (Plate 7, Figure 6). Rammelsbergite and glaucodot were brecciated before the period of skutterudite deposition. Skutterudite is replaced by schirmerite in Plate 8, Figure 2, and apparently replaces schirmerite in Plate 7, Figures 7 and 8. Thus it appears that the skutterudite and schirmerite precipitation was generally contemporaneous.

Schirmerite

As previously stated, schirmerite is present in samples 4, 4557, and 5. In sample 5, it occurs as replacement bands along skutterudite growth layers (Plate 8, Figure 2) and as irregular brecciated masses (Plate 7, Figure 8). In Plate 8, Figure 4, it is shown forming part of the dendritic structure where it has replaced bismuth.

PLATE 7

FIGURE 1: Photomicrograph of sample 5. Pitchblende (p) replaced by niccolite (nic) and rammelsbergite (ram). x40

FIGURE 2: Photomicrograph of sample 5. Rammelsbergite (ram) - glaucodot (glau) contact. x255

FIGURE 3: Photomicrograph of sample 5. Rammelsbergite (ram) is rimmed and veined by glaucodot (glau). x255

FIGURE 4: Photomicrograph of sample 3. Dendritic and disseminated glaucodot (glau) in gangue. Sp is disseminated sphalerite. x40

FIGURE 5: Photomicrograph of sample 3. Brecciated pitchblende (p) veinlet replaced by disseminated glaucodot (glau) and carbonate x40

FIGURE 6: Photomicrograph of sample 5. Pitchblende (light grey) replaced by rammelsbergite (ram) which is in turn replaced by cellular skutterudite (sk). Schirmerite (very light grey) has replaced skutterudite along growth bands or indicates rhythmic precipitation of skutterudite - schirmerite. x40

FIGURE 7: Photomicrograph of sample 5. Cellular skutterudite (sk) replaced by schirmerite.(sch) or replaces schirmerite. The two minerals are replaced by dolomite (black). x100

FIGURE 8: Photomicrograph of sample 5. Skutterudite (sk) apparently replacing schirmerite (sch). Black triangular area is dolomite. x625

PLATE 7

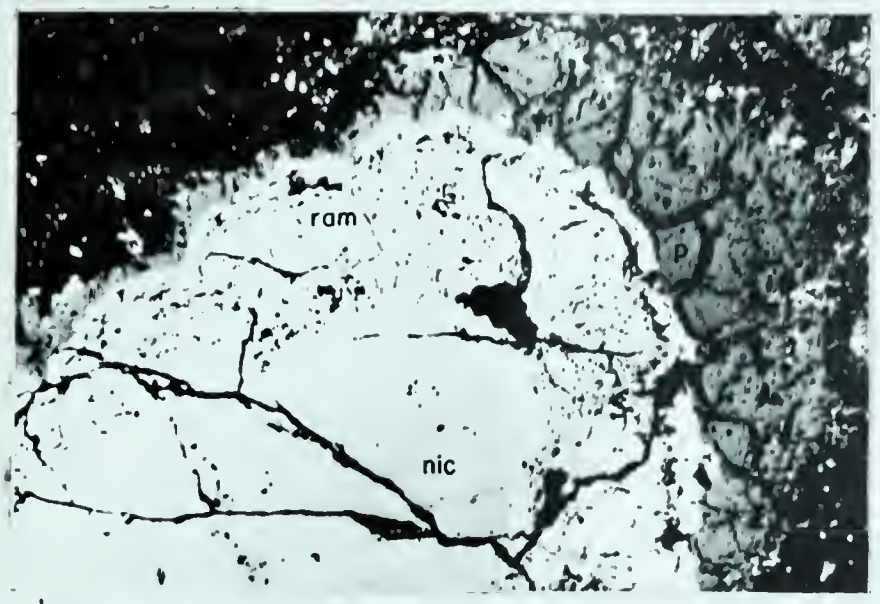


1 X40

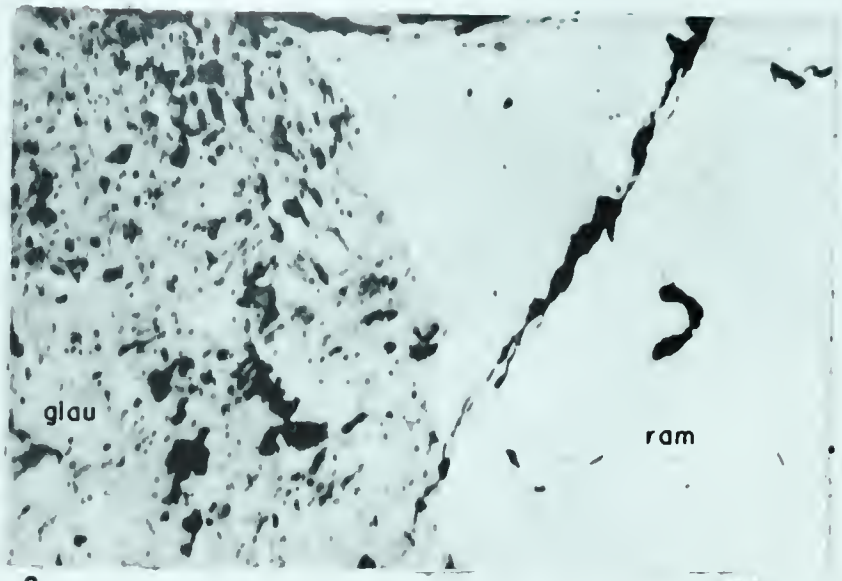


2 X 255

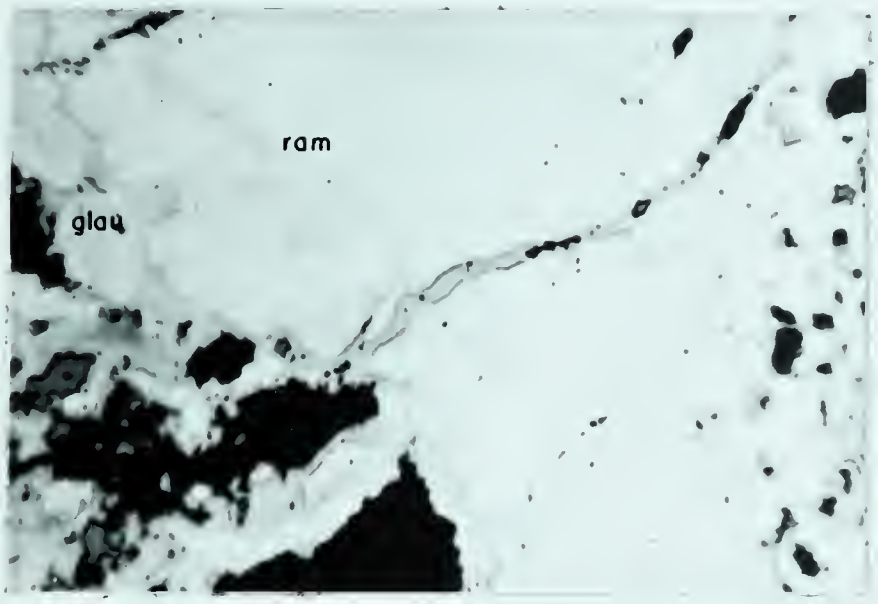


3 X255

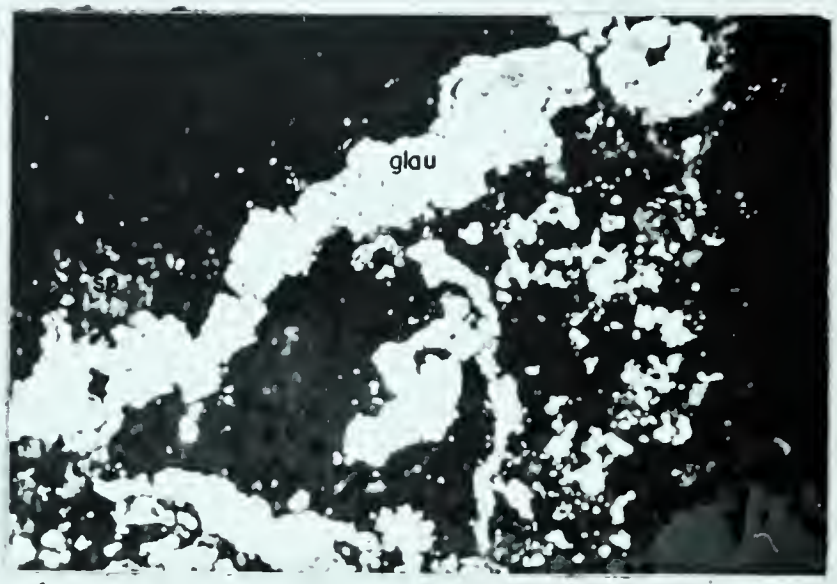


4 X40

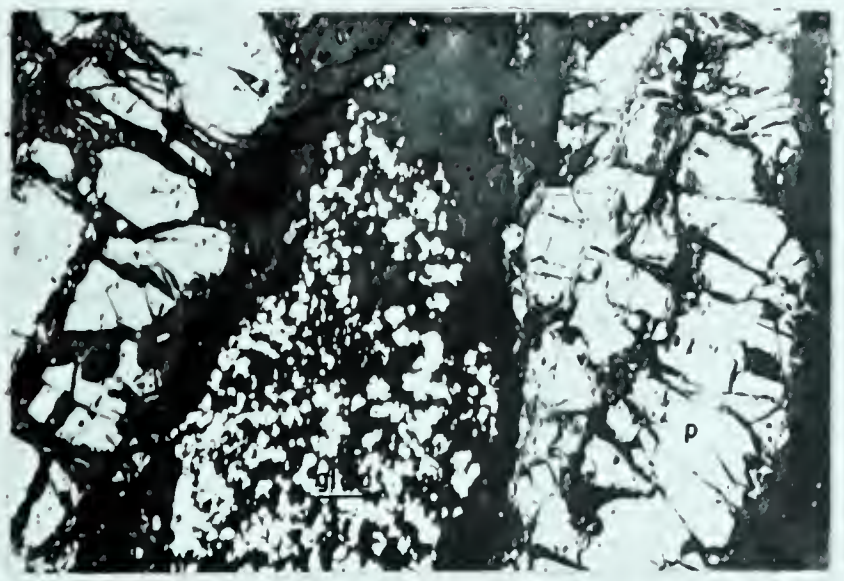


5 X40

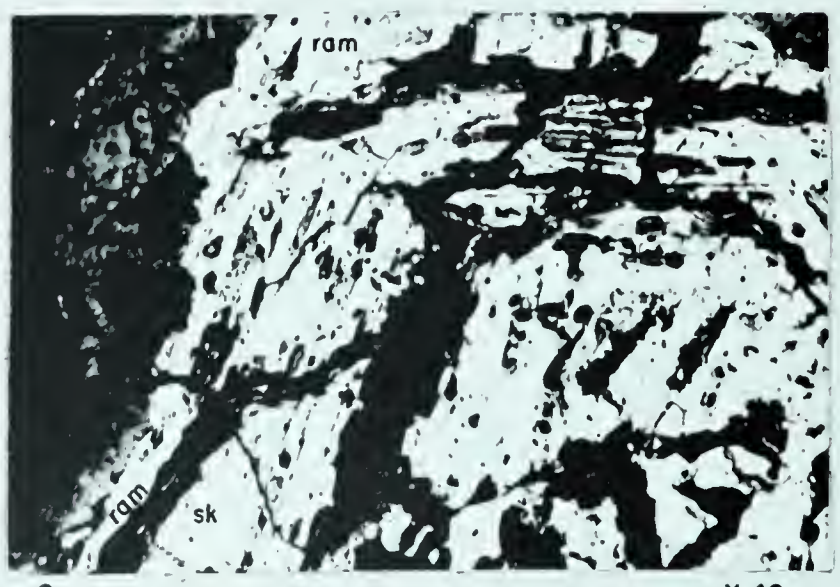


6 X 40


7 X100

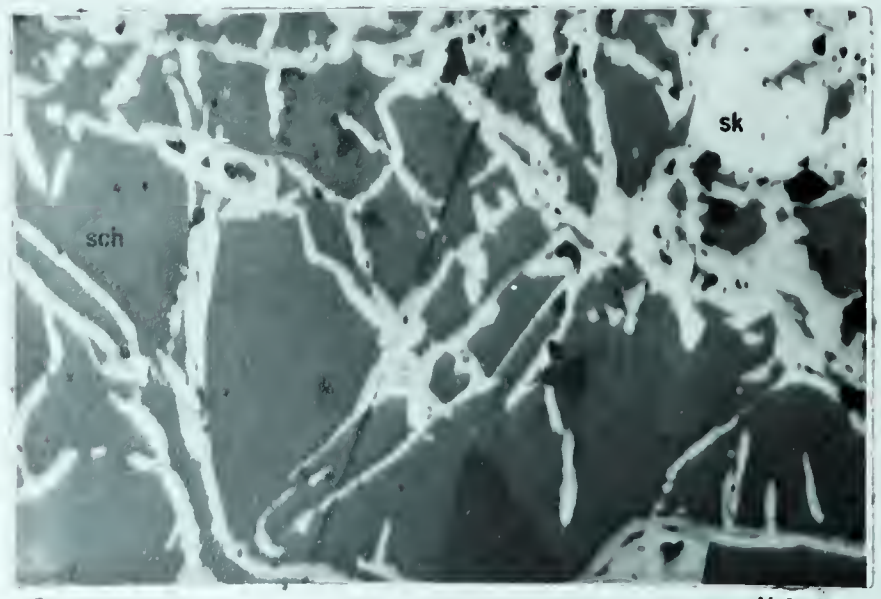


8 X625

It also occurs as irregular masses replaced or enclosed by copper sulfides in sample 4 (Plate 8, Figures 3 and 4). Schirmerite may occur as veins as shown in Plate 8, Figure 5 or may form rims around bismuth as shown in Plate 7, Figure 8.

Klaprothite

Schirmerite and klaprothite are intimately associated, and invariably klaprothite replaces schirmerite. In Plate 7, Figure 8, klaprothite replaces schirmerite which has in turn replaced niccolite. In sample 4557, klaprothite forms rims around spider-like bismuth or replaces the bismuth (Plate 8, Figure 6). It occurs as irregular dendritic patches that appear to have been deposited in openings in arsenide dendrites (Plate 8, Figure 7). It should be noted that klaprothite dendrites consist of irregular patches whereas schirmerite occurs in rhombohedral shapes after bismuth. Schirmerite was deposited in skeletal openings in glaucodot grains (Plate 8, Figure 1), whereas by the time klaprothite was being deposited, skeletal crystals of glaucodot had been attacked and partially dissolved, and the klaprothite was deposited in the irregular openings. As shown in Plate 8, Figure 8 klaprothite has replaced schirmerite.

Pyrite

The time of pyrite deposition is uncertain. Some euhedral pyrite is veined by the comb quartz (Plate 9, Figures 1 and 2). Carbonate also occurs along fractures in

PLATE 8

FIGURE 1: Photomicrograph of sample 5. Schirmerite (sch) filling skeletal glaucodot (glau). Glaucodot is replacing rammelsbergite (ram) along growth layers of dendritic rammelsbergite. x100

FIGURE 2: Photomicrograph of sample 5. Cellular skutterudite (sk) replaced by schirmerite (sch) along growth bands (or indicates schirmerite - skutterudite rhythmic deposition). Replaced by dolomite (black). x255

FIGURE 3: Photomicrograph of sample 4. Granular tarnished bismuth (bi) is rimmed or replaced by schirmerite (sch). Bornite (bor) encloses bismuth and schirmerite. x625

FIGURE 4: Photomicrograph of sample 4. Granular schirmerite (sch) replaced (or rimmed) by galena (gn), tetrahedrite (tet), and chalcopyrite (cp) x625

FIGURE 5: Photomicrograph of sample 4. Schirmerite (sch) veining brecciated pitchblende (p). Chalcopyrite (cp) is disseminated and along syneresis cracks of pitchblende. x255

FIGURE 6: Photomicrograph of sample 4557. Klaprothite (kla) has replaced spider-like skeletal bismuth or rimmed spider-like bismuth which has been replaced by carbonate. x100

FIGURE 7: Photomicrograph of sample 5. Irregular klaprothite (kla) cores of arsenide dendrites (rammelsbergite - ram and glaucodot - glau). x625

FIGURE 8: Photomicrograph of sample 5. 85° crossed - nicols. Isotropic schirmerite (sch) is replaced by anisotropic klaprothite (kla) x255

PLATE 8

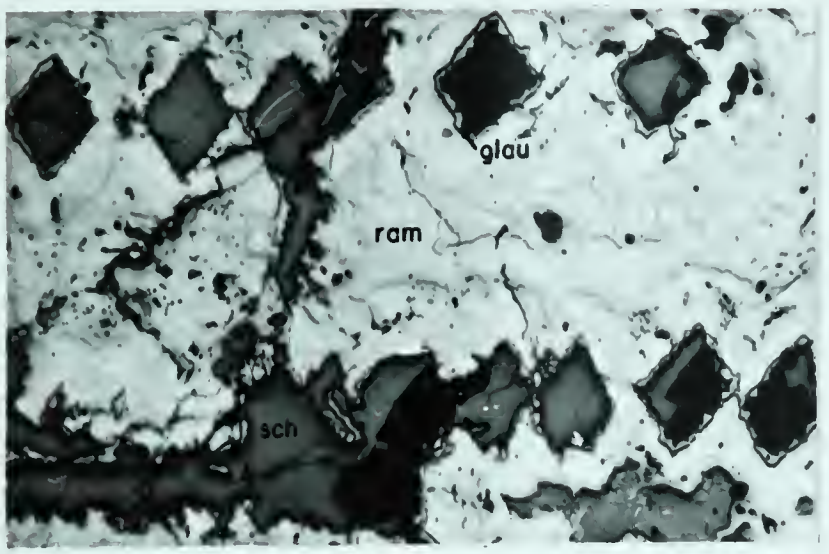


1 X100

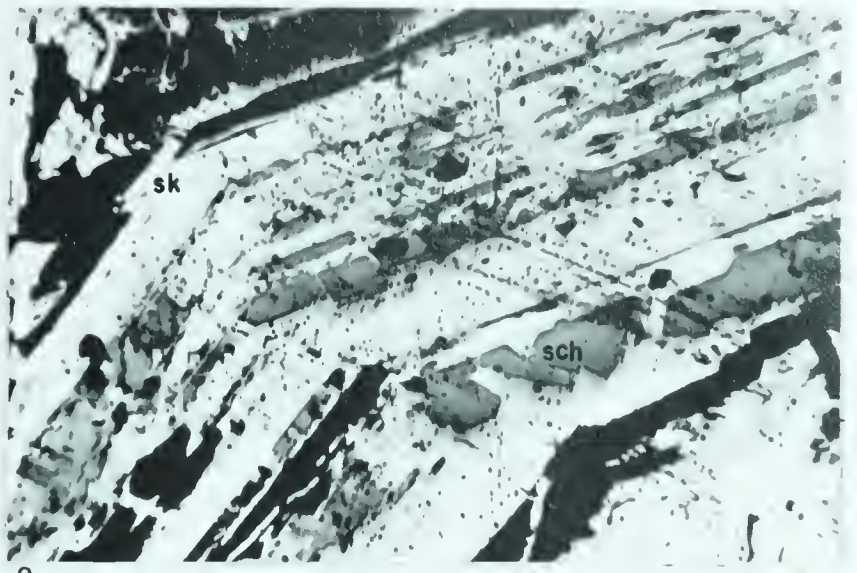


2 X255

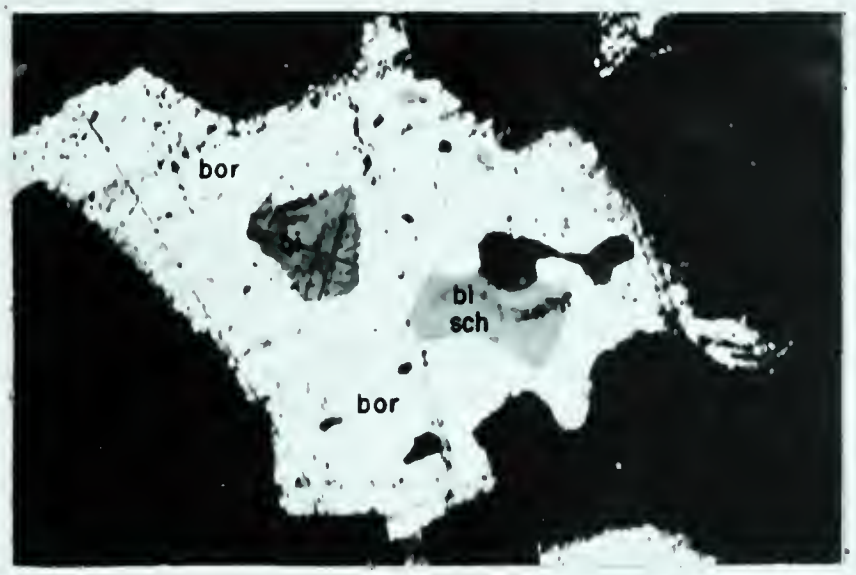


3 X625

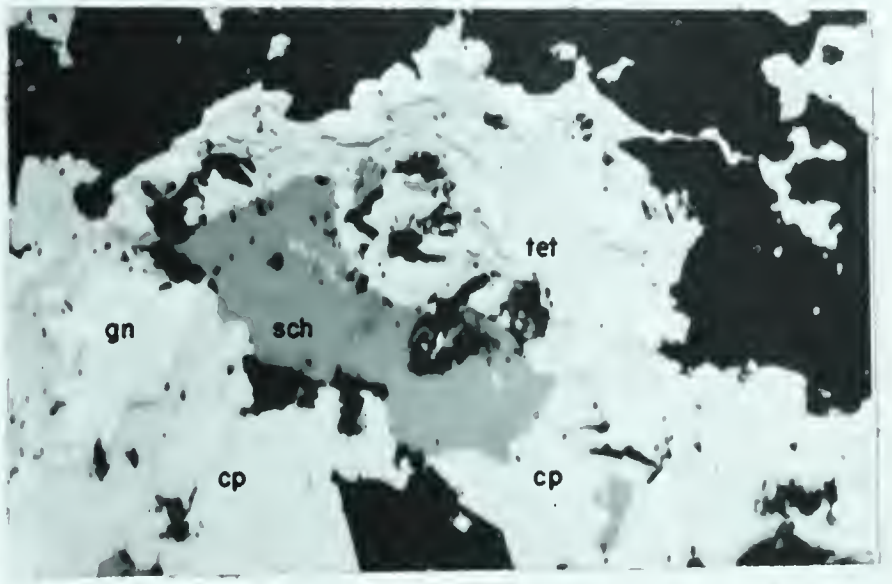


4 X625

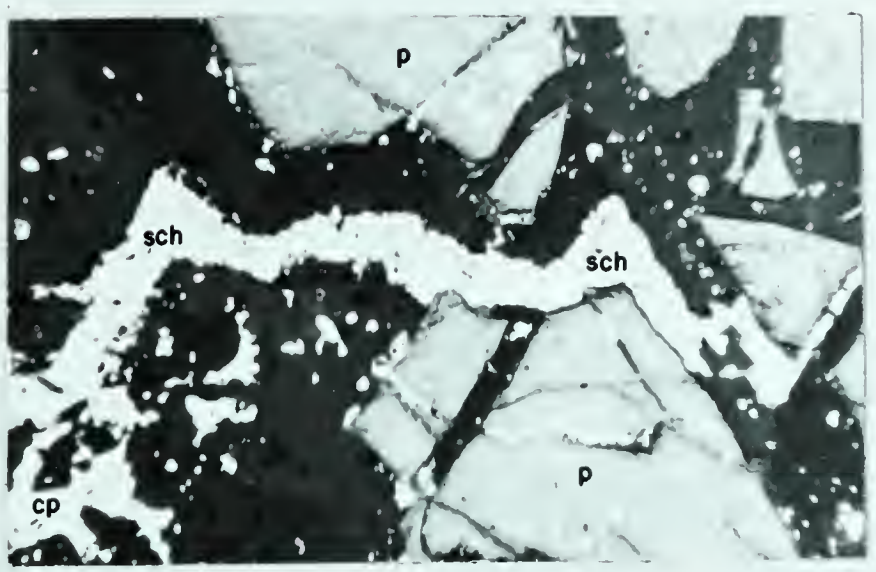


5 X255

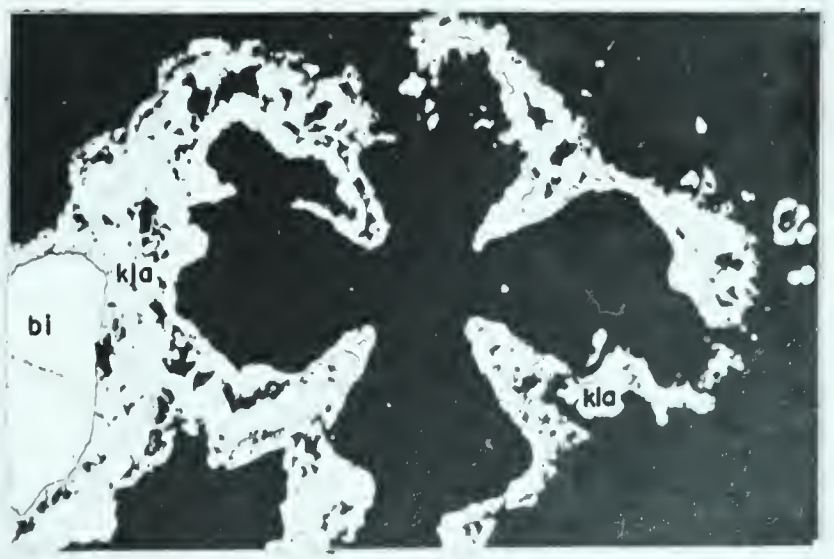


6 X100

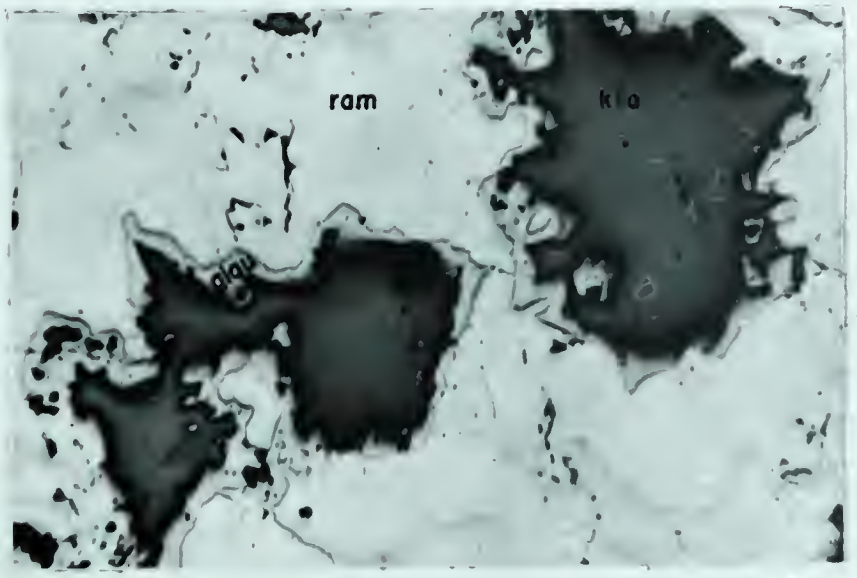


7 X625

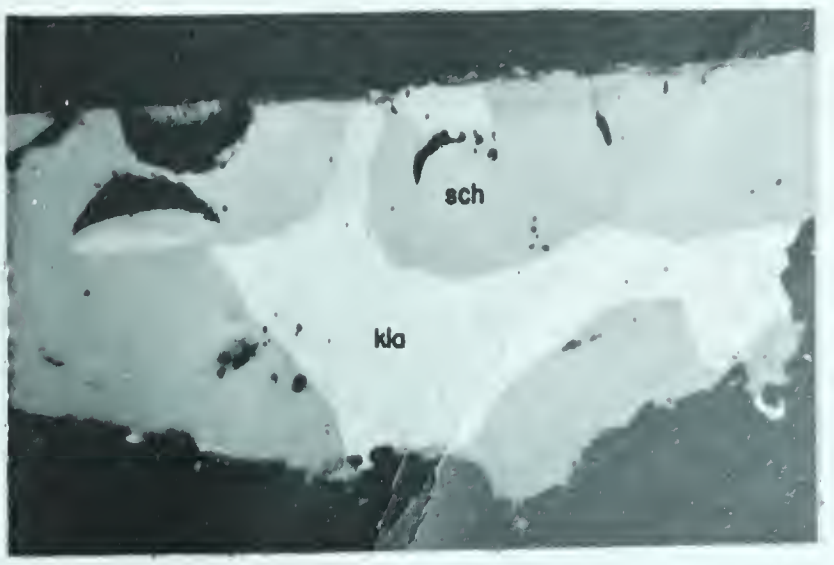


8 X255

pyrite crystals (Plate 8, Figure 3). Massive pyrite is also quite common and replaces late quartz. Thus, it appears that pyrite deposition started after the pitchblende and hematite mineralization and continued until the carbonate veining, which followed iron sulfide and sphalerite deposition. Pyrite is present in samples 2, 3, 6, 7, 8, and GB.28.3.

Marcasite

This mineral occurs in samples 1, 3, 4, 6, and 8. In samples 1, 3, 6, and 8, it occurs as single crystals (Plate 9, Figure 8 and Plate 10, Figure 1). Sample 4 contains an aggregate of acicular crystals (Plate 10, Figure 3) in a veinlet occurring with massive pyrite (Plate 10, Figure 2) and burr-shaped pyrrhotite (Plate 9, Figure 4).

Pyrrhotite

Pyrrhotite occurs dominantly as irregular masses (Plate 9, Figure 7) and as burr-shaped bodies. In the latter case, it is partly replaced by dolomite. The burr-shaped pyrrhotite (Plate 9, Figure 4) is due to subparallel aggregation on (0001) (Palache, Berman, and Frondel, 1946, p.232). As previously indicated, the pyrrhotite is near troilite in composition.

Sphalerite

Sphalerite occurs mainly in very small disseminated irregular masses. Some areas of sphalerite in pyrrhotite resemble an exsolution texture, (Plate 9, Figure 7). The relationships in Plate 10, Figure 7, may indicate sphalerite-

PLATE 9

FIGURE 1: Photomicrograph of sample GB.28.3. Pyrite (py) crystal fractured and veined by gangue (quartz). Light grey is mica. x100

FIGURE 2: Photomicrograph of sample 7. Pyrite crystal (py) replaced by quartz (black) and sphalerite (sp). p is pitchblende. x100

FIGURE 3: Photomicrograph of sample 7. Shattered pyrite (py) crystal replaced by dolomite (dol), which also replaces quartz (q), and by sphalerite (sp) x100

FIGURE 4: Photomicrograph of sample 7. Irregular pyrite (py) replacing oxidized pitchblende and quartz (both black). x625

FIGURE 5: Photomicrograph of sample 9. Irregular masses of pyrrhotite (po) exsolving sphalerite (sp) x625

FIGURE 6: Photomicrograph of sample 8. Marcasite (ma) - pyrite (py) in a dolomite veinlet (black). x625

PLATE 9


1 X100


2 X 100

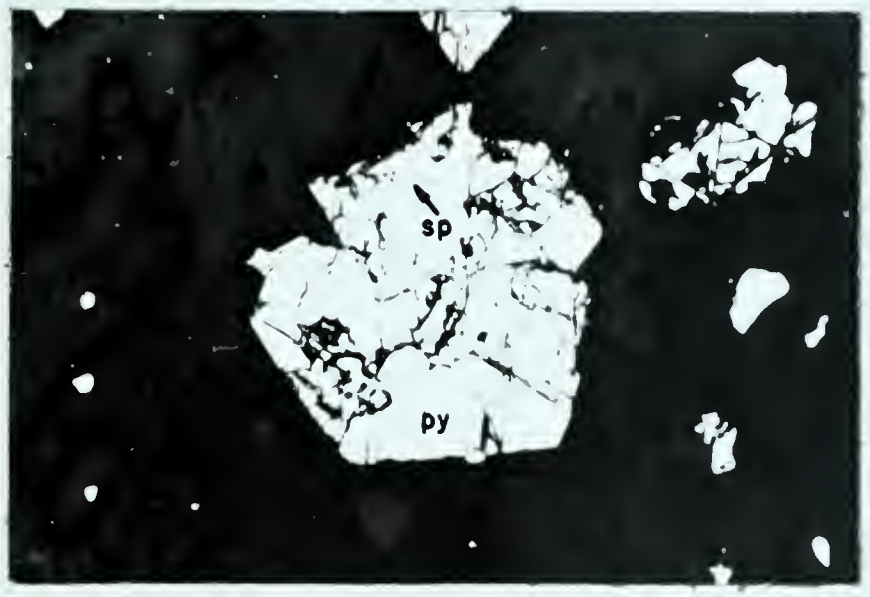


3 X 100

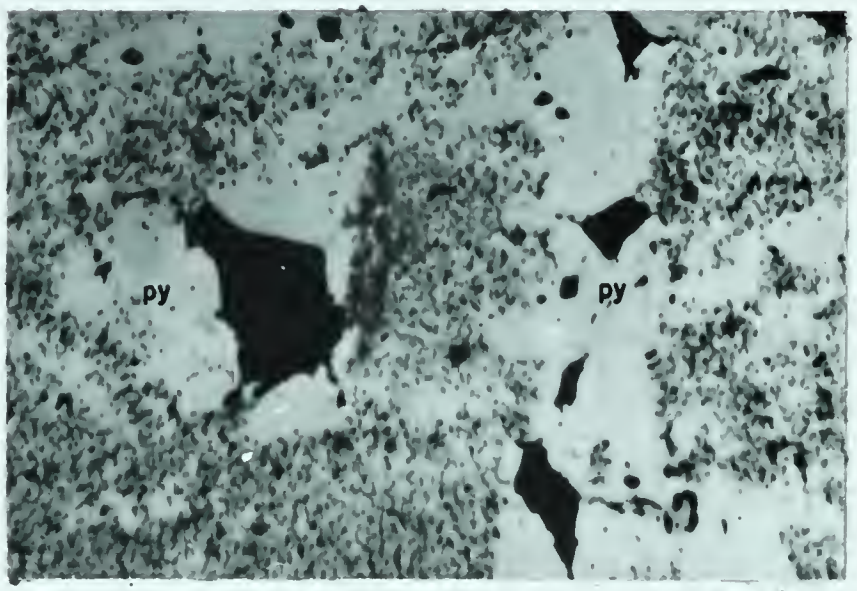


4 X 625

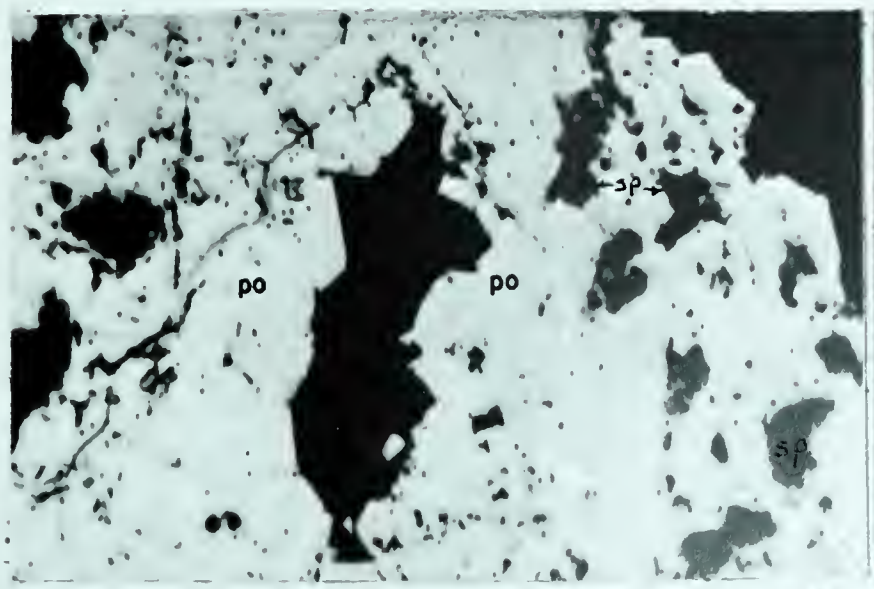


5 X625

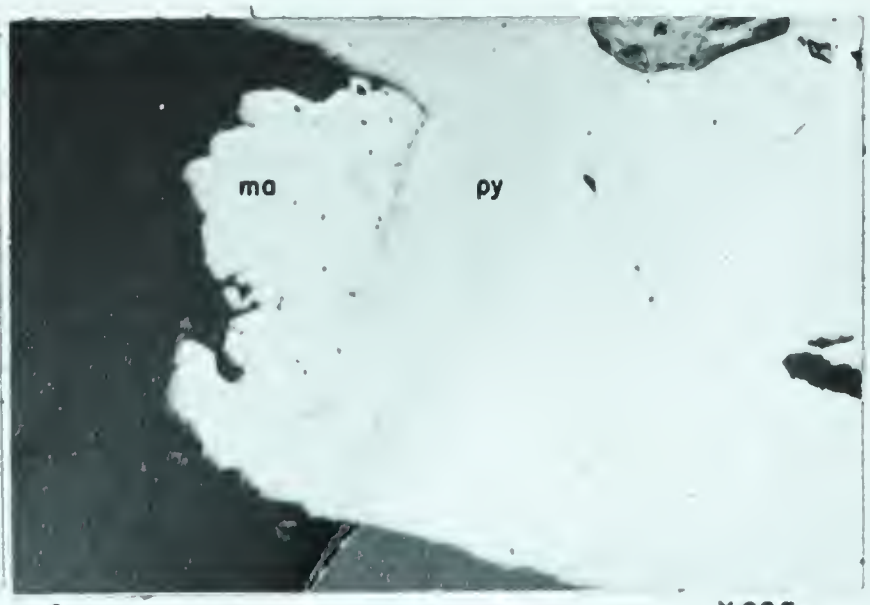


6 X625

PLATE 10

FIGURE 1: Photomicrograph of sample 3. Marcasite (ma) in exploded - form hematite (hem). Medium-grey and black is carbonate gangue. x625

FIGURE 2: Photomicrograph of sample 4. Massive pyrite (py) in a veinlet, replaced by chalcopyrite (cp). x625

FIGURE 3: Photomicrograph of sample 4. Randomly oriented acicular marcasite (ma) in same veinlet as pyrite in Figure 2. Gangue (black) is carbonate. x625

FIGURE 4: Photomicrograph of sample 4. Pyrrhotite burrs (po) in same dolomite (dol) veinlet as marcasite (Figure 3) and pyrite (Figure 2). x100

FIGURE 5: Photomicrograph of sample GB.28.3. Sphalerite (sp) enclosed by chalcopyrite (cp). x255

FIGURE 6: Photomicrograph of sample 6. Sphalerite (sp) - galena (gn) segregation veinlet in a carbonate veinlet (medium grey). Cp is chalcopyrite. x625

PLATE 10.

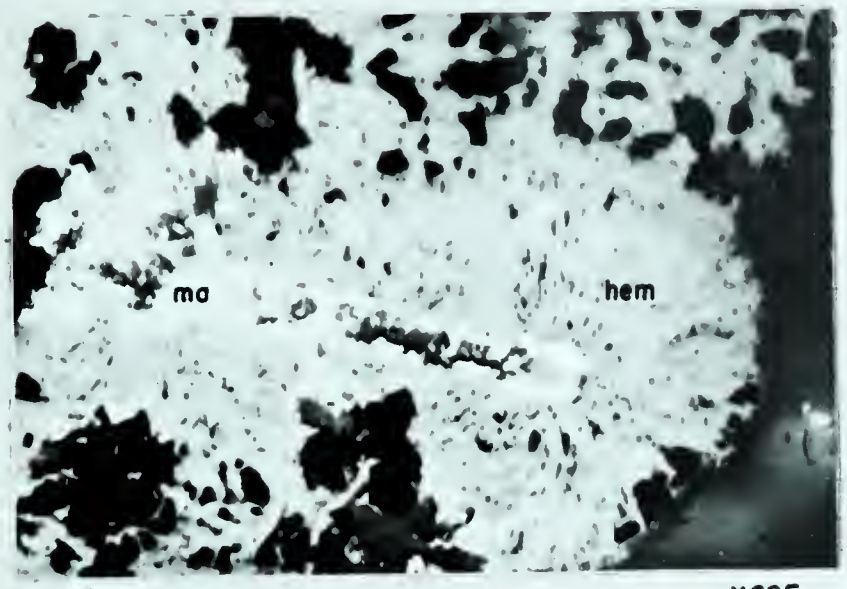


1 X625

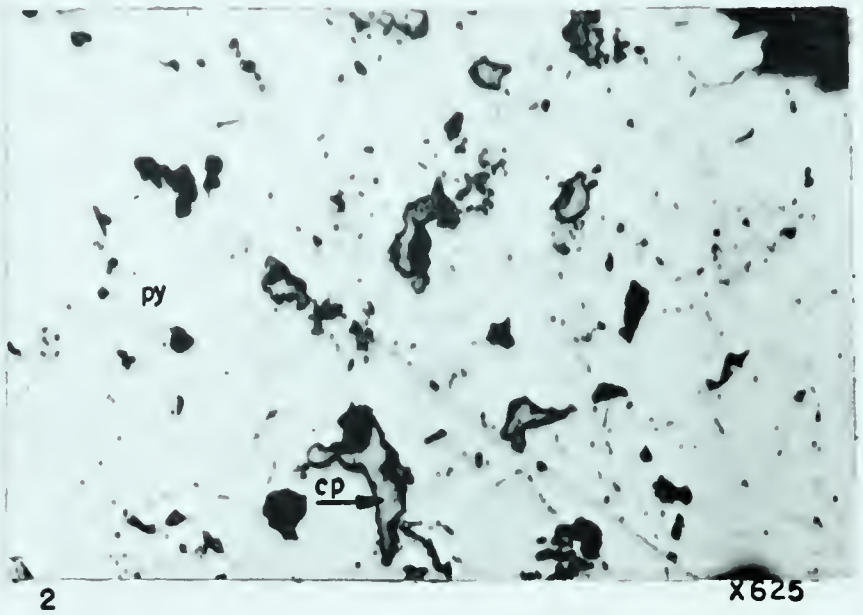


2 X625

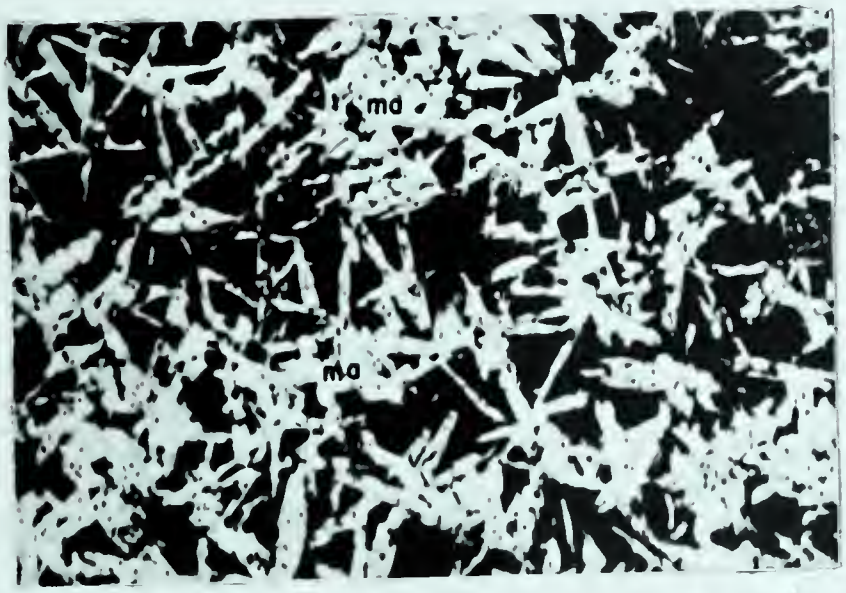


3 X625

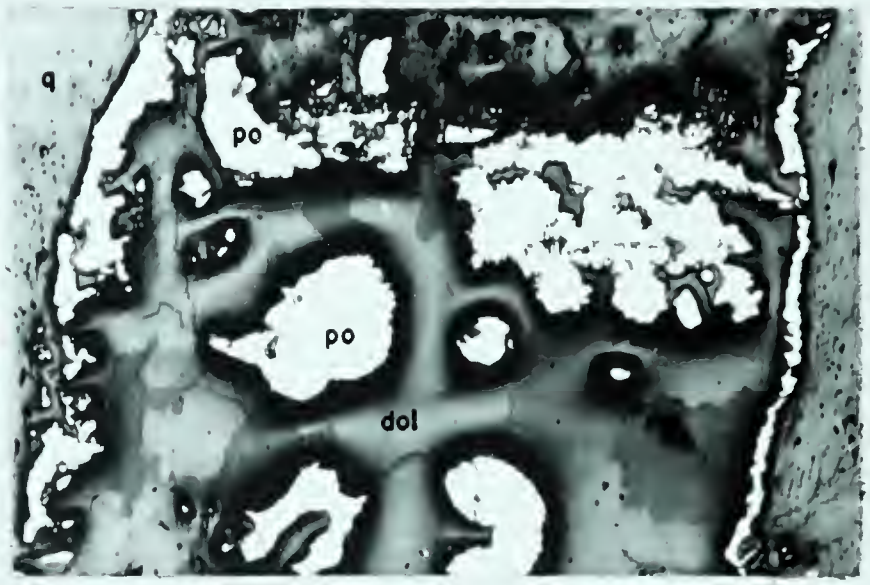


4 X100


5 X255


6 X625

chalcopyrite exsolution or that chalcopyrite is replacing sphalerite. Plate 9, Figure 2, indicates that sphalerite has replaced pyrite, and in Plate 11, Figure 1, it appears sphalerite has replaced glaucodot. A veinlet of sphalerite which is partly replaced by galena is shown in Plate 10, Figure 8. This is a segregation type veinlet containing sphalerite, galena, and chalcopyrite.

Dolomite

Dolomite is the only carbonate identified. Dolomite is present in larger amounts than quartz in samples 3, 4, 1812, 4557. It occurs as irregular replacements, replacements of rhombohedral bismuth, replacements along pitchblende layers, and massive deposits and veinlets.

Guanajuatite

Guanajuatite, a rare mineral, was observed in sample 1812 in one small vug. It occurs in irregularly arranged acicular crystals in dolomite (Plate 11, Figure 2). The crystals appear to have developed from native bismuth. Other occurrences reported (Palache, Berman, and Frondel, 1946) are from the Santa Catarina and La Industrial Mines, Sierra de Santa Rosa, near Guanajuato, Mexico; Andreasberg, Harz Mountains, Germany; Fahlun, Sweden; and near Salmon, Lemhi County, Idaho.

Galena

Galena occurs as irregular masses (Plate 11, Figure 3), and as replacements of pitchblende (Plate 11, Figure 7 and Plate 12, figure 3). Flecks of galena are seen

PLATE 11

FIGURE 1: Photomicrograph of sample 9. Irregular sphalerite (sp) is replacing granular masses of glaucodot (glau). Sphalerite is replaced by tetrahedrite (tet) which contains white specks of chalcopyrite. x255

FIGURE 2: Photograph of sample 1812. Acicular crystals of guanajuatite (gua) in a dolomite vug. Earlier dolomite is massive; later dolomite (in vug) consists of small crystals, partly pink. x2.5

FIGURE 3: Photomicrograph of sample 4. Irregular galena (gn) replacing schirmerite (sch). Galena is replaced by bornite (bor). x625

FIGURE 4: Photomicrograph of sample 4. Irregular schirmerite (sch) rimmed by chalcopyrite (cp). x625

FIGURE 5: Photomicrograph of sample 5. Bornite (bor) and chalcopyrite (cp) in a segregation - type deposit with klaprothite (kla). Py is pyrite. x625

FIGURE 6: Photomicrograph of sample 5. This shows typical occurrence of 4 or 5 transparent crystals (epidote, sphene or zircon) with bornite (bor) and gangue (dark grey). x625

FIGURE 7: Photomicrograph of sample 9. Massive galena (gn) with chalcopyrite (cp) replacing, rimming, and veining massive pitchblende (p). x625

FIGURE 8: Photomicrograph of sample 7 where galena (gn) occurs in syneresis cracks of massive pitchblende (p) x255

PLATE II.

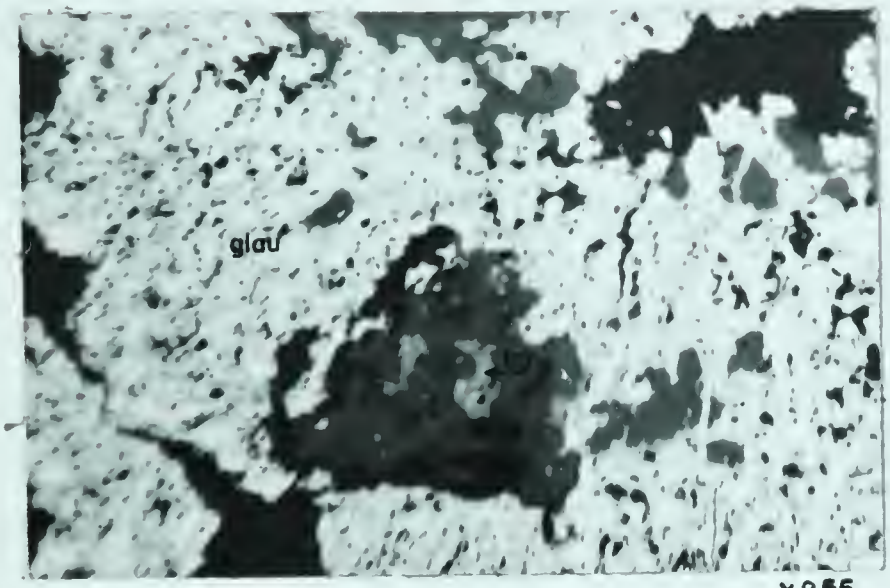


1 X255

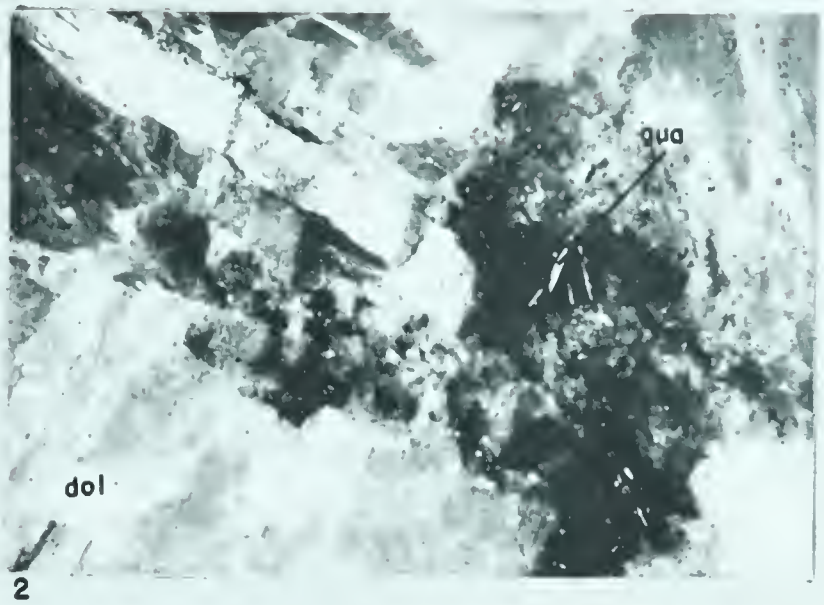


2

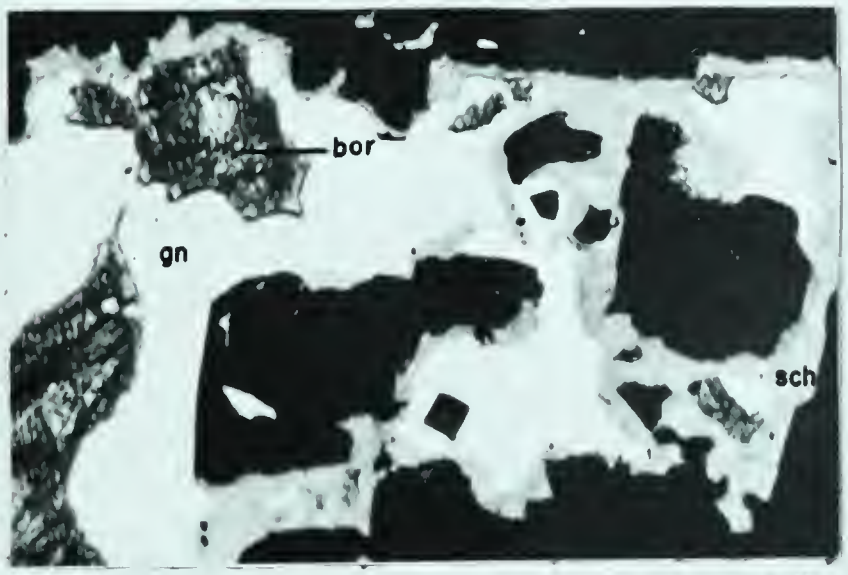


3 X625


4 X625

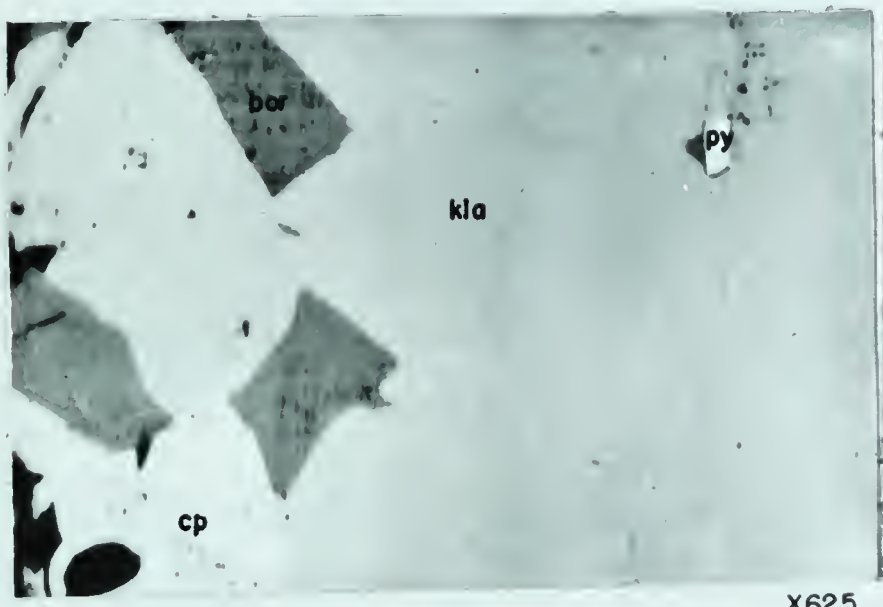


5 X625


6 X625

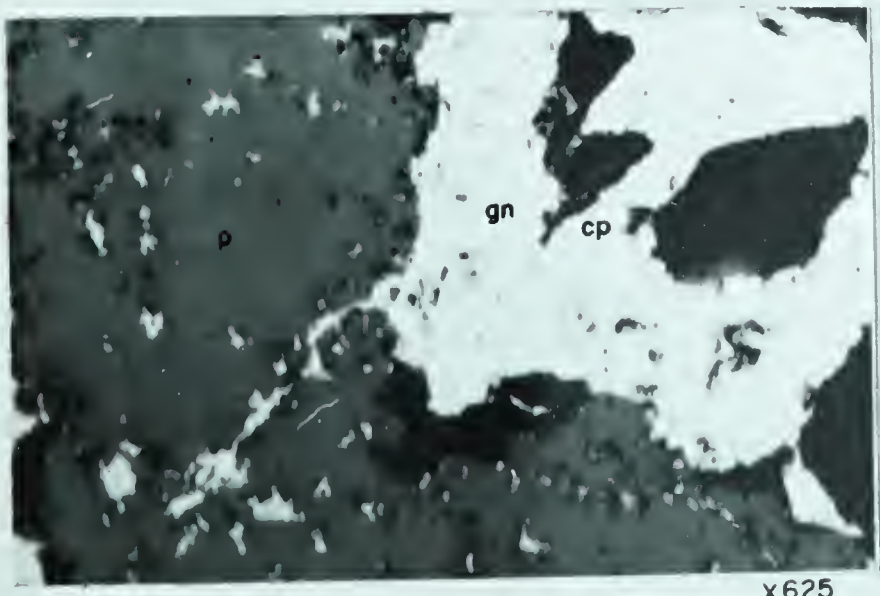


7 X625

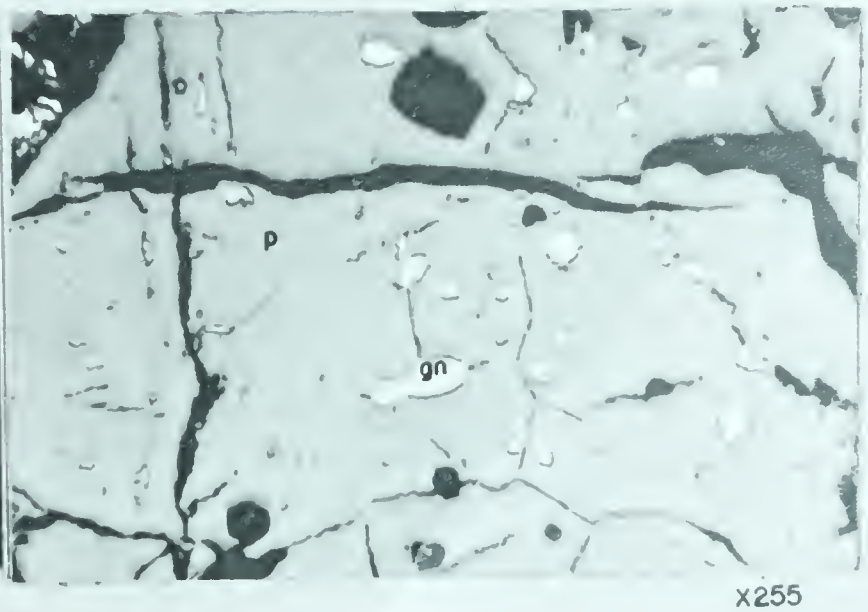


X255

in places in the pitchblende (Plate 11, Figure 8). Segregation veinlets of galena-bornite-chalcopyrite are seen in Plate 12, Figure 4, and a galena-tetrahedrite veinlet is seen in Plate 12, Figure 10. Most of the lead in the galena is probably not radiogenic, but a complex mixture of normal and radiogenic material.

Tetrahedrite

This mineral is present in sample 9 where it occurs with galena and chalcopyrite. Plate 12, Figure 1, shows a veinlet comprising galena and tetrahedrite. This may be an exsolution relationship (Edwards, 1960, p. 93) or simply a segregation veinlet. Plate 12, Figure 2 shows an occurrence of tetrahedrite with chalcopyrite and some galena along syneresis cracks in pitchblende. Edwards (1960, p. 92), gives chalcopyrite-tetrahedrite in a table showing possible solid solution series. This may explain the omnipresence of chalcopyrite with tetrahedrite.

Bornite

Bornite occurs along syneresis cracks in pitchblende (Plate 12, Figure 4), replaces klaprothite (Plate 11, Figure 5), and occurs in klaprothite-bornite-chalcopyrite segregations. Bornite replaces galena (Plate 11, Figure 3), and encloses galena (Plate 12, Figure 5).

An occurrence of 4 or 5 transparent crystals with klaprothite and bornite in sample 5 should be mentioned here, (Plate 11, Figure 6). They are believed to be either epidote, sphene, or zircon.

PLATE 12

FIGURE 1: Photomicrograph of sample 9. Segregation veinlet of galena (gn) and tetrahedrite (tet) or exsolution of tetrahedrite from galena (Edwards, 1960). x255

FIGURE 2: Photomicrograph of sample 9. Massive pitchblende (p) rimmed and veined (along syneresis cracks) by tetrahedrite (tet), chalcopyrite (cp), and very fine grained galena. x255

FIGURE 3: Photomicrograph of sample 9. Massive pitchblende (p) rimmed and veined (along syneresis cracks) by tetrahedrite (tet) and chalcopyrite (cp). x100

FIGURE 4: Photomicrograph of sample 2. Segregation veinlet along syneresis crack of pitchblende (p) of galena (gn), bornite (bor), and chalcopyrite(cp). x625

FIGURE 5: Photomicrograph of sample 2. Paragenetic sequence of galena (gn) - bornite (bor) - chalcopyrite (cp) in order of earliest to latest deposited as shown by ~~x625~~ order of rimming. x625

FIGURE 6: Photomicrograph of sample 2. Exsolution blades of chalcopyrite (cp) in bornite (bor). x100

FIGURE 7: Photomicrograph of sample 9. Chalcopyrite (cp) has largely replaced massive pitchblende (p).

FIGURE 8: Photomicrograph of sample 4. Botryoidal layered pitchblende (p) has been replaced by chalcopyrite (cp). x40

PLATE 12

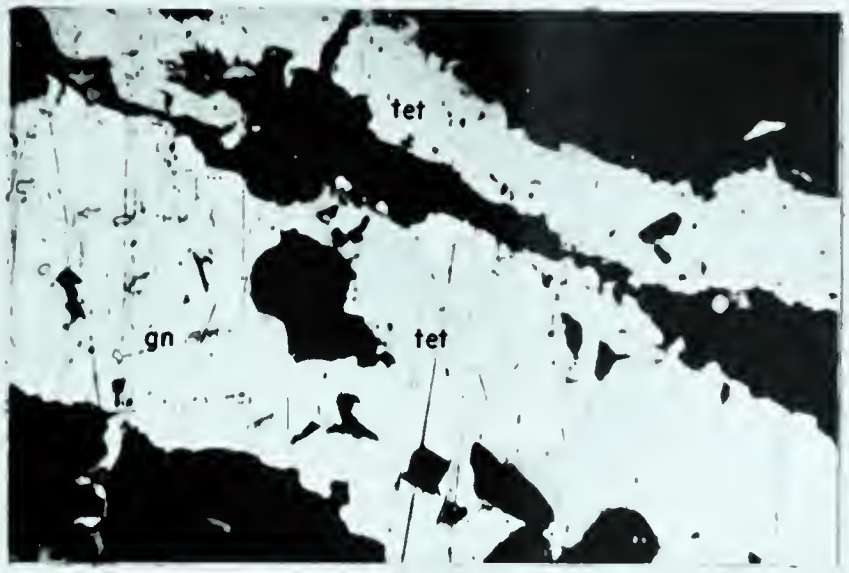


1 X255

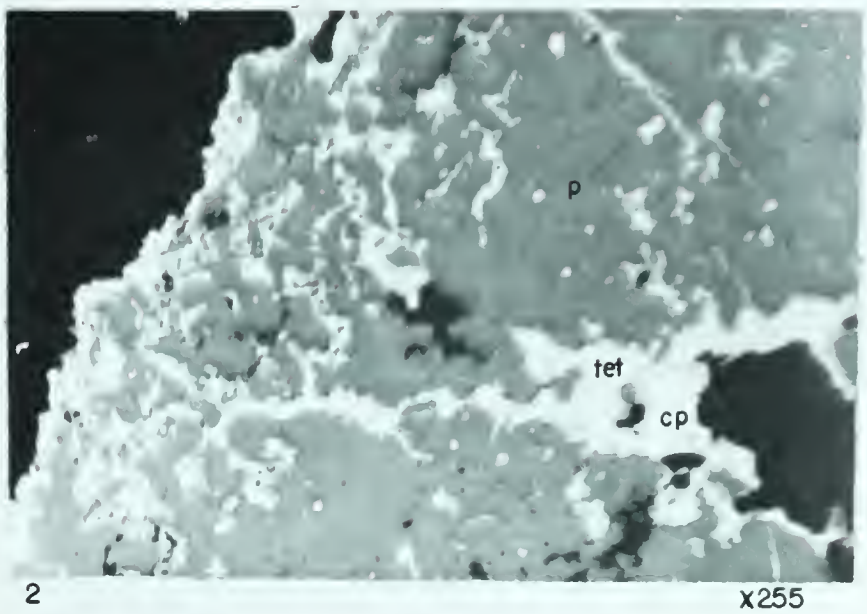


2 X255

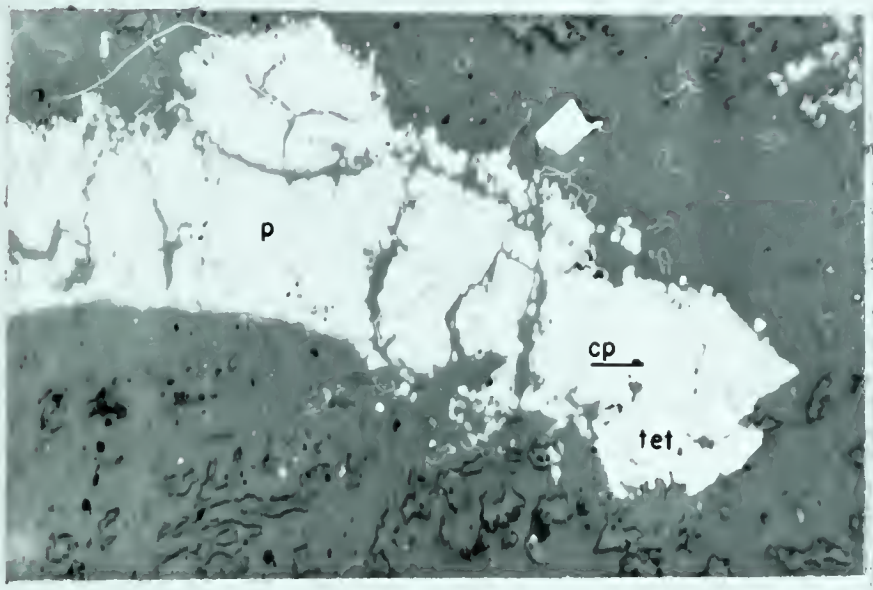


3 X100

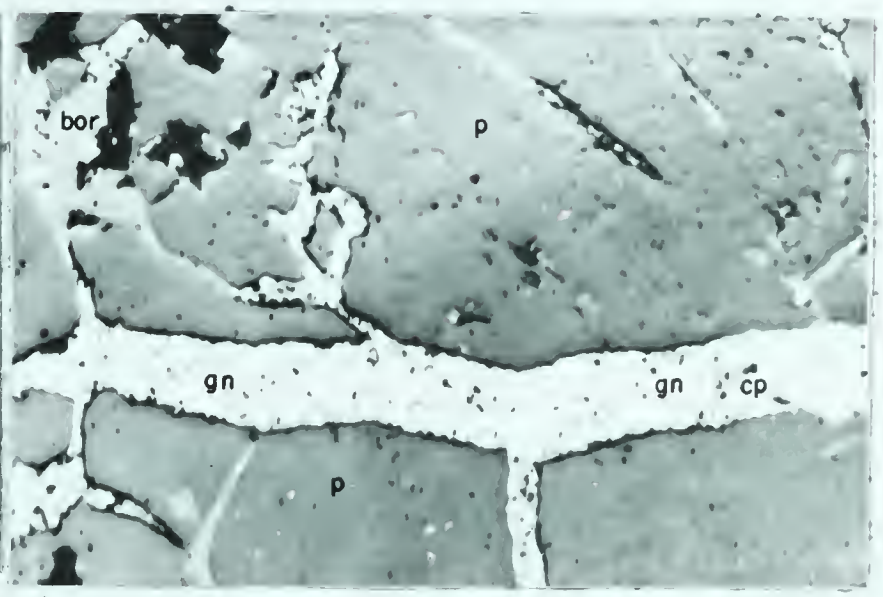


4 X625

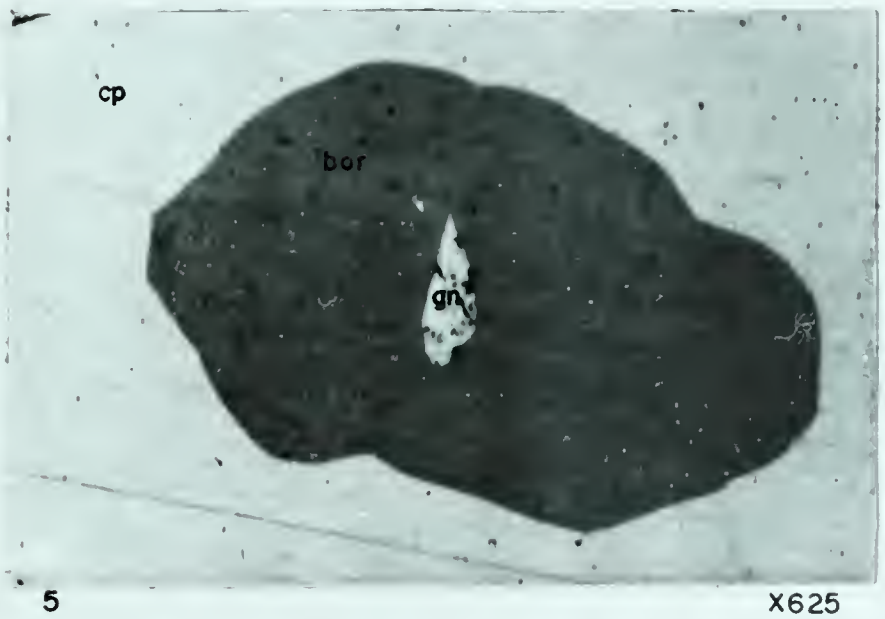


5 X625

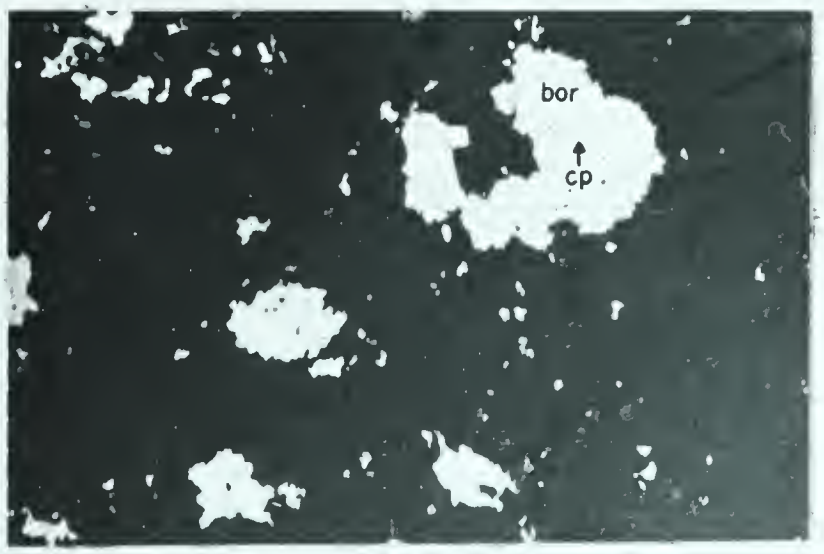


6 X100

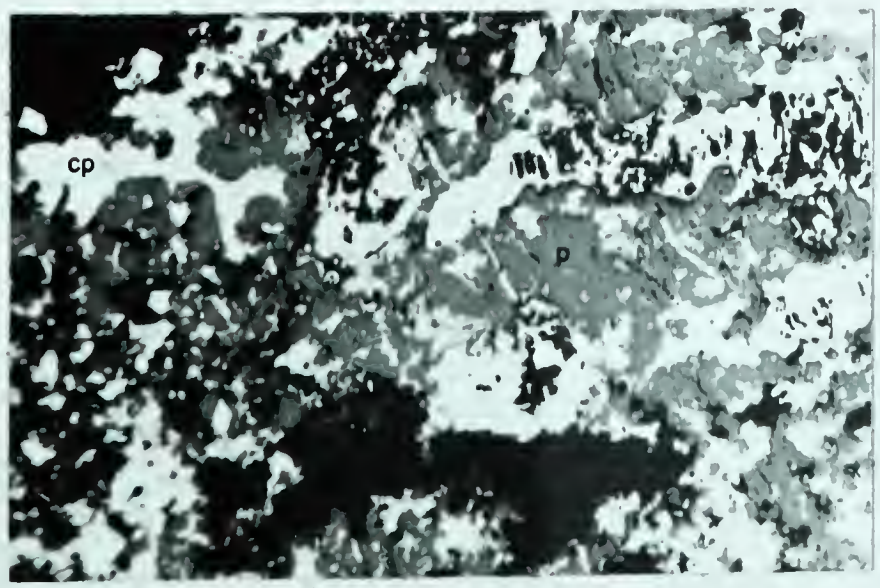


7 X100


8 X 40

Chalcopyrite

Next to pitchblende, chalcopyrite is the most abundant metallic mineral, and is present in all the samples studied. The most common occurrence of chalcopyrite is in syneresis cracks of pitchblende. A common occurrence, also, is the replacement of pitchblende which is seen in Plate 12, Figure 7 and 8 and Plate 13, Figure 2. The veining of pitchblende by chalcopyrite is shown in Plate 13, Figure 1. Chalcopyrite is present as irregular masses replacing schirmerite (Plate 11, Figure 4) and klaprothite (Plate 11, Figure 5). Disseminated chalcopyrite occurs in tetrahedrite as seen in Plate 12, Figures 2 and 3. Chalcopyrite rims bornite and galena (Plate 12, Figure 5). Segregation veinlets are seen in Plate 12, Figure 4. Residual pyrite in chalcopyrite is observed in Plate 13, Figures 2, 3, and 4, and shattered pyrite, veined by chalcopyrite, as seen in plate 13, Figure 5. The residual pyrite in chalcopyrite indicates that chalcopyrite was deposited at the expense of pyrite. Sample 2 contains blades or veinlets of chalcopyrite in bornite (Plate 12, Figure 6).

The occurrence of chalcopyrite blades in bornite is noteworthy. Lyon (1959) discusses the solid solution of bornite and chalcopyrite. He states that bladed intergrowth could be produced by unmixing. Unmixing occurs at 475$^{o}$C, a temperature which is unreasonable for the 2 Zone. It must be noted that no mention of bulk

PLATE 13

FIGURE 1: Photomicrograph of sample 6. Chalcopyrite (cp) veinlet and irregular patches in unoxidized pitchblende (medium grey - p) and oxidized pitchblende (dark grey - p). x40

FIGURE 2: Photomicrograph of sample 7. Chalcopyrite (cp) rimming and in syneresis cracks of pitchblende (p). Pyrite (py) islands occur in chalcopyrite. x255

FIGURE 3: Photomicrograph of sample 4. Pyrite (py) islands in chalcopyrite (cp). x625

FIGURE 4: Photomicrograph of sample 3. Similar to Figure 3. Pyrite (py) island in chalcopyrite (cp). x625

FIGURE 5: Photomicrograph of sample GB.28.3. Shattered pyrite (py) veined and rimmed by chalcopyrite (cp). x255

FIGURE 6: Photomicrograph of sample 5. Stromeyerite (str) replacing rammelsbergite (ram) which has replaced pitchblende (dark grey - p). x100

FIGURE 7: Photomicrograph of sample 4. Covellite (cov) along cleavage planes of chalcopyrite (cp).

PLATE 13

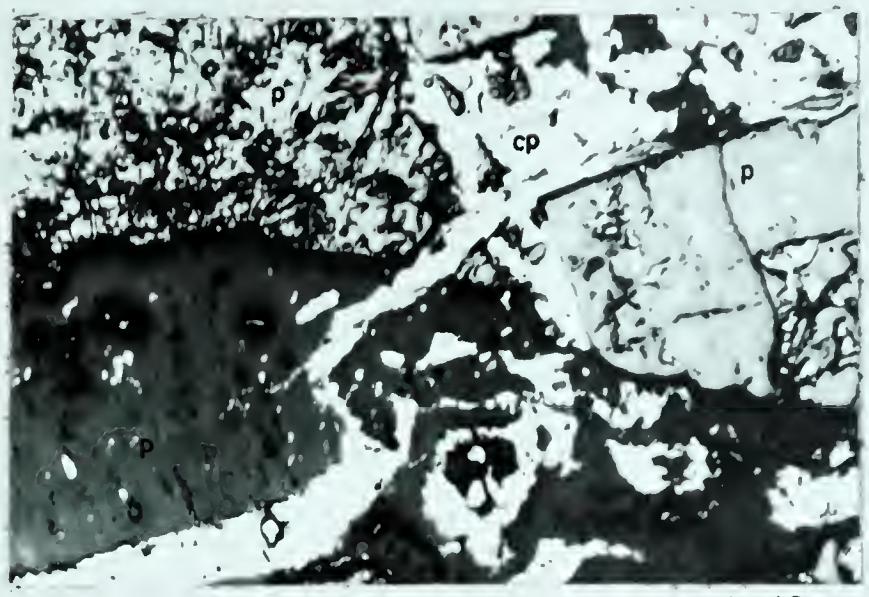


1 X 40

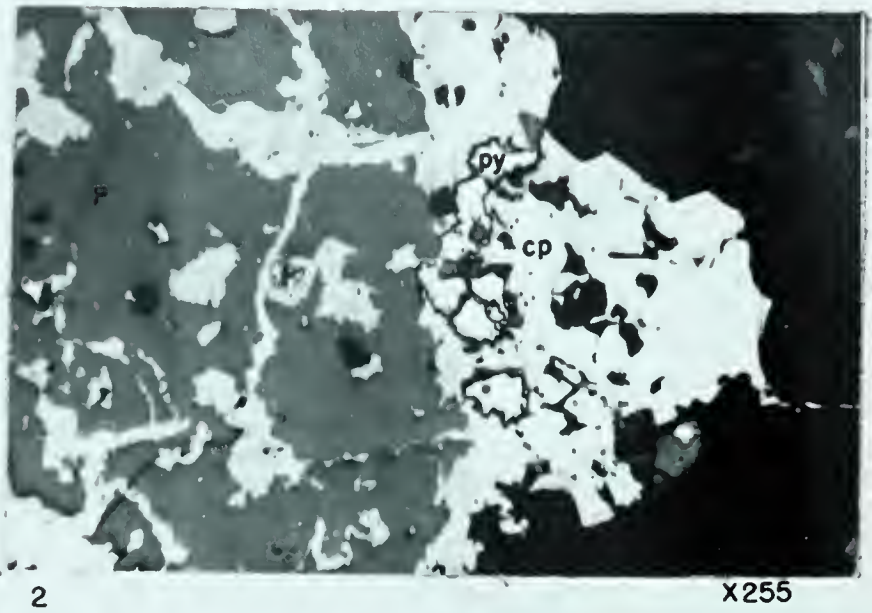


2 X255

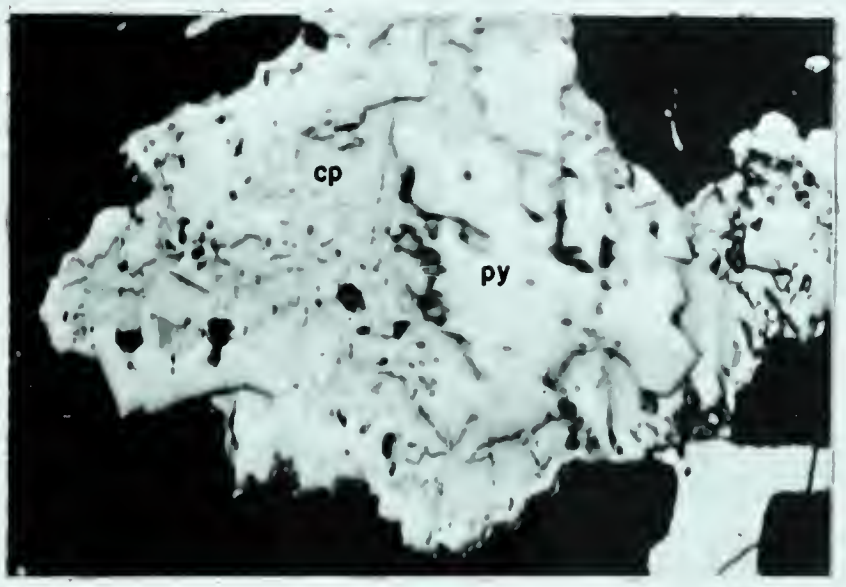


3 X625


4 X625

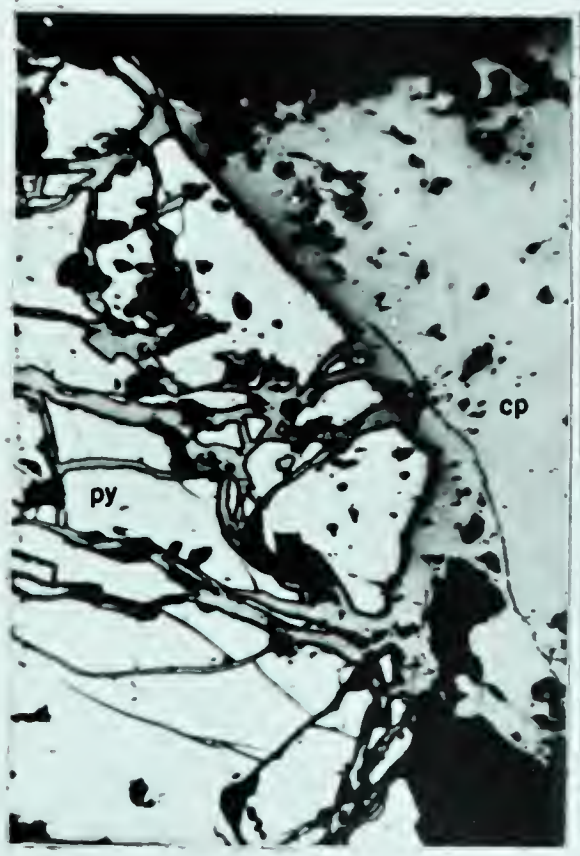


5 X255

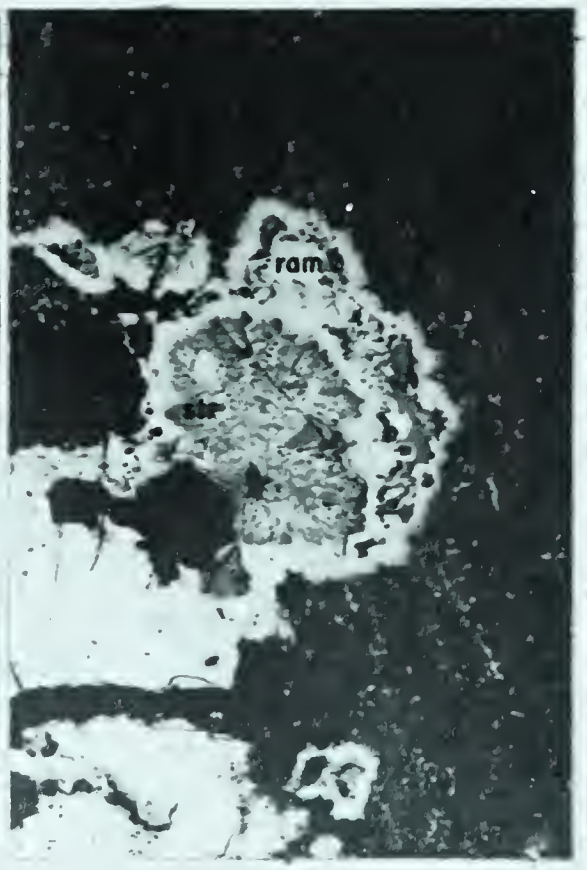


6 X 100

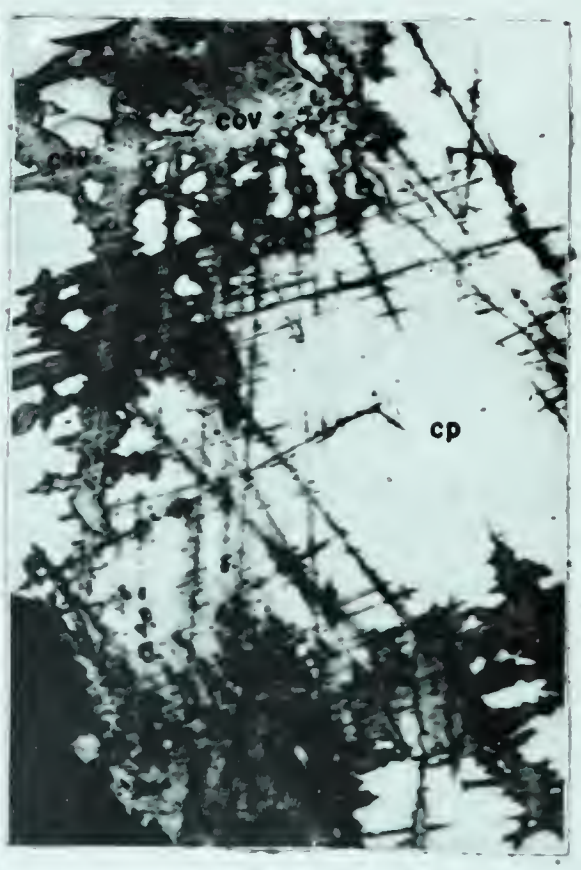


7 X 625

composition is made. Therefore, unmixing probably occurs at much lower temperatures than 475°C where the bulk composition is close to either of the end members, bornite or chalcopyrite. In the case of the No 2 Zone the bulk composition is very near chalcopyrite. Lyon shows photomicrographs in which a large number of chalcopyrite blades are oriented in bornite. This large quantity of chalcopyrite signifies the bulk composition near 50 percent of each of the constituents, and this composition would give a temperature near maximum on the solvus. Lyon does state that Latsky has observed an appreciable diffusion rates of chalcopyrite in bornite occurring even at 220°C.

Stromeyerite

Stromeyerite occurs in sample 5 where it replaces arsenides (Plate 3, Figure 6). Some replacement of cores of arsenide dendrites was also observed. The cores were probably originally bismuth or dolomite.

Covellite

Covellite is present in most of the samples in small disseminated plates associated with copper minerals. It coats the previously described copper minerals and in some places may be supergene. In some places covellite occurs along chalcopyrite cleavage planes (Plate 13, Figure 8).

Supergene minerals:

Besides pitchblende 4, already described, other supergene minerals observed were alteration products of

Table 26 : Mineralogy and paragenesis of the No. 2 Zone

| MINERALS | oldest ——► PARAGENESIS ——► youngest |
|---|---|
| HYPOGENE | |
| Magnetite | ——— |
| Massive quartz | ——————— |
| Pitchblende 0 (1) | ——— |
| Hematite | ——————— |
| Pitchblende 2 (3) | ——— |
| Comb quartz | ——————— |
| Native bismuth | — |
| Niccolite | — |
| Rammelsbergite | — |
| Gersdorffite | — |
| Glaucodot | — |
| Skutterudite | — |
| Schirmerite | — |
| Klaprothite | — |
| Pyrite | ——— — — |
| Marcasite | — ——— |
| Pyrrhotite | —— |
| Sphalerite | — |
| Dolomite | ——— |
| Guanajuatite | — |
| Galena | — |
| Tetrahedrite | — |
| Bornite | — |
| Chalcopyrite | — |
| Stromeyerite | — |
| Covellite | — |
| SUPERGENE | |
| Uranium minerals | |

pitchblende. Sample 1 has a coating, and is veined, by supergene uranium minerals. A very small amount of supergene uranium minerals was noted in some of the underground samples. For the most part supergene mineralization has been minor except at the surface.

The paragenetic sequence interpreted from the textural data described is given in Table 26. As previously discussed the time of the deposition for niccolite, rammelsbergite, and pyrite has not been definitely established. In addition, the pyrite-marcasite-pyrrhotite relationships in places are so complex that the sequence cannot be stated with certainty. Marcasite deposition may have occurred before pyrite, and even earlier than the bismuth and arsenide deposition.

## SPATIAL ZONING

The twelve samples studied do not exhibit any marked zoning, either vertically or laterally. This does not mean that there is no spatial zoning but rather that too few samples were examined to determine mineral distribution. Dolomite is dominant over quartz in some localities. Arsenides occur between the 375 level and the 1675 level. Bornite decreases markedly with depth whereas chalcopyrite persists. This indicates an increase in iron with depth. Pyrite and pyrrhotite are more common in the deeper parts of the zone.

Robinson (1958, p. 181), states that silver diminished with depth, and pitchblende is botryoidal at

the surface and is massive at depth.

Kidd and Haycock (1935, p. 892), when discussing the No. 2 Zone, note,

> "Throughout the greater part it (No. 2 Zone) is a quartz vein stockwork like No. 1 Zone, but at its northeast end quartz is absent, and the gangue is carbonate."

They also note that native silver is present at several places, but especially in the northeast section of the zone. It occurs, they state, where galena and chalcopyrite is extensive.

## GEOTHERMOMETRY

Murphy states that the early massive quartz and massive pitchblende were deposited under mesothermal conditions. Botryoidal pitchblende, comb quartz, and quartz veinlets indicate low mesothermal temperatures (Kidd and Haycock, 1935).

Bismuth deposition must have occured below 271$^{o}$C, the melting point of the metal. Brown (1948, p. 69) discusses the possibility of bismuth separating from the solutions above 271$^{o}$C in liquid form. Rhombohedral bismuth dendrites rimmed by later minerals indicates that bismuth was solid before arsenide mineralization, although bismuth may have originally separated as a liquid. Assuming a dropping temperature, this puts a maximum temperature limit of arsenide deposition and all mineralization after the bismuth at 271$^{o}$C. The writer believes that the botryoidal pitchblende and comb quartz throughout the whole zone indicates that temperatures after pitchblende and quartz

deposition were mesothermal, probably below 271°C.

Pyrrhotite formed in equilibrium with pyrite may be used as a geothermometer. Temperatures are determined from the iron content of the pyrrhotite. As previously stated the iron content of the pyrrhotite from No 2 Zone is greater than 48 atomic percent. Arnold (1962, p. 73) has given equilibrium relationships in the system FeS-S between stoichiometric FeS and $FeS_2$ (pyrite) as a function of temperature. Assuming equilibrium with pyrite iron content greater than 48 percent in pyrrhotite indicates temperature of deposition much lower than 200°C.

Sphalerite as a geothermometer was found to be less reliable. Small errors in reading to obtain d-spacings and small shrinkage of the film cause significant deviation in the extrapolated cell edge. This produces a large variation in the mole percent FeS in sphalerite and gives very large temperature variations since the curve used (Ingerson 1955, p. 470) is steep. Considering the large possible errors 9 percent FeS calculated for one sample seems reasonable. The sphalerite is a bright-ruby-red suggesting a low iron sulfide content. The minimum temperature for 9 percent FeS in sphalerite using Ingerson's curve is 280°C. This is higher than expected since sphalerite was deposited after pyrrhotite and pyrrhotite was deposited below 200°C. The sample analysed is a sphalerite from a veinlet that has filled vuggy dolomite. The fact that sphalerite has not replaced dolomite faces

suggests low temperatures, but it is not known how low.

Another more general temperature indicator is the occurrence of pyrite and marcasite, apparently in equilibrium (Plate 9, figures 2 and 3). This limits the maximum temperature to about 400°C, as above this termperature marcasite will invert to pyrite (Clark 1960, p. 1349).

Finally oxidation of $UO_2$ to a tetragonal compound occurs only at temperatures below 220°C (Brooker and Nuffield, 1952). Assuming this oxidation took place before comb quartz deposition, the temperature must not have been greater than 220°C.

## ORE GENESIS

Robinson (1958) has classified Canadian uranium deposits, and he believes that the Eldorado ore was deposited from hypogene solutions. Lang (1952) classifies the Eldorado deposit as a complex mineral association of hydrothermal origin. The outstanding problem regarding the genesis of the deposit has been, which exposed intrusive, if any, supplied these solutions.

### Source of the Mineralization

Many have considered that the granite exposed at LaBine Point is the source. However, the granite is fractured by the same ore-bearing zones in the Eldorado Mine. Furthermore the granite is 1930 million years old whereas U/Pb ages have given an average of 1400 million years (Gastil, 1960 and Cumming, Wilson, Farquhar, and Russell, 1955). Did 530 million years elapse before

solutions from the granite entered and deposited the minerals in fractures occurring in the granite and earlier sedimentary and volcanic rocks? This granite was assayed for uranium content and contains 0 p.p.m. whereas average assay of granite is 4 p.p.m. Does this indicate a diffusion of uranium and other elements? Perhaps, but it is not likely. The small difference from the average could be due to analytical errors. Wasserstein (1951, 1954) has presented a new method of 'uraninite' age determination. This is a shrinkage of the cell edge due to decay from 0.0025 Å to 0.0051 Å for every 100 million years. The cell edge is 5.4682 Å for 0 age material. The calculated age of the X-rayed pitchblende sample for a 5.455 Å cell edge is 366 million years to 600 million years. This of course is unreasonable. The low ages do indicate that the Eldorado deposit is much younger than any of the igneous bodies. The large age discrepancy from the published U/Pb ages could be due to some thorium in pitchblende. Thorium content increases the cell edge of pitchblende. However, Robinson (1958) states that thorium content for such deposits is low. But this does not mean that a low thorium content will not effect the cell edge.

Eldorado ore originated from unexposed rocks, perhaps closely related to the exposed mafic dikes. The general theory is that uranium deposits are related to acid rocks. Page (1960) states, in his abstract,

"Recent work indicates that in many places

> these hypogene solutions start escaping from magmas long before the formation of granite and continue, perhaps intermittently, until the end of fractional crystallization. There seems to be evidence for the escape of uraniferous solutions from the magma at about the same time that diabase and lamprophyre dikes were intruded. Uranium escaping from the more acid members of magmatic sequences seems to be less important volumetrically. The spatial relation of epigenetic uranium deposits to various types of igneous bodies and to major structural elements strongly suggests that the source of uranium in most districts is at considerable depth."

One syenodiorite sample from the 10 level of the No. 2 Zone sample No. GB.28.4, contains 110 $\pm$ 10 p.p.m. uranium. This is anomalous in that the average syenodiorite content is approximately 1 p.p.m. The high anomalous content may indicate a mutual source of the pitchblende and syenodiorite.

Another possibility may be that the source of the uranium and other elements is the sedimentary and volcanic rocks of the LaBine Point area. A siliceous argillite contains 750 p.p.m. uranium whereas a high uranium content for shales is 200 p.p.m. The author feels this high content indicates that hydrothermal solutions carried the uranium into fractures in the country rocks and not from the sedimentary and volcanic rocks into the fractures. Thus the solutions are hydrothermal in origin and not due to lateral secretion.

Type of Solutions and Their Environment

The early hypogene solution was acidic and strongly reducing, and contained iron, uranium, and silica.

Pressure, temperature, and the chemical conditions were favorable for pitchblende 0, hematite, and quartz deposition. The conditions were then changed so that the solution became strongly oxidizing, facilitating oxidation of pitchblende 0 to pitchblende 1. During oxidation, another hydrothermal solution, containing arsenic, sulfur, bismuth, cobalt, nickel, iron, zinc, selenium, lead, antimony, copper, silver, and other elements, entered the fracture zones and mingled with the earlier iron-uranium-rich solutions. Due to an interaction with the wall rocks, conditions changed from an acid and oxidizing environment to a basic and strongly reducing one. This environment allowed the precipitation of pitchblende 2 and all the other minerals that were deposited after pitchblende 2. Finally, deposition from supergene water occurred at the surface dominantly.

BIBLIOGRAPHY

Arnold, A. G., 1962, Equioibrium relations between pyrrhotite and pyrite from 325° to 743°C: Ec. Geol., Vol. 57, No. 1 (Jan. - Feb.), pp. 72 - 91.

Arnold, A.G. and Reichen, Laura E., 1962, Measurement of the metal content of naturally occurring, metal-deficient hexagonal pyrrhotite by an X-ray spacing method: Am. Min., Vol. 47, Nos. 1 and 2 (Jan. - Feb.), pp. 105 - 112.

A.S.T.M., 1957 and 1960, Index to the X-ray powder data file.

Bastin, E.S., 1950, Interpretation of ore textures: G.S.A., Mem. 45.

Brooker, E.J. and Nuffield, E.W., 1952, Studies of radioactive compounds - pitchblende from Lake Athabasca, Canada: Am. Min., Vol. 37, pp. 363 - 385.

Brown, J.S. 1948, Ore genesis: The Hopewell Press, Hopewell, N.J. p. 69.

Buddington, A.F., 1959, Granite emplacement with Special reference to North America: G.S.A. Bul., Vol. 70, No. 6.

Campbell, D.D., 1955, Geology of the pitchblende deposits of Port Radium, Great Bear Lake, N.W.T.: California Inst. of Technology (Ph.D. thesis), Vols. 1 and 2.

Campbell, D.D., 1957, Port Radium Mine: Structural deposits of Canadian ore deposits, C.I.M.M., Vol. 2, pp. 177 - 189.

Clark, L.A., 1960, The Fe-As-S System: Phase relations and applications. Pt. 1 : Ec. Geol., Vol. 55, No. 7, Page 1349.

Cumming, G.L., Wilson, J.T., Farquhar, R.M. and Russell, R.D., 1955, Some dates and subdivisions of the Canadian Shield: Proceedings of the G.A.C., Vol. 7, Pt. 2, pp. 74 - 77.

Edmonton Journal, 1960, North uranium mine closing; played part in first A-bomb: Edmonton Journal, Sept. 9, p. 3.

Edwards, A.B., 1960, Textures of the ore minerals and their significance: Aust. Inst. M.M.

Feniak, M., 1948, MacAlpine Channel, District of MacKenzie, N.W.T.: G.S.C., Map 1011 A (1 inch = 1 mile).

Feniak, M., 1949, MacAlpine Channell Map Area, N.W.T. (Report and Map): G.S.C., Paper 49 - 19.

Gastil, G. 1960, The distribution of mineral dates in time and space: Am. Jour. Sci., Vol. 258, p. 19.

Holmes, R.J., 1947, Higher mineral arsenides of cobalt, nickel, and iron: G.S.A., Vol. 58, pp. 299 - 392.

Ingerson, Earl, 1955, Geologic Thermometry: G.S.A., Special Paper 62, p. 470.

Kidd, D.F., 1931, Great Bear Lake - Coppermine River Area, MacKenzie District, N.W.T.: G.S.C. Summ. Rept., Pt. C., pp. 47 - 69.

Kidd, D.F. 1932, Great Bear Lake Area, Northwest Territories: G.S.C. Summ. Rept., Pt. C, pp. 1 - 37.

Kidd, D.F. and Haycock, M.H., 1935, Mineralography of the ores of Great Bear Lake: Bull. of the G.S.A., Vol. 46, pp. 879 - 960.

Lang, A.H., 1952, Canadian deposits of uranium and thorium: G.S.C. No. 16, Ec. Geol. Series.

Lord, C.S., 1942, Snare River - Ingray Lake Map Areas: G.S.C., Mem. 235.

Lord, C.S., 1946, and Parsons, W.H., 1947, Camsell River, District of MacKenzie, N.W.T.: G.S.C., Map 1014 A, (1 inch = 4 miles).

Lowdon, J.A., 1961, Age determinations by the G.S.C.: G.S.C., Paper 61 - 17, pp. 21 - 36.

Lyon, J.P., 1959, Time aspects of geothermometry: Mining Engineering, pp. 1145 - 1151.

Mason, B., 1958, Principles of Geochemistry: John Wiley and Sons, Inc.

Murphy, R., 1946, Geology and mineralogy at Eldorado Mine: C.I.M.M. Vol. 49, pp. 423 - 438.

Nelson, J.B. and Riley, D.P. 1944, An experimental investigation of extrapolation methods in the derivation of accurate unit-cell dimensions of crystals: Cavendish Laboratory, Cambridge, pp. 160 - 177.

Page, L.R., 1960, The sources of uranium in ore deposits: International Geological Congress: Genetic Problems of Uranium and Thorium Deposits, Pt. 15, p. 149.

Palache, C., Berman, H., and Frondel, C., 1946, Dana's System of Mineralogy: John Wiley and Sons, Vol. 7, 7th Ed.

Parsons, W.H., 1948, Camsell River Map Area, N.W.T. (Report and Map): G.S.C., Paper 48 - 19.

Robinson, S.C., 1958, A genetic classification of Canadian uranium deposits: Can. Min., Vol. 16, Pt. 2.

Short, M.N., 1940, Microscopic determination of the ore minerals: U.S.G.S., Bull. 914.

Skinner, B.J., Barton, Jr., P.B., and Kullerud, G., 1959, Effect of FeS on the unit cell edge of sphalerite: Ec. Geol., Vol. 54, No. 6 (Sept. - Oct.), pp. 1040 - 1047.

Todd, E.W., 1926, Gowganda vein minerals: Ont. Dept. of Mines, Vol. 35, Pt. 3, p. 73.

Wasserstein, B., 1951, Cube edge of uraninites as a criterion of age: Nature, Vol. 168, p. 380.

Wasserstein, B., 1954, Ages of uraninites by a new method: Nature, Vol. 174, pp. 1004 - 1005.